Optimal Shape Design for Polymer Electrolyte Membrane Fuel Cell Cathode Air Channel: Modelling, Computational and Mathematical Analysis

Jamal Hussain Al-Smail

Thesis submitted to the Faculty of Graduate and Postdoctoral Studies
in partial fulfillment of the requirements for the degree of Doctor of Philosophy in Mathematics [1]

Department of Mathematics and Statistics
Faculty of Science
University of Ottawa

[1]The Ph.D. program is a joint program with Carleton University, administered by the Ottawa-Carleton Institute of Mathematics and Statistics

Abstract

Hydrogen fuel cells are devices used to generate electricity from the electrochemical reaction between air and hydrogen gas. An attractive advantage of these devices is that their byproduct is water, which is very safe to the environment. However, hydrogen fuel cells still lack some improvements in terms of increasing their life time and electricity production, decreasing power losses, and optimizing their operating conditions. In this thesis, the cathode part of the hydrogen fuel cell will be considered. This part mainly consists of an air gas channel and a gas diffusion layer. To simulate the fluid dynamics taking place in the cathode, we present two models, a general model and a simple model both based on a set of conservation laws governing the fluid dynamics and chemical reactions. A numerical method to solve these models is presented and verified in terms of accuracy. We also show that both models give similar results and validate the simple model by recovering a polarization curve obtained experimentally. Next, a shape optimization problem is introduced to find an optimal design of the air gas channel. This problem is defined from the simple model and a cost functional, E, that measures efficiency factors. The objective of this functional is to maximize the electricity production, uniformize the reaction rate in the catalytic layer and minimize the pressure drop in the gas channel. The impact of the gas channel shape optimization is investigated with a series of test cases in long and short fuel cell geometries. In most instances, the optimal design improves efficiency in on- and off-design operating conditions by shifting the polarization curve

vertically and to the right.

The second primary goal of the thesis is to analyze mathematical issues related to the introduced shape optimization problem. This involves existence and uniqueness of the solution for the presented model and differentiability of the state variables with respect to the domain of the air channel. The optimization problem is solved using the gradient method, and hence the gradient of E must be found. The gradient of E is obtained by introducing an adjoint system of equations, which is coupled with the state problem, namely the simple model of the fuel cell. The existence and uniqueness of the solution for the adjoint system is shown, and the shape differentiability of the cost functional E is proved.

Acknowledgements

I would like first to express my deep appreciation to my beloved and great mother Zahra, who strove for me to be successful. I also greatly thank my grandfather Hussan, for his care and support to us since our childhood. I thank every member of my family for their good wishes to me.

I would like to express my love and gratitude to the person I admire my wife, Nada– for her care and support in my life with her.

It is my deep pleasure to express my gratitude to my supervisor Prof. Yves Bourgault– who made completing my thesis possible. I thank him for his good wishes, strong support and continuous encouragement to me. I would also like to express my gratitude to my first supervisor Prof. Arian Novruzi; I really appreciate his advices and previous support to me.

I would like to thank my teachers and everyone who taught me and cared about me, in particular my uncle Mohamed and my aunt Afifa.

Thanks to everyone who makes my success possible.

Dedication

It is my honor to dedicate my PhD thesis to my parents–Zahra and Hussain, my grandparents Hussan and Khaireyya, my wife Nada and my children Mohamed and Kendeel.

I also like to dedicate my thesis to my family and my city–Awamia.

Contents

List of Figures

List of Tables

0.1 Nomenclature

Latin symbols:

a, b, e	coefficients appearing in the cost functional E
A	air channel
$\hat{c}$, $\hat{c}_o$	oxygen mass fraction
c_i, c_{in}, $\hat{c}_{o,in}$	oxygen mass fraction at the air channel inlet
$\hat{c}_{n,in}$	nitrogen mass fraction at the air channel inlet
$\hat{c}_{o,ref}$	oxygen reference mass fraction
D_j^{eff}	effective diffusion constant of species j (m^2/s)
E, $E(\Gamma)$, $E(\zeta)$	cost functional
E_{cell}	cell voltage (V)
E_{rev}	reversible cell voltage (V)
F	Faraday's constant $(A \cdot s/mol)$
G, GDL	gas diffusion layer
h_A	with of the air channel (m)
$h_{A,max}$	maximum width of the air channel (m)
$h_{A,min}$	minimum width of the air channel (m)
h_G	width of GDL (m)
H_m	reaction rate of oxygen $(kg/(m^2 \cdot s))$
i	current density on M (A/m^2)
I_{av}	average current density on M (A/m^2)
i_0	exchange current density (A/m^2)
J_j	diffusive flux of species j $(kg/(m^2 \cdot s))$
K	GDL permeability (m^2)
l	length of the fuel cell (m)

M	cathode/anode membrane
M_j	molar mass of species j (kg/mol)
N_j	total flux of species j $(kg/(m^2 \cdot s))$
$\hat{p}$	gas pressure (Pa)
p_A, p_G	gas pressure in A and G, respectively (Pa)
p_i, p_{in}	gas pressure at the air channel inlet (Pa)
p_o, p_{out}	gas pressure at the air channel outlet (Pa)
r	ohmic resistance of the fuel cell (Ωm^2)
R	the universal ideal gas law constant $(J/(mol \cdot K))$
R_j	reaction rate of species j $(kg/(m^2 \cdot s))$
T	gas temperature (K)
$\hat{\mathbf{u}}$	gas velocity (m/s)
x	x-coordinate (m)
x_j	molar fraction of species j
y	y-coordinate (m)

Greek symbols:

α, β, σ	coefficients appearing in the cost functional E
α_c	cathode transfer coefficient
α_m	net water cross the membrane M from the anode to the cathode
η	activation over-potential (V)
ε	porosity of the GDL
ϕ	volumetric flow rate at the air channel inlet (kg/s)
Γ	air channel wall
Γ_i, Γ_{in}	air channel inlet
Γ_o, Γ_{out}	air channel outlet
Γ_w	walls of G

μ	gas viscosity $(kg/(m \cdot s))$
μ_{air}	air viscosity $(kg/(m \cdot s))$
μ_w	water vapor viscosity $(kg/(m \cdot s))$
ν, ν_A, ν_G	the exterior unit normal vectors to Ω, A, G, resp.
$\nu_{\partial\Gamma_i}$, $\nu_{\partial\Gamma_o}$	the exterior unit normal vectors to $\partial\Gamma_i$ and $\partial\Gamma_o$, resp.
Ω	$A \cup G$
ρ_i	density of species i (kg/m^3)
Σ	interface separating A and G
τ	the counterclockwise tangential unit vector to Ω
ξ	direction to which Ω is deformed
ζ	parameterizing variable to deform Ω to Ω_ζ

Chapter 1

Introduction

1.1 Fuel Cells and main objective of the thesis

Fuel cells are devices used to generate electricity from electrochemical reactions occurring inside the cell between the fuel and the air. Fuel cells are classified by means of the fuel used, which lead to different electrochemical reactions.

In a polymer electrolyte membrane fuel cell, there are three main parts: the cathode, the membrane(M) and the anode, see Figure 1.1. Both the cathode and the anode have a fluid (gas) flow channel, a gas diffusion layer (GDL or G) and a catalyst layer (CL). The flow channel is used to deliver the fluid or the reactant. The gas diffusion layer is a porous medium that helps to distribute the gas to the catalyst layer, by which it speeds up the reactions taking place in the cathode or the anode.

In the thesis, hydrogen fuel cells are considered, which use hydrogen gas H_2 as their fuel. The hydrogen gas is delivered into the anode flow channel, diffuses through the anode GDL and then spreads over the anode CL. In the anode CL, hydrogen molecules react to produce electrons and protons:

$$H_2 \longrightarrow 2H^+ + 2e^-. \tag{1.1.1}$$

The two electrons, $2e^-$, are transported to the cathode through an external circuit.

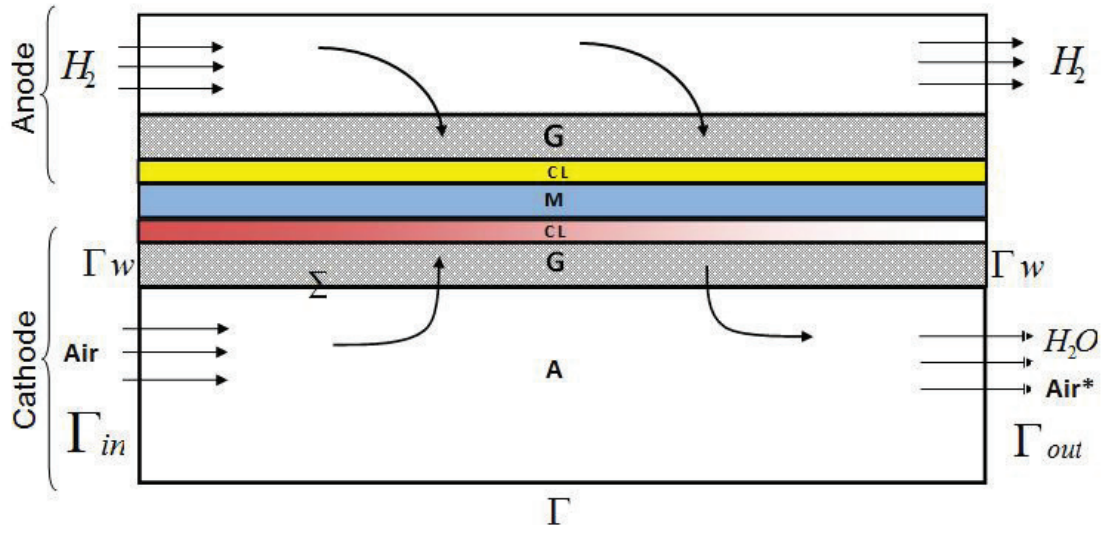

Figure 1.1: 2d cross-section of a hydrogen fuel cell

However, the protons, $2H^+$, are drained into the membrane. On the surface of the membrane, these protons bind with water molecules to produce two ions of hydronium:

$$2H^+ + 2H_2O \quad \longrightarrow \quad 2H_3O^+. \tag{1.1.2}$$

Next, the hydronium ions travel through the membrane towards the cathode side. In the cathode, air (or oxygen gas) is delivered into the cathode air channel. The air diffuses in the cathode GDL and then spreads over the cathode CL, where the oxygen molecules enter a reduction reaction by means of the two electrons coming from the anode:

$$\frac{1}{2}O_2 + 2e^- \quad \longrightarrow \quad O^{-2}. \tag{1.1.3}$$

Finally, the hydronium ions react with the oxygen atom to produce three molecules of water and heat:

$$2H_3O^+ + O^{-2} \quad \longrightarrow \quad 3H_2O + \quad Heat. \tag{1.1.4}$$

Hence, the overall reaction taking place at the cathode CL is

$$2H^+ + \frac{1}{2}O_2 + 2e^- \quad \longrightarrow \quad H_2O + \quad Heat, \tag{1.1.5}$$

where water, as the main product, is a great advantage to have a safe environment. However, the products of the reaction (1.1.5), namely water and heat, may lead to ineffective operation of the fuel cell. The heat, resulting from the exothermic reaction at the cathode, can cause the membrane to dry out. In this case, the membrane cannot transport the protons $2H^+$ from the anode to the cathode, therefore the electricity generation decreases or stops. On the other hand, water can accumulate in the cathode part of the cell. This, as well, prevents the reaction (1.1.5) to take place, as all catalytic reaction sites are eventually flooded by water.

The main goal of the thesis is to investigate avenues for solving these issues, for instance by improving the transport of reactants and products in the cathode. It is noted experimentally that the reaction rate (1.1.5) is not uniform on the cathode CL(decreasing along the channel direction), see for instance [14] and [22], where this is remarkable for long air channel fuel cells. This leads to accumulation of heat in regions where the reaction rate is high, and accumulation of water where the reaction rate is low, see [22] where regions of water accumulation in cathode has been studied. Improving the performance of hydrogen fuel cells becomes a concern today for researchers. In [30], the current density is maximized by finding the optimal composition of membrane electrode assembly(MEA), that is, finding the optimal platinum loading, platinum to carbon ratio, electrolyte content and gas diffusion layer porosity. The optimal assembly for the cathode was done in [27] and [29], and for the anode in [28]. In [19], the goal was to maximize the current density with respect to operating conditions. In [32], the objective was find the optimal thickness of the cathode CL that maximizes the current density. In [10] and [11], the objective was to find the optimal cathode dimensions and optimal inlet pressure that maximize the

current density. In [16], finding an optimal geometry of the cathode air channels was considered to maximize the current density, by testing rectangular, triangular and hemispherical air channels. Only maximizing the current density is widely considered in the literature, while considering uniform current density as an objective is rarely seen though it is crucial, as explained above and for instance in [13]. However, in [26], results show an optimal cathode catalyst (platinum) loading that makes the current distribution even. Yet in this work, maximizing the current density is not considered.

This thesis combines three objectives through finding an optimal design of the cathode air channel: maximizing the current density, uniformizing the current density, and reducing the pressure drop along the gas channel.

1.2 Plan of the thesis

Chapter 2 is dedicated to the modeling of the cathode part of hydrogen fuel cells. It considers two models: a general model and simplified model. A shape optimization problem is defined to minimize an objective function representing the efficiency of hydrogen fuel cells.

Chapter 3 presents a mathematical analysis of the shape optimization problem. The first part is about finding the shape gradient of the cost functional defined in chapter 2. The second part investigates the shape differentiability of the variables involved, by which the cost functional is defined. Also, the shape differentiability of the cost functional is proved. The last part studies existence and uniqueness of an adjoint problem, which is used to calculate the shape gradient of the cost functional.

Chapter 4 presents the numerical methods used to solve the optimization problem.

In chapter 5, the simplified and general models are first compared. The simplified model is next validated with the model studied in [15]. The optimization problem is solved and discussed for both long and short air channels.

Chapter 2

Statement of Problems

2.1 Mathematical Modeling

The goal of this section is to present mathematical modeling background to explain the fluid dynamics taking place in the cathode part of hydrogen fuel cells. Of the cathode part, two main domains are considered: the air channel A and the gas diffusion layer G, see Figure 2.1.

In this figure, Γ_i is the channel inlet, Γ_o the channel outlet, Γ and Γ_w walls, M the catalytic interface between the GDL and the membrane, Σ the interface between A and G. In the thesis, M will be called the "membrane".

Air is delivered at Γ_i while some water vapor, nitrogen and oxygen gases exit at

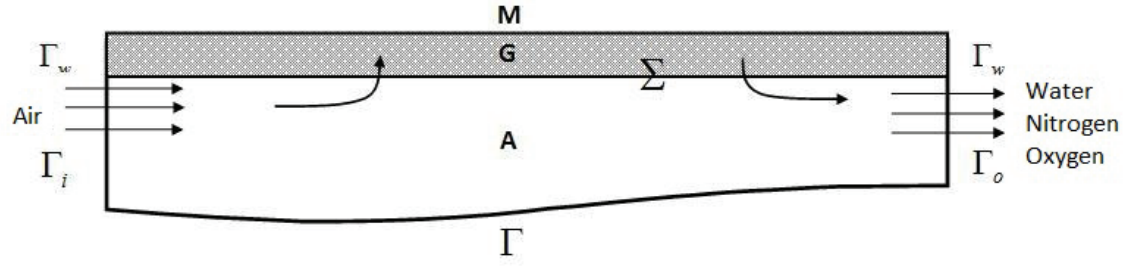

Figure 2.1: 2d cross-section of the cathode part of hydrogen fuel cells.

Γ_o.

Let $\hat{c}_o, \hat{c}_w$ and $\hat{c}_n$ denote the mass fractions of oxygen, water vapor and nitrogen, respectively, and ρ_o, ρ_w, ρ_n and ρ_g the densities of oxygen, water, nitrogen and the gas mixture, respectively. Let also $\hat{p}_g$ denote the pressure of the gas mixture and $\hat{\mathbf{u}}_g$ the velocity of the gas mixture.

The system is assumed to be in steady state, isothermal and has only gas phase.

Two models will be considered in this section. The first model, a general model, takes into account the variation of both the gas density and the dynamic viscosity due to change in the mass fractions of species. The second model, a simplified model, assumes the gas density, the dynamic viscosity and the nitrogen mass fraction to be constant. The later model improves the one presented in [21], a simplification of the model considered in [22]. In both models, a particular attention is given to the porosity of the domain G and specifying the reaction rate at the membrane as well as the dynamic viscosity of the gas mixture.

The assumptions of constant dynamic viscosity and constant gas density are clearly not valid due to high change of mass fractions.

Comparing the two models will serve for two benefits. The first benefit is to verify the assumptions taken in the simplified model. The second benefit is to consider the simplified model in the analysis part.

2.1.1 The General Model

In the general model, $\hat{c}_o, \hat{c}_n, \hat{c}_w, \hat{\mathbf{u}}_g, \hat{p}_g, \rho_g$ and μ are all variables.

The mixture density ρ_g is interpreted in terms of partial densities:

$$\rho_g = \rho_o + \rho_w + \rho_n, \tag{2.1.1}$$

and the mass fraction of each species is given by

$$\hat{c}_o = \frac{\rho_o}{\rho_g}, \quad \hat{c}_w = \frac{\rho_w}{\rho_g}, \quad \hat{c}_n = \frac{\rho_n}{\rho_g}. \tag{2.1.2}$$

Hence, (2.1.2) gives the total mass fraction

$$\hat{c}_o + \hat{c}_w + \hat{c}_n \;\; = \;\; 1. \tag{2.1.3}$$

Since no reaction happens in both domains A and G, the gas temperature T is assumed to be constant in $A \cup G$; see also [3] and [22], where the variation of temperature is small.

Assuming that the gases are ideal in both domains A and G, then their partial pressures are given by

$$\hat{p}_o = \frac{\rho_o RT}{M_o}, \quad \hat{p}_w = \frac{\rho_w RT}{M_w}, \quad \hat{p}_n = \frac{\rho_n RT}{M_n}, \tag{2.1.4}$$

where M_o, M_w and M_n are the molar masses of oxygen, water, and nitrogen, respectively, and R is the universal ideal gas constant.

The mixture pressure or the total pressure $\hat{p}_g$ is given by

$$\hat{p}_g \;\; = \;\; \hat{p}_o + \hat{p}_w + \hat{p}_n. \tag{2.1.5}$$

From (2.1.2), it follows that $\rho_o = \hat{c}_o \rho_g$, $\rho_w = \hat{c}_w \rho_g$ and $\rho_n = \hat{c}_n \rho_g$. Then using (2.1.3),(2.1.4) and (2.1.5) results in

$$\begin{aligned} \hat{p}_g &= \hat{p}_o + \hat{p}_w + \hat{p}_n \\ &= \rho_g RT \left(\frac{\hat{c}_o}{M_o} + \frac{1 - \hat{c}_o - \hat{c}_n}{M_w} + \frac{\hat{c}_n}{M_n} \right) \\ &= \frac{\rho_g RT}{M_w} \left(\beta_o \hat{c}_o + \beta_n \hat{c}_n + 1 \right), \end{aligned} \tag{2.1.6}$$

where $\beta_o = \frac{M_w}{M_o} - 1$ and $\beta_n = \frac{M_w}{M_n} - 1$.

Therefore, ρ_g is written as

$$\rho_g \;\; = \;\; \frac{M_w \hat{p}_g}{RT \left(\beta_o \hat{c}_o + \beta_n \hat{c}_n + 1 \right)}. \tag{2.1.7}$$

It also follows from the ideal gas law that

$$x_o = \frac{\hat{p}_o}{\hat{p}_g}, \quad x_n = \frac{\hat{p}_n}{\hat{p}_g}, \quad x_w = \frac{\hat{p}_w}{\hat{p}_g}. \tag{2.1.8}$$

Using (2.1.4), partial pressures in (2.1.8) are written in terms of the main variables:

$$x_o = \frac{RT\rho_g \hat{c}_o}{M_o \hat{p}_g}, \quad x_n = \frac{RT\rho_g \hat{c}_n}{M_n \hat{p}_g}, \quad x_w = \frac{RT\rho_g \hat{c}_w}{M_w \hat{p}_g}. \tag{2.1.9}$$

Dynamic Viscosity

The dynamic viscosity of the mixture , μ, is not constant in general as it is a function of the molar fractions of the species, see [33] and [35]. For this, let x_o, x_n and x_w denote the molar fractions of oxygen, nitrogen and water, respectively. Let also μ_{air} and μ_w be the dynamic viscosities of dry air and water, respectively, at the temperature T. Then according to [33], the dynamic viscosity of moist air or the mixture is well-approximated by

$$\mu \;=\; (\mu_{air} x_{air} + \mu_w x_w)\,(1 + x_{air} x_w / 2.75)\,, \tag{2.1.10}$$

where the molar fraction of air $x_{air} = x_o + x_n$ and x_w are obtained from (2.1.9). The dynamic viscosity of the gas mixture (2.1.10) depends on the temperature T. In our models presented below, the gas temperature T is chosen within the validity rage of this equation.

Relative Humidity

The system is assumed to be only in gas phase. To check the validity of this assumption, the so called "relative humidity", denoted by RH, is calculated.

Relative humidity measures the amount of water vapor in a mixture relative to that in the mixture saturated with water vapor. Let n_w denote the number of moles of water molecules in the mixture. Let also n_s be the total number of water moles in the saturated mixture. Then, the relative humidity is defined as

$$RH \;=\; \frac{n_w}{n_s}, \tag{2.1.11}$$

see [35]. From the ideal gas law, (2.1.11) is written as

$$RH = \frac{\hat{p}_w}{\hat{p}_s}, \tag{2.1.12}$$

where $\hat{p}_s$ is the pressure of water vapor at the saturation point. Also, $\hat{p}_s$ is approximated by a polynomial in terms of temperature, see [35].

Dry air means $RH = 0$ while saturated air with water means $RH = 1$. When the relative humidity of a system is greater than one, the system is called over-saturated, and a liquid phase exists. In the numerical results presented in Chapter 5, the relative humidity always remains below 1.

Fluid dynamics in the air channel

In the air channel, the system is governed by fluid dynamics laws: conservation of momentum and conservation of mass.

Conservation of momentum gives

$$\nabla \cdot \left[-\mu \left(\nabla \hat{\mathbf{u}}_g + \nabla \hat{\mathbf{u}}_g^T\right) + \hat{p}_g I\right] = 0 \ \ in \ \ A, \tag{2.1.13}$$

where μ is the dynamic viscosity of the flowing fluid. The first term of (2.1.13) represents the change of momentum due to shear stress and the second term the change of momentum due to pressure drop. Equation(2.1.13) is the Stokes equation for creeping flow [2].

Mass conservation of the mixture results in the continuity equation:

$$\frac{\partial \rho_g}{\partial t} + \nabla \cdot (\rho_g \hat{\mathbf{u}}_g) = 0 \ \ in \ \ A, \tag{2.1.14}$$

where t denotes the time. Since the system is assumed to be in steady state, (2.1.14) simplifies to

$$\nabla \cdot (\rho_g \hat{\mathbf{u}}_g) = 0 \ \ in \ \ A. \tag{2.1.15}$$

Equation (2.1.15) is the usual mass conservation equation for compressible fluids, see [2].

Let J_k be the diffusive mass flux of species k, and N_k denote the combined (diffusive and convective) mass flux of species k. Then from Fick's law [2], the combined mass flux of oxygen and nitrogen are given by

$$\begin{aligned} N_{\hat{c}_o} &= -D_o \rho_g \nabla \hat{c}_o + \rho_g \hat{\mathbf{u}}_g \hat{c}_o, \\ N_{\hat{c}_n} &= -D_n \rho_g \nabla \hat{c}_n + \rho_g \hat{\mathbf{u}}_g \hat{c}_n \quad in \quad A \end{aligned} \tag{2.1.16}$$

where D_o and D_n are the diffusivity constants for oxygen and nitrogen, respectively. The first term of the fluxes (2.1.16) represents the diffusive flux and the second term the convective flux. The mass conservation of oxygen and nitrogen results in

$$\begin{aligned} \nabla \cdot N_{\hat{c}_o} &= R_{\hat{c}_o}, \\ \nabla \cdot N_{\hat{c}_n} &= R_{\hat{c}_n} \quad in \quad A \end{aligned} \tag{2.1.17}$$

where $R_{\hat{c}_o}$ and $R_{\hat{c}_n}$ are the reaction rates for $\hat{c}_o$ and $\hat{c}_n$, respectively. Since the flow is non-reactive in A, $R_{\hat{c}_o} = R_{\hat{c}_n} = 0$. Using equation (2.1.15), it follows that

$$\begin{aligned} \nabla \cdot (\rho_g \hat{\mathbf{u}}_g \hat{c}_o) &= \rho_g \hat{\mathbf{u}}_g \cdot \nabla \hat{c}_o \\ \nabla \cdot (\rho_g \hat{\mathbf{u}}_g \hat{c}_n) &= \rho_g \hat{\mathbf{u}}_g \cdot \nabla \hat{c}_n \quad in \quad A. \end{aligned} \tag{2.1.18}$$

Then equations (2.1.17) reduce to

$$\begin{aligned} -\nabla \cdot (D_o \rho_g \nabla \hat{c}_o) + \rho_g \hat{\mathbf{u}}_g \cdot \nabla \hat{c}_o &= 0, \\ -\nabla \cdot (D_n \rho_g \nabla \hat{c}_n) + \rho_g \hat{\mathbf{u}}_g \cdot \nabla \hat{c}_n &= 0 \quad in \quad A. \end{aligned} \tag{2.1.19}$$

Therefore in the air channel, A, the following problem must be solved : Find $\hat{\mathbf{u}}_g$, $\hat{p}_g$, $\hat{c}_o$, $\hat{c}_n$ and ρ_g such that

$$\begin{aligned} \nabla \cdot \left[-\mu \left(\nabla \hat{\mathbf{u}}_g + \nabla \hat{\mathbf{u}}_g^T \right) + \hat{p}_g I \right] &= 0, \\ \nabla \cdot (\rho_g \hat{\mathbf{u}}_g) &= 0, \\ -\nabla \cdot (D_o \rho_g \nabla \hat{c}_o) + \rho_g \hat{\mathbf{u}}_g \cdot \nabla \hat{c}_o &= 0, \quad in \quad A \end{aligned} \tag{2.1.20}$$

$$\begin{aligned} -\nabla \cdot (D_n \rho_g \nabla \hat{c}_n) + \rho_g \hat{\mathbf{u}}_g \cdot \nabla \hat{c}_n &= 0, \\ \frac{M_w \hat{p}_g}{RT\left(\beta_o \hat{c}_o + \beta_n \hat{c}_n + 1\right)} &= \rho_g. \end{aligned}$$

Fluid dynamics in the gas diffusion layer

In the gas diffusion layer, the fluid dynamics of the system is modeled by Darcy's equation and conservation of mass.

Darcy's equation [2] models the gas velocity and the gas pressure in porous media:

$$\frac{\mu}{K}\hat{\mathbf{u}}_g + \nabla \hat{p}_g = 0 \quad in \quad G, \tag{2.1.21}$$

where K is the permeability of the porous medium. Here $\hat{\mathbf{u}}_g$ is the superficial velocity or the extrinsic velocity, which is the averaged velocity over the porous domain G. The pressure $\hat{p}$ is the intrinsic gas pressure.

Mass conservation of the mixture yields the continuity equation:

$$\frac{\partial \rho_g}{\partial t} + \nabla \cdot (\rho_g \hat{\mathbf{u}}_g) = 0 \quad in \quad G, \tag{2.1.22}$$

Since the system is assumed to be in steady state, equation (2.1.22) simplifies to

$$\nabla \cdot (\rho_g \hat{\mathbf{u}}_g) = 0 \quad in \quad G. \tag{2.1.23}$$

Like in the air channel, A, the mass conservation of oxygen and nitrogen gives

$$\begin{aligned} -\nabla \cdot (\varepsilon D_o^{eff} \rho_g \nabla \hat{c}_o) + \varepsilon \rho_g \hat{\mathbf{u}}_g \cdot \nabla \hat{c}_o &= 0, \\ -\nabla \cdot (\varepsilon D_n^{eff} \rho_g \nabla \hat{c}_n) + \varepsilon \rho_g \hat{\mathbf{u}}_g \cdot \nabla \hat{c}_n &= 0, \quad in \quad G \\ \frac{M_w \hat{p}_g}{RT\left(\beta_o \hat{c}_o + \beta_n \hat{c}_n + 1\right)} &= \rho_g, \end{aligned} \tag{2.1.24}$$

where ε is the porosity, the ratio of pore area (volume) to the total area (volume) of the domain G.

The diffusivity of each of oxygen and nitrogen, D_o^{eff} and D_n^{eff}, is the effective diffusivity which takes into account the effect of porosity of the domain G. In fact

for species i, the effective diffusivity $D_i^{eff} := \varepsilon^{1.5} D_i$, see [14]. Note also that $\hat{\mathbf{u}}_g$ is the fluid velocity obtained from (2.1.21) since the medium is porous.

In summary, the following problem has to be solved in the gas diffusion layer, G: Find $\hat{\mathbf{u}}_g$, $\hat{p}_g$, $\hat{c}_o$, $\hat{c}_n$ and ρ_g such that

$$\begin{aligned}
\frac{\mu}{K}\hat{\mathbf{u}}_g + \nabla \hat{p}_g &= 0, \\
\nabla \cdot (\rho_g \hat{\mathbf{u}}_g) &= 0, \\
-\nabla \cdot (\varepsilon D_o^{eff} \rho_g \nabla \hat{c}_o) + \varepsilon \rho_g \hat{\mathbf{u}}_g \cdot \nabla \hat{c}_o &= 0, \quad in \;\; G \\
-\nabla \cdot (\varepsilon D_n^{eff} \rho_g \nabla \hat{c}_n) + \varepsilon \rho_g \hat{\mathbf{u}}_g \cdot \nabla \hat{c}_n &= 0, \\
\frac{M_w \hat{p}_g}{RT\,(\beta_o \hat{c}_o + \beta_n \hat{c}_n + 1)} &= \rho_g.
\end{aligned} \tag{2.1.25}$$

Boundary Conditions

The above system of equations (2.1.20) and (2.1.25) are coupled with boundary conditions. These boundary conditions are introduced in [3], [15], [21] and [22].

On the channel inlet, Γ_i, the following boundary conditions are prescribed.

$$\hat{u}_2 = 0, \tag{2.1.26}$$

$$\int_{\Gamma_i} \hat{u}_1 = \phi, \tag{2.1.27}$$

$$-\mu \partial_1 \hat{u}_1 + \hat{p}_g = \frac{1}{|\Gamma_i|} \int_{\Gamma_i} \hat{p}_g = p_{in}, \tag{2.1.28}$$

$$\hat{c}_o = c_{o,in}, \tag{2.1.29}$$

$$\hat{c}_n = c_{n,in}, \tag{2.1.30}$$

where ϕ, $c_{o,in}$ and $c_{n,in}$ are given constants. Condition (2.1.26) implies that the tangential velocity component is zero, and condition (2.1.27) specifies the volumetric flow rate at the inlet. Condition (2.1.28) implies that the total stress tensor equals to the average pressure p_{in} on Γ_i, where p_{in} here is an unknown constant. Conditions

(2.1.29) and (2.1.30), respectively, mean that oxygen and nitrogen mass fractions are known at the channel inlet.

On the channel outlet, Γ_o, the following boundary conditions are considered.

$$\begin{aligned} \hat{u}_2 &= 0, && (2.1.31)\\ -\mu\partial_1\hat{u}_1 + \hat{p}_g &= p_{out}, && (2.1.32)\\ J_{\hat{c}_o}\cdot\nu &= 0, && (2.1.33)\\ J_{\hat{c}_n}\cdot\nu &= 0, && (2.1.34) \end{aligned}$$

where p_{out} is a given constant. Condition (2.1.31) is the same as on the channel inlet. Condition (2.1.32) specifies the total stress tensor. In conditions (2.1.33) and (2.1.34), the diffusive flux of oxygen and nitrogen are zero; or equivalently that oxygen and nitrogen mass fractions are constant along the x-direction near the outlet.

On the wall Γ, the boundary conditions are

$$\begin{aligned} \hat{u}_1 = \hat{u}_2 &= 0, && (2.1.35)\\ J_{\hat{c}_o}\cdot\nu &= 0, && (2.1.36)\\ J_{\hat{c}_n}\cdot\nu &= 0, && (2.1.37) \end{aligned}$$

where ν denotes the exterior normal vector to $\partial\Omega$, and $\Omega := A\cup G$. The first condition (2.1.35) specifies the usual no-slip velocity on a wall. Conditions (2.1.36) and (2.1.37) state that diffusive fluxes for oxygen and nitrogen are zero. Hence, with condition (2.1.35) the combined fluxes of oxygen and nitrogen are zero.

On the interface, Σ, it is assumed that

$$\begin{aligned} [\hat{u}_2] &= 0, && (2.1.38)\\ -\mu\partial_2\hat{u}_2 + \hat{p}_g &= \hat{p}_g(\cdot, 0^+), && (2.1.39)\\ \hat{u}_1(., 0^-) &= 0, && (2.1.40) \end{aligned}$$

$$[\hat{c}_o] = \left[\varepsilon D_o^{eff} \rho_g \partial_2 \hat{c}_o\right] = 0, \tag{2.1.41}$$

$$[\hat{c}_n] = \left[\varepsilon D_n^{eff} \rho_g \partial_2 \hat{c}_n\right] = 0, \tag{2.1.42}$$

$$[\rho_g] = 0, \tag{2.1.43}$$

where $[\cdot]$ denotes the jump across Σ, and $\hat{p}_g(x, 0^+) = lim_{y\to 0^+} \hat{p}_g(x, y)$, for every $x \in \Sigma$. In domain A, $\varepsilon = 1$ and $D^{eff} = D$. Conditions (2.1.38), (2.1.41) and (2.1.42) as well as (2.1.43) ensure that the diffusive and the convective fluxes of oxygen and nitrogen are continuous on Σ. Consequently, these are used to couple equations (2.1.19) and (2.1.24). Condition (2.1.39) implies that the total stress tensor equals to $\hat{p}|_{\Sigma_G}$. In condition (2.1.40), it is assumed that the gas in domain A does not slip along the interface Σ.

On the walls, Γ_w, the boundary conditions are

$$\hat{u}_1 = 0, \tag{2.1.44}$$

$$J_{\hat{c}_o} \cdot \nu = 0, \tag{2.1.45}$$

$$J_{\hat{c}_n} \cdot \nu = 0. \tag{2.1.46}$$

Conditions (2.1.45), (2.1.46) and (2.1.44) imply that the combined fluxes of oxygen and nitrogen are zero.

In the catalyst layer M, the following reaction takes place:

$$4H^+ + 4e^- + O_2 \longrightarrow 2H_2O + Heat. \tag{2.1.47}$$

This means that for every mole of oxygen consumed (or $\frac{1}{M_o} N_{\hat{c}_o} \cdot \nu$), there will be two moles of water vapor produced ($\frac{1}{M_w} N_{\hat{c}_w} \cdot \nu$). Hence

$$\frac{1}{M_o} N_{\hat{c}_o} \cdot \nu = -\frac{1}{2M_w} N_{\hat{c}_w} \cdot \nu. \tag{2.1.48}$$

In addition, the reaction (2.1.47) implies that for every mole of oxygen consumed (or $\frac{1}{M_o} N_{\hat{c}_o} \cdot \nu$), there will be four moles of electrons (or $4F$ of charges) used, where F is the Faraday constant. These electrons pass through an external circuit to generate

electricity. Let i denote the current density on M, which is the transport rate of electrons per unit area or the flux of electrons. Then the current density is related to the oxygen mass flux as follow

$$\begin{aligned} i &= (O_2 \; molar \; transport \; rate) \times 4F \\ &= \frac{4F}{M_o} N_{\hat{c}_o} \cdot \nu. \end{aligned} \tag{2.1.49}$$

Hence, the normal component of oxygen mass flux is then determined to be

$$N_{\hat{c}_o} \cdot \nu = \frac{M_o}{4F} i. \tag{2.1.50}$$

Also, due to consumption of oxygen and production of water vapor on M, the total mass is written as

$$\rho_g \hat{u}_2 = N_{\hat{c}_o} \cdot \nu + (1 + 2\alpha_m) N_{\hat{c}_w} \cdot \nu, \tag{2.1.51}$$

where the factor $2\alpha_m$ accounts for the water crossing the membrane from the anode side. Now using equations (2.1.48), (2.1.49), and (2.1.50), it follows that

$$\rho_g \hat{u}_2 = \frac{M_o}{4F} i - \frac{M_w}{2F} (1 + 2\alpha_m) i. \tag{2.1.52}$$

The nitrogen mass flux is assumed to be zero, which means that the nitrogen gas cannot cross the membrane:

$$N_{\hat{c}_n} \cdot \nu = 0. \tag{2.1.53}$$

To find the current density i, the Butler-Volmer equation is used

$$i = i_0 \left(\frac{\hat{c}_o}{\hat{c}_{o,ref}} \right) \left[exp\left(\frac{\alpha_c F}{RT} \eta \right) - exp\left(-\frac{\alpha_c F}{RT} \eta \right) \right], \tag{2.1.54}$$

where i_0 is the exchange current density, $\hat{c}_{o,ref}$ oxygen reference mass fraction, and α_c the cathode side transfer coefficient, which are all fixed parameters, see [15].

Finally, the variable η, which is the catalyst layer activation over-potential, satisfies the cell voltage formula:

$$E_{cell} = E_{rev} - \eta - r I_{av}, \tag{2.1.55}$$

where E_{cell} is the cell voltage, E_{rev} the reversible cell voltage, r the ohmic resistance of the cell, and I_{av} is the averaged current density on M:

$$I_{av} = \frac{1}{|M|}\int_M i(x)dx. \tag{2.1.56}$$

Then the boundary conditions considered on M are

$$\begin{aligned} N_{\hat{c}_o}\cdot\nu &= \frac{M_o}{4F}i, \\ N_{\hat{c}_w}\cdot\nu &= -\left(1+2\alpha_m\right)\frac{M_w}{2F}i, \\ N_{\hat{c}_n}\cdot\nu &= 0, \\ \rho_g\hat{u}_2 &= \frac{M_o}{4F}i-\left(1+2\alpha_m\right)\frac{M_w}{2F}i, \end{aligned} \tag{2.1.57}$$

where i is determined by the following equations

$$\begin{aligned} i &= i_0\left(\frac{\hat{c}_o}{\hat{c}_{o,ref}}\right)\left[exp\left(\frac{\alpha_c F}{RT}\eta\right)-exp\left(-\frac{\alpha_c F}{RT}\eta\right)\right], \\ E_{cell} &= E_{rev}-\eta-rI_{av}. \end{aligned} \tag{2.1.58}$$

Then the above boundary conditions are summarized below.

$$\begin{aligned} &\Gamma_i: && \hat{c}_o-c_{o,in}=\hat{c}_n-c_{n,in} &&= \phi-\textstyle\int_{\Gamma_i}\hat{u}_1=\hat{u}_2=-\mu\partial_1\hat{u}_1+\hat{p}_g-p_{in}=0, \\ &\Gamma: && N_{\hat{c}_o}\cdot\nu=N_{\hat{c}_n}\cdot\nu &&= \hat{u}_1=\hat{u}_2=0, \\ &\Gamma_o: && J_{\hat{c}_o}\cdot\nu=J_{\hat{c}_n}\cdot\nu &&= \hat{u}_2=-\mu\partial_1\hat{u}_1+\hat{p}_g-p_{out}=0, \\ &\Sigma: && [\hat{c}_o]=[N_{\hat{c}_o}\cdot\nu]=[\hat{c}_n]=[N_{\hat{c}_n}\cdot\nu] &&= \hat{u}_1\left(.,0^-\right)=[\hat{u}_2]=-\mu\partial_2\hat{u}_2+\hat{p}_g-\hat{p}(\cdot,0^+)=0, \\ &\Gamma_w: && N_{\hat{c}_o}\cdot\nu=N_{\hat{c}_n}\cdot\nu &&= \hat{u}_1=0, \\ &M: && N_{\hat{c}_o}\cdot\nu-\tfrac{M_o}{4F}i=N_{\hat{c}_n}\cdot\nu &&= \rho_g\hat{u}_2-\left(\tfrac{M_o}{4F}-\left(1+2\alpha_m\right)\tfrac{M_w}{2F}\right)i=0, \end{aligned} \tag{2.1.59}$$

where $K, \phi, c_{o,in}, c_{n,in}, p_{out}$ are given constants, while p_{in} is an unknown constant.

In the following remark, the oxygen mass flux is written in terms of the oxygen mass fraction, $\hat{c}_o$. This remark will be used in Chapter 3 to calculate shape derivatives; in particular, it clarifies notations used there.

Remark 2.1.1 Let H_m denote the consumption rate of oxygen on the membrane, M. Then using the first equation of (2.1.57) gives

$$N_{\hat{c}_o} \cdot \nu = H_m \hat{c}_o = \frac{M_o}{4F} i, \tag{2.1.60}$$

where it follows from the first equation of (2.1.58) that

$$H_m = \frac{M_o i_0}{4F \hat{c}_{o,ref}} \left[exp\left(\frac{\alpha_c F}{RT}\eta\right) - exp\left(-\frac{\alpha_c F}{RT}\eta\right)\right]. \tag{2.1.61}$$

Also, from the last equation of (2.1.57), it follows that

$$\begin{aligned} \varepsilon \rho_g \hat{u}_2 &= -\varepsilon \left[\frac{M_w}{2F}(1+2\alpha_m) - \frac{M_o}{4F}\right] \frac{4F}{M_o} H_m \hat{c}_o \\ &= -\varepsilon \left(\frac{2M_w}{M_o}(1+2\alpha_m) - 1\right) H_m \hat{c}_o. \end{aligned} \tag{2.1.62}$$

Set

$$\beta_m = \varepsilon \left(\frac{2M_w}{M_o}(1+2\alpha_m) - 1\right), \tag{2.1.63}$$

which is a positive quantity as $\frac{2M_w}{M_o} > 1$. Then,

$$\varepsilon \rho_g \hat{u}_2 = -\beta_m H_m \hat{c}_o. \tag{2.1.64}$$

Since

$$N_{\hat{c}_o} \cdot \nu = -\varepsilon \rho_g D^{eff} \partial_\nu \hat{c}_o + \varepsilon \rho_g \hat{\mathbf{u}} \hat{c}_o \cdot \nu, \tag{2.1.65}$$

it follows from (2.1.60) and (2.1.64) that the normal component of the diffusive flux on the membrane is given by

$$-\varepsilon \rho_g D^{eff} \partial_\nu \hat{c}_o = H_m \left(1 + \beta_m \hat{c}_o\right) \hat{c}_o. \tag{2.1.66}$$

2.1.2 The Simplified Model

In the simplified model, the gas density and nitrogen mass fraction are assumed to be constant. The general model: equations (2.1.20) and (2.1.25) are simplified after dividing by ρ_g. Then the following problem has to be solved: Find $\hat{\mathbf{u}}_g$, $\hat{p}_g$, $\hat{c}_o$ such that

$$\begin{aligned} -\nabla \cdot (D_o \nabla \hat{c}_o) + \hat{\mathbf{u}}_g \cdot \nabla \hat{c}_o &= 0, \\ -\mu \Delta \hat{\mathbf{u}}_g + \nabla \hat{p}_g &= 0, \\ \nabla \cdot \hat{\mathbf{u}}_g &= 0 \end{aligned} \tag{2.1.67}$$

in A, and

$$\begin{aligned} -\nabla \cdot \left(\varepsilon D_o^{eff} \nabla \hat{c}_o\right) + \varepsilon \hat{\mathbf{u}}_g \cdot \nabla \hat{c}_o &= 0, \\ \frac{\mu}{K} \hat{\mathbf{u}}_g + \nabla \hat{p}_g &= 0, \\ \nabla \cdot \hat{\mathbf{u}}_g &= 0 \end{aligned} \tag{2.1.68}$$

in G.

The above system of equations are grouped, and the problem is to find $\hat{\mathbf{u}}_g$, $\hat{p}_g$, $\hat{c}_o$ such that

$$-\nabla \cdot \left(\varepsilon D_o^{eff} \nabla \hat{c}_o\right) + \varepsilon \hat{\mathbf{u}}_g \cdot \nabla \hat{c}_o = 0 \quad in \ \Omega, \tag{2.1.69}$$

$$\left(-\mu \Delta \hat{\mathbf{u}}_g + \nabla \hat{p}_g\right) \chi(A) + \left(\frac{\mu}{K} \hat{\mathbf{u}}_g + \nabla \hat{p}_g\right) \chi(G) = 0 \quad in \ A \cup G, \tag{2.1.70}$$

$$\nabla \cdot \hat{\mathbf{u}}_g = 0 \quad in \ A \cup G, \tag{2.1.71}$$

coupled with the same boundary conditions (2.1.59). Here $\chi(.)$ denotes the characteristic function, and $\varepsilon = 1$ in A.

2.2 Optimization Problem

Based on experimental observations [13],[19] and [26], hydrogen fuel cells are made more efficient under the following conditions.

First, the current density i must be uniformly distributed on the membrane M. This makes the reaction of oxygen and hydrogen molecules occur uniformly at the same rate on the entire membrane. In addition, having this uniform distribution takes advantage of the cathode platinum catalyst layer, which is the most expensive part in the fuel cell. But the current density (2.1.50) is proportional to the normal component of the oxygen mass flux. Therefore, minimizing the total variance of the current density or that of the normal component of the oxygen mass flux are the same. Hence, the integral

$$\int_M \left(N_{\hat{c}_o} \cdot \nu - \frac{1}{|M|} \int_M N_{\hat{c}_o} \cdot \nu \right)^2, \tag{2.2.1}$$

must be minimized.

Second, the current density should be maximized as well on the membrane in order to increase the production of electricity. This is achieved when the normal component of the oxygen mass flux is maximized on the membrane. Then,

$$\int_M N_{\hat{c}_o} \cdot \nu, \tag{2.2.2}$$

must be maximized. Note also that maximizing the oxygen mass transport towards the membrane usually decreases the amount of oxygen reaching the channel outlet. This makes a maximum benefit of the oxygen gas delivered at the channel inlet.

Third, the pressure drop between the inlet and the outlet,

$$p_{in} - p_{out}, \tag{2.2.3}$$

must be minimized. This leads to a lower operating cost for the fuel cell. This term is proportional to the energy that is drawn from the fuel cell to maintain a flow through the gas channel, for instance with a compressor that is attached to the fuel cell.

Now, taking a weighted average of the above functionals leads to the following cost functional $E(\Gamma)$,

$$E(\Gamma) := \frac{1}{2}a\int_M \left(N_{\hat{c}_o}\cdot\nu - \frac{1}{|M|}\int_M N_{\hat{c}_o}\cdot\nu\right)^2 - b\int_M N_{\hat{c}_o}\cdot\nu + e\left(p_{in}-p_{out}\right), \quad (2.2.4)$$

where Γ is the design parameter controlling the shape of the air channel, A, and a, b, and e are some given nonnegative parameters. The coefficients (a, b, and e) should come with proper units for $E(\Gamma)$ to be non-dimensional if the variables in each term are dimensional.

The optimal shape of the wall of the air channel, Γ_*, is defined to be the solution of the following problem: Find $\Gamma_* \in C^2(\mathbb{R})$ such that

$$\Gamma_* \;=\; arg\ min_{\Gamma\in C^2(\mathbb{R})}\ E(\Gamma), \quad (2.2.5)$$

subjected to the state equations (2.1.69)-(2.1.71) and (2.1.59).

Remark 2.2.1 The regularity of Γ is needed to show the shape differentiability of the cost functional $E(\Gamma)$ as well as the state variables.

Chapter 3

Mathematical Analysis

The goal of this chapter is to discuss some mathematical analysis issues related to the optimization problem introduced in Section 2.2. To recall, our optimization problem is to find an optimal shape Γ, see Figure 2.1, minimizing a cost functional $E = E(\Gamma, W(\Gamma))$, where $W(\Gamma)$ denotes steady state variables, which satisfies a system of equations represented by $F(\Gamma, W(\Gamma)) = \mathbf{0}$. Therefore, our problem reads:

$$min_{\Gamma} \qquad E(\Gamma, W(\Gamma)), \tag{3.0.1}$$

$$subject\ \ to \qquad F(\Gamma, W(\Gamma)) = \mathbf{0}. \tag{3.0.2}$$

To solve this problem, we need to differentiate E with respect to Γ:

$$\frac{dE}{d\Gamma} \;=\; \frac{\partial E}{\partial \Gamma} + \frac{\partial E}{\partial W}\frac{dW}{d\Gamma}, \tag{3.0.3}$$

where $\frac{dW}{d\Gamma}$ is taken as a new variable. However, differentiating the state equation (3.0.2) with respect to Γ gives an equation for the variable $\frac{dW}{d\Gamma}$:

$$\frac{\partial F}{\partial \Gamma} + \frac{\partial F}{\partial W}\frac{dW}{d\Gamma} \;=\; 0. \tag{3.0.4}$$

To derive equations (3.0.3) and (3.0.4), some background in differentiation with respect to domains is presented in the first section of this chapter. This will help to calculate derivatives with respect to Γ, which appear in the above equations (3.0.3)

and (3.0.4). In the second section, the gradient of E is calculated using an adjoint problem. Existence of the shape derivative of the state variable, $\frac{dW}{d\Gamma}$, will be discussed in the third section. Finally, existence and uniqueness of the adjoint problem will be proved.

In the course of this chapter, the domains A, G, and $\Omega = A \cup G$ as well as their boundaries refer to the ones given in Figure 2.1, unless otherwise stated. These domains are open sets of $\mathbb{R}^2$ with Lipchitz boundaries. Also, ν_A, ν_G and ν denote the exterior unit normal vectors to A, G and Ω, respectively.

3.1 Some Background in Shape Calculus

This section presents some background in shape calculus, that will be needed in this chapter. The notations and proofs of this section are found in [31]. For comprehensive and self-contained details in this subject, we refer the reader to [5].

Let Ω be a bounded open set of $\mathbb{R}^n$ with a regular boundary $\partial\Omega$. Let also ζ be a regular vector field defined on $\mathbb{R}^n$. Then a variable set Ω_ζ, parametrized by ζ, is defined as follows

$$\Omega_\zeta \;:=\; \{x_\zeta = x + \zeta(x), x \in \Omega\}\,. \tag{3.1.1}$$

Let $u(\zeta)$ be a real-valued function depending on Ω_ζ, and defined on Ω_ζ. Then,

$$u(\zeta)(x_\zeta) \;:=\; u(\zeta, x_\zeta), \quad x_\zeta \in \Omega_\zeta. \tag{3.1.2}$$

The above equation can be considered in the fixed domain Ω using the change of variables $x_\zeta = (I + \zeta)(x)$, where I is the identity vector field on $\mathbb{R}^n$:

$$u(\zeta) \circ (I + \zeta)(x) \;:=\; u(\zeta, (I + \zeta)(x)), \quad x \in \Omega. \tag{3.1.3}$$

Note that $u(0)$ is defined on the fixed domain $\Omega_0 = \Omega$.

The function $u(\zeta)$ either solves an equation (a PDE system, for instance), or is involved in a cost functional that needs to be minimized or maximized. The goal of this section is to present the main results to calculate derivatives with respect to ζ of equations and cost functionals involving $u(\zeta)$.

First, let us introduce a diffeomorphism space, C_k, that is used to map the fixed domain Ω to the transformed domain Ω_ζ, as given above.

Definition 3.1.1 *Let $k \geq 1$, where k is an integer. Then a diffeomorphism space C_k on $\mathbb{R}^n$ is defined as follows:*

$$C_k = \left\{ \zeta = (\zeta_1, \zeta_2, ..., \zeta_n) \mid \ D^\alpha \zeta_i \in C_0^b(\mathbb{R}^n),\ i \leq n,\ |\alpha| \leq k \right\}, \tag{3.1.4}$$

where C_0^b denotes the space of bounded, continuous functions with compact support on $\mathbb{R}^n$. This space is equipped with the norm

$$\|\zeta\|_k = \sup \left\{ \left| D^\alpha \zeta(x) \right|, x \in \mathbb{R}^n, 0 \leq |\alpha| \leq k \right\}. \tag{3.1.5}$$

The following lemma shows the differentiability of the Jacobian function, $Jac(I+\zeta)$. This lemma will be used to change the variable x_ζ to x.

Lemma 3.1.2 *Denote*

$$Jac(I+\zeta) = \left| \det \left(\frac{\partial (I+\zeta)_i}{\partial x_j} \right) \right|. \tag{3.1.6}$$

Then the map $\zeta \to Jac(I+\zeta)$ is differentiable at $\zeta = 0$ from C_k into $C^{k-1}(\mathbb{R}^n)$, and for every $\xi \in C_k$, its derivative in the direction ξ is equal to

$$\frac{\partial Jac(I+\zeta)}{\partial \zeta}(0)\,\xi = div(\xi). \tag{3.1.7}$$

Lemma 3.1.3 *Let*

$$[\nabla(I+\zeta)] = \left[\frac{\partial(I+\zeta)_i}{\partial x_j}\right] \tag{3.1.8}$$

denote the matrix derivative of the map $I+\zeta$ *of* $\mathbb{R}^n$ *and* $[\nabla(I+\zeta)]^{-T}$ *be the transposed inverse matrix. Then the function* $\zeta \to [\nabla(I+\zeta)]^{-T}$ *is differentiable at* $\zeta = \mathbf{0}$ *from* C_k *into* $(C_{k-1})^n$*, and for every* $\xi \in C_k$*, its derivative in the direction* ξ *is equal to*

$$\frac{\partial\left[\nabla(I+\zeta)\right]^{-T}}{\partial\zeta}(0)\,\xi = -\left[\nabla\xi\right]^T. \tag{3.1.9}$$

The following remark gives a relation between the gradient operators ∇_{x_ζ} and ∇_x, which is needed to change variables.

Remark 3.1.4 For every $f \in W^{1,1}(\mathbb{R}^n)$ and $\zeta \in C_k$ small enough, it follows that

$$\left(\nabla_{x_\zeta} f\right) \circ (I+\zeta) = \left[\nabla(I+\zeta)\right]^{-T} \nabla_x \left(f \circ (I+\zeta)\right). \tag{3.1.10}$$

3.1.1 Differentiation of $\zeta \to f \circ (I+\zeta)$ and $\zeta \to f(\zeta) \circ (I+\zeta)$

Let f be a function on $\mathbb{R}^n$, which does not depend on ζ, and $I+\zeta$ be a diffeomorphism on $\mathbb{R}^n$. Then $f \circ (I+\zeta)$ is a function on $\mathbb{R}^n$.

Lemma 3.1.5 *Let* $f \in H^1(\mathbb{R}^n)$*. Then the map* $\zeta \to f \circ (I+\zeta)$ *is differentiable at* $\zeta = 0$ *from* C_k *into* $L^2(\mathbb{R}^n)$ *and , for every* $\xi \in C_k$*, its derivative at* $\zeta = \mathbf{0}$ *in the direction* ξ *is equal to*

$$\frac{\partial f \circ (I+\zeta)}{\partial\zeta}(0)\,\xi = \xi \cdot \nabla f. \tag{3.1.11}$$

Now, the above lemma is extended by considering $f(\zeta)$, a function of ζ.

Lemma 3.1.6 *Let* $f(\zeta) \in H^1(\mathbb{R}^n)$*, and suppose that* $\zeta \to f(\zeta) \circ (I+\zeta)$ *is differentiable at* $\zeta = 0$ *from* C_k *into* $H^1(\mathbb{R}^n)$*. Then* $\zeta \to f(\zeta)$ *is differentiable at* $\zeta = 0$

from C_k *into* $L^2(\mathbb{R})$ *and , for every* $\xi \in C_k$, *its derivative in the direction* ξ *is equal to*

$$\frac{\partial f(\zeta)}{\partial \zeta}(0)\,\xi = \frac{\partial f(\zeta) \circ (I+\zeta)}{\partial \zeta}(0)\,\xi - \xi \cdot \nabla f(0). \tag{3.1.12}$$

3.1.2 Local differentiation

For every $\zeta \in C_k$ small enough, let Ω_ζ and $u(\zeta)$ be defined as in (3.1.1) and (3.1.2), respectively, and $u(\zeta) \in H^1(\Omega_\zeta)$. Note first that for $x \in \Omega$, the directional derivative

$$\frac{\partial u(\zeta)}{\partial \zeta}(\mathbf{0})(x)\xi \;\; = \;\; lim_{t \longrightarrow 0} \frac{u(t\xi)(x) - u(\mathbf{0})(x)}{t} \tag{3.1.13}$$

is not defined in general as $x \in \Omega$ may not belong to the domain of definition of $u(t\xi)$. Therefore, this directional derivative must be defined locally.

For $x \in \Omega$, let Ω' be an open set such that $x \in \Omega'$, and $\Omega' \subset\subset \Omega$, meaning that Ω' is strictly included in Ω and $\overline{\Omega'} \subset \Omega$. Then, $u(\zeta)|_{\Omega'}$ is defined for small ζ as $\Omega' \subset\subset (I+\zeta)(\Omega)$. Hence the differentiation of $\zeta \to u(\zeta)|_{\Omega'}$ at $\zeta = 0$ has a meaning.

Definition 3.1.7 *The map* $\zeta \to u(\zeta)$ *is said to be differentiable into* $W^{m,r}_{loc}(\Omega)$, *or locally differentiable, if the map* $\zeta \to u(\zeta)|_{\Omega'}$ *is differentiable from* C_k *into* $W^{m,r}(\Omega')$ *for every* $\Omega' \subset\subset \Omega$. *Also, its local derivative* $\frac{\partial u(\zeta)}{\partial \zeta}(0)\,\xi$ *is defined in the whole domain* Ω, *for any direction* $\xi \in C_k$, *by*

$$\frac{\partial u(\zeta)}{\partial \zeta}(0)\,\xi = \frac{\partial u(\zeta)|_{\Omega'}}{\partial \zeta}(0)\,\xi, \tag{3.1.14}$$

for every $\Omega' \subset\subset \Omega$.

Lemma 3.1.8 *Let* $u(\zeta) \in H^1(\Omega_\zeta)$ *and* $\zeta \to u(\zeta) \circ (I+\zeta)$ *be differentiable at* $\zeta = 0$ *from* C_k *into* $H^1(\Omega_\zeta)$. *Then* $\zeta \to u(\zeta)$ *is differentiable at* $\zeta = 0$ *from* C_k *into* $L^2_{loc}(\Omega)$ *and , for every* $\xi \in C_k$, *its derivative in the direction* ξ *is equal to*

$$\frac{\partial u(\zeta)}{\partial \zeta}(0)\,\xi = \frac{\partial u(\zeta) \circ (I+\zeta)}{\partial \zeta}(0)\,\xi - \xi \cdot \nabla u(0).$$

Lemma 3.1.9 *Suppose that* $\partial\Omega$ *is a piecewise* C^1 *curve,* $u(\zeta) \in W^{1,1}(\Omega_\zeta)$ *and* $\zeta \to u(\zeta) \circ (I+\zeta)$ *is differentiable at* $\zeta = 0$ *from* C_k *into* $W^{1,1}(\Omega)$*. Assume also that* $u(\zeta) = 0$ *on* $\partial\Omega_\zeta$*, and that* $u(0) \in W^{2,1}(\Omega)$*. Then,* $\zeta \to u(\zeta)$ *is differentiable at* $\zeta = 0$ *from* C_k *into* $L^1_{loc}(\Omega)$ *and , for every* $\xi \in C_k$*, its derivative at* $\zeta = 0$ *in the direction* ξ *satisfies* $\frac{\partial u(\zeta)}{\partial \zeta}(0)\,\xi \in W^{1,1}(\Omega)$ *, and*

$$\frac{\partial u(\zeta)}{\partial \zeta}(0)\,\xi = -(\xi \cdot \nu)\,\partial_\nu u(0) \qquad on \quad \partial\Omega, \tag{3.1.15}$$

where ν *denotes the outward unit normal vector to* $\partial\Omega$*.*

3.1.3 Differentiation of cost functionals defined through an integral form over Ω_ζ or $\partial\Omega_\zeta$

Consider a function $u(\zeta) \in H^1(\Omega_\zeta)$ and the cost functionals $J(\zeta)$ and $K(\zeta)$ given by

$$J(\zeta) = \int_{\Omega_\zeta} C(u(\zeta)), \tag{3.1.16}$$

$$K(\zeta) = \int_{\partial\Omega_\zeta} G(u(\zeta)) \tag{3.1.17}$$

where C and G are partial differential operators given in $\mathbb{R}^n$. For the problem to make sense, we assume, for ζ small enough, that the operators C and G map $H^1(\Omega_\zeta)$ into $L^1(\Omega_\zeta)$ and $W^{1,1}(\Omega_\zeta)$, respectively. We also assume, for ζ small enough, that C and G are differentiable from $L^2(\Omega_\zeta)$ into $\mathcal{D}'(\Omega_\zeta)$. In other words, C is differentiable if $v \to (C(v), \varphi)$ is differentiable for every $\varphi \in \mathcal{D}(\Omega_\zeta)$.

Let us assume that $\zeta \to u(\zeta) \circ (I+\zeta)$ is differentiable at $\zeta = 0$ from C_k into $H^1(\Omega)$. Then by lemma 3.1.8, $\zeta \to u(\zeta)$ is differentiable at $\zeta = 0$ from C_k into $L^2_{loc}(\Omega)$ and , for every $\xi \in C_k$, its derivative at $\zeta = 0$ in the direction ξ is equal to

$$u' := \frac{\partial u(\zeta)}{\partial \zeta}(0) \quad in \quad \in L^2(\Omega). \tag{3.1.18}$$

Moreover, we have the following results.

Theorem 3.1.10 *Suppose, for ζ small enough, that $u(\zeta) \in H^1(\Omega_\zeta)$, $\zeta \to u(\zeta) \circ (I+\zeta)$ is differentiable at $\zeta = 0$ from C_k into $H^1(\Omega)$, C is differentiable from $L^2(\Omega_\zeta)$ into $\mathcal{D}'(\Omega_\zeta)$, $\zeta \to C(u(\zeta)) \circ (I+\zeta)$ is differentiable at $\zeta = 0$ from C_k into $L^1(\Omega)$, and $C(u(0)) \in W^{1,1}(\Omega)$. Then, $\zeta \to J(\zeta)$ is differentiable at $\zeta = 0$ from C_k into $\mathbb{R}$, and its derivative at $\zeta = 0$ in the direction ξ is equal to*

$$\frac{dJ(0)}{d\zeta}\xi = \int_\Omega \frac{\partial C(u(\mathbf{0}))}{\partial u}u' + \int_{\partial\Omega} (\xi \cdot \nu)\ C(u(0)). \tag{3.1.19}$$

Definition 3.1.11 *For every $x \in \partial\Omega$, let $\{\tau_j\}_{j=1}^{n-1}$ be an orthonormal system spanning the tangent plane to $\partial\Omega$ at x. Then the tangential divergence of $\mathbf{v} \in (C^1(\partial\Omega))^n$ is defined to be*

$$div_{\partial\Omega}(\mathbf{v})(x) \ := \ \Sigma_{j=1}^{n-1}\tau_j \cdot \partial_{\tau_j}\tilde{\mathbf{v}}(x) \ \ on \ \ \partial\Omega, \tag{3.1.20}$$

where $\tilde{\mathbf{v}} \in (C^1(\mathbb{R}^n))^n$ extends $\mathbf{v}$.

Theorem 3.1.12 *Let $\partial\Omega$ be a C^2 curve and Ω locally on one side of $\partial\Omega$. Suppose, for ζ small enough, that $u(\zeta) \in H^1(\Omega_\zeta)$, $\zeta \to u(\zeta) \circ (I+\zeta)$ is differentiable at $\zeta = 0$ from C_k into $H^1(\Omega)$, G is differentiable from $L^2(\Omega_\zeta)$ into $\mathcal{D}'(\Omega_\zeta)$, $\zeta \to G(u(\zeta)) \circ (I+\zeta)$ is differentiable at $\zeta = 0$ from C_k into $W^{1,1}(\Omega)$, and $G(u(0)) \in W^{2,1}(\Omega)$. Then, $\zeta \to K(\zeta)$ is differentiable at $\zeta = 0$ from C_k into $\mathbb{R}$, and its derivative at $\zeta = 0$ in the direction ξ is equal to*

$$\frac{dK(0)}{d\zeta}\xi \ = \ \int_{\partial\Omega}\left[\frac{\partial G(u(\mathbf{0}))}{\partial u}u' + (\xi \cdot \nu)\,\partial_\nu G(u(0)) + div_{\partial\Omega}(\xi G(u(0))\right], \tag{3.1.21}$$

where $div_{\partial\Omega}$ is defined above.

3.2 Derivative of the Cost Functional, E

To solve the optimization problem (2.2.5), the steepest gradient method is used to find a minimizer, Γ_*. For this, the shape gradient of the cost functional E is needed, where

$$E(\zeta) := \frac{1}{2}\alpha \int_M \left(N_{\hat{c}_o} \cdot \nu - \frac{1}{|M|} \int_M N_{\hat{c}_o} \cdot \nu \right)^2 - \beta \int_M N_{\hat{c}_o} \cdot \nu + \sigma \left(p_{in}(\zeta) - p_{out} \right), \quad (3.2.1)$$

where ζ is the parameter controlling the shape of the air channel A, and α, β and σ are some given nonnegative parameters.

From the boundary conditions (2.1.57) and (2.1.58), $N_{\hat{c}_o} \cdot \nu$ is written as

$$N_{\hat{c}_o} \cdot \nu = H_m(\eta)\hat{c}_o, \quad (3.2.2)$$

where

$$H_m(\eta) = \frac{M_o i_o}{4F\hat{c}_{o,ref}} \left[exp\left(\frac{\alpha_c F}{RT}\eta \right) - exp\left(-\frac{\alpha_c F}{RT}\eta \right) \right], \quad (3.2.3)$$

and η is a function of ζ:

$$\eta(\zeta) = E_{rev} - E_{cell} - rI_{av}. \quad (3.2.4)$$

Hence, $N_{\hat{c}_o} \cdot \nu$ contains both factors, $H_m(\eta)$ and $\hat{c}_o$, each depending on ζ.

Remark 3.2.1 From (3.2.3), H_m depends only on the overpotential η, which from the simple model in (3.2.4) is constant over M. This implies that H_m can be moved in and out of any integral. This will be used below.

Definition 3.2.2 *Let*

$$E_1 := \frac{1}{2} \int_M \left(H_m \hat{c}_o - \frac{1}{|M|} \int_M H_m \hat{c}_o \right)^2, \quad (3.2.5)$$

$$E_2 := \int_M H_m \hat{c}_o, \quad (3.2.6)$$

where H_m is a positive constant for every ζ, and

$$E(\zeta) \;=\; \alpha E_1(\zeta) - \beta E_2(\zeta) + \sigma\left(p_{in}(\zeta) - p_{out}\right). \tag{3.2.7}$$

As defined in the previous section $\Gamma_\xi = (I+\xi)(\Gamma)$, where $\xi \in C^2(\mathbb{R}^2;\mathbb{R}^2)$. The vector ξ is chosen such that each point of Γ is perturbed vertically, that is $\xi = (\xi_1, \xi_2) = (0, \xi_2)$. The space of perturbation, V, is defined as follows.

Definition 3.2.3 *Let $\xi \in V$,*

$$V \;:=\; C^2\left(\mathbb{R}^2;\mathbb{R}^2\right) \cap \left\{(0,\zeta_2)\,, \zeta_2 = \mathbf{0} \text{ on } \overline{G}\right\}. \tag{3.2.8}$$

Let also E' denotes the derivative of E at $\zeta = 0$ in a direction $\xi \in V$:

$$E' := E'(\mathbf{0})\xi = lim_{t\longrightarrow 0}\frac{E(t\xi) - E(\mathbf{0})}{t}$$

The notation $(.)'$ will only be used below for the directional derivative at $\zeta = \mathbf{0}$ in a direction $\xi \in V$.

The objective of the following lemmas is to first find the shape derivative of the cost functional E, and then to find the shape gradient of E using an adjoint system of differential equations.

Lemma 3.2.4 *The shape derivative of H_m at $\zeta = \mathbf{0}$ in the direction ξ is given by*

$$H'_m \;=\; -\frac{ri_o\alpha_c F}{\hat{c}_{o,ref}RT|M|}\left[exp\left(\frac{\alpha_c F}{RT}\eta\right) + exp\left(-\frac{\alpha_c F}{RT}\eta\right)\right]\left(\int_M H_m\hat{c}_o\right)'. \tag{3.2.9}$$

Proof:

Using Definition 3.2.3 and 3.2.4, it follows that

$$H'_m \;=\; \frac{\partial H_m}{\partial \eta}\frac{d\eta}{d\zeta}(\mathbf{0})\xi$$

$$= \frac{M_o i_o}{4F\hat{c}_{o,ref}} \frac{\alpha_c F}{RT} \left[exp\left(\frac{\alpha_c F}{RT}\eta\right) + exp\left(-\frac{\alpha_c F}{RT}\eta\right)\right] (-rI'_{av}), \quad (3.2.10)$$

where I'_{av} is given by

$$I'_{av} = \frac{4F}{M_o|M|}\left(\int_M H_m \hat{c}_o\right)'. \quad (3.2.11)$$

∎

Now let

$$B(\eta) := \frac{ri_o\alpha_c F}{\hat{c}_{o,ref}RT}\left[exp\left(\frac{\alpha_c F}{RT}\eta\right) + exp\left(-\frac{\alpha_c F}{RT}\eta\right)\right], \quad (3.2.12)$$

then $B(\eta)$ is always positive.

Lemma 3.2.5 *Using lemma 3.2.4, the shape derivative of E_2 at $\zeta = \mathbf{0}$ in the direction ξ is given by*

$$E'_2(\mathbf{0})\xi = \frac{H_m}{1 + \frac{B(\eta)}{|M|}\int_M \hat{c}_o} \int_M \hat{c}'_o. \quad (3.2.13)$$

Proof:

Multiplying equation (3.2.9) by $\hat{c}_o$ and integrating over M gives

$$\int_M H'_m \hat{c}_o = -\frac{B(\eta)}{|M|}\int_M \hat{c}_o \int_M (H'_m \hat{c}_o + H_m \hat{c}'_o), \quad (3.2.14)$$

which results in

$$\int_M H'_m \hat{c}_o = -\frac{B(\eta)\int_M \hat{c}_o}{|M| + B(\eta)\int_M \hat{c}_o}\int_M H_m \hat{c}'_o. \quad (3.2.15)$$

Hence using (3.2.15) gives

$$\begin{aligned}\left(\int_M H_m\hat{c}_o\right)' &= \int_M H_m'\hat{c}_o + \int_M H_m\hat{c}_o' \\ &= \frac{H_m}{1+\frac{B(\eta)}{|M|}\int_M \hat{c}_o}\int_M \hat{c}_o'. \end{aligned} \tag{3.2.16}$$

∎

Lemma 3.2.6 *The shape derivative of E_1 at $\zeta = \mathbf{0}$ in the direction ξ is given by*

$$E_1'(\mathbf{0})\xi = \int_M \left[\frac{-2B(\eta)E_1}{|M|+B(\eta)\int_M \hat{c}_o} + \alpha H_m^2\left(\hat{c}_o - \frac{1}{|M|}\int_M \hat{c}_o\right)\right]\hat{c}_o'. \tag{3.2.17}$$

Proof:

For this, note that

$$\begin{aligned}E_1'(\mathbf{0})\xi &= H_m H_m'\int_M \left(\hat{c}_o - \frac{1}{|M|}\int_M \hat{c}_o\right)^2 \\ &\quad + H_m^2\int_M \left[\left(\hat{c} - \frac{1}{|M|}\int_M \hat{c}\right)\left(\hat{c}' - \frac{1}{|M|}\int_M \hat{c}'\right)\right]. \end{aligned} \tag{3.2.18}$$

The first term in (3.2.18) is simplified using lemma 3.2.4 and lemma 3.2.5 since

$$\begin{aligned}H_m' &= -\frac{B(\eta)}{|M|}E_2'(\mathbf{0})\xi \\ &= -\frac{H_m B(\eta)}{|M|+B(\eta)\int_M \hat{c}_o}\int_M \hat{c}_o'. \end{aligned} \tag{3.2.19}$$

For the second term in equation (3.2.18), note that

$$\begin{aligned}&\int_M \left[\left(\hat{c}_o - \frac{1}{|M|}\int_M \hat{c}_o\right)\left(\hat{c}_o' - \frac{1}{|M|}\int_M \hat{c}_o'\right)\right] \\ &= \left(\int_M \hat{c}_o\hat{c}_o' - \frac{2}{|M|}\int_M \hat{c}_o\int_M \hat{c}_o' + \frac{1}{|M|}\int_M \hat{c}_o\int_M \hat{c}_o'\right) \\ &= \int_M \left(\hat{c}_o - \frac{1}{|M|}\int_M \hat{c}_o\right)\hat{c}_o'. \end{aligned} \tag{3.2.20}$$

Hence, equations (3.2.19) and (3.2.20) give the result. ∎

The following lemma gives the shape derivative of E.

Lemma 3.2.7 *The shape derivative of E at $\zeta = \mathbf{0}$ in the direction ξ is given by*

$$E'(\mathbf{0})\xi = \int_M g\hat{c}_o' + \sigma p_{in}', \tag{3.2.21}$$

where

$$g = \frac{-2B(\eta)E_1\alpha - |M|H_m\beta}{|M| + B(\eta)\int_M \hat{c}_o} + \alpha H_m^2\left(\hat{c}_o - \frac{1}{|M|}\int_M \hat{c}_o\right). \tag{3.2.22}$$

Proof:

The proof follows from the definition of the cost functional E from equation (3.2.1), Lemma 3.2.5 and 3.2.6. ∎

We now take the shape derivatives of $\hat{c}$, $\hat{\mathbf{u}}$ and $\hat{p}$ assuming that the system, (2.1.69)-(2.1.71) and (2.1.59), has a smooth solution. The following lemmas will be needed to find the shape gradient of the cost functional E.

Lemma 3.2.8 *Let $\varphi \in C^\infty(\mathbb{R}^2)$ such that $\varphi = 0, \Gamma_o(\mathbf{0})$ be a test function independent of ζ. Then the shape derivative $\hat{c}'$ satisfies*

$$\begin{aligned}
&-\int_\Omega \nabla\cdot\left(\varepsilon D^{eff}\nabla\varphi + \varepsilon\varphi\hat{\mathbf{u}}\right)\hat{c}' + \int_\Omega \varepsilon\varphi\nabla\hat{c}\cdot\hat{\mathbf{u}}' \\
&= \int_M \left[-\varepsilon D^{eff}\partial_2\varphi + \varphi H_m(3\beta_m\hat{c}+1)\right]\hat{c}' - \int_{\Gamma_o}\left(D^{eff}\partial_\nu\varphi + \varphi\hat{\mathbf{u}}\cdot\nu\right)\hat{c}' \\
&\quad - \int_{\Gamma\cup\Gamma_w}\left(\varepsilon D^{eff}\partial_\nu\varphi\right)\hat{c}' - \int_\Gamma (\xi\cdot\nu)\left(D^{eff}\nabla\hat{c}\cdot\nabla\varphi\right),
\end{aligned} \tag{3.2.23}$$

where

$$\beta_m \;=\; \varepsilon\left(\frac{2M_w}{M_o}(1+2\alpha_m)-1\right). \tag{3.2.24}$$

Proof:

Multiplying the advection-diffusion equation (2.1.69) by φ and integrating by parts give

$$\int_{\Omega_\zeta}\varepsilon\left(D^{eff}\nabla\hat{c}\cdot\nabla\varphi+\varphi\hat{\mathbf{u}}\cdot\nabla\hat{c}\right)=\int_{\partial\Omega_\zeta}\varepsilon D^{eff}\varphi\partial_\nu\hat{c}. \tag{3.2.25}$$

From (2.1.59), $\partial_\nu\hat{c}=0$ on $\Gamma\cup\Gamma_o\cup\Gamma_w$. Also, Remark 2.1.1 gives $-\varepsilon D^{eff}\partial_\nu\hat{c}=H_m\hat{c}(1+\beta_m\hat{c})$ on M, assuming that $\rho_g=1$ on Ω. Then (3.2.25) simplifies to

$$\int_{\Omega_\zeta}\varepsilon\left(D^{eff}\nabla\hat{c}\cdot\nabla\varphi+\varphi\hat{\mathbf{u}}\cdot\nabla\hat{c}\right)=-\int_{\Gamma_{i,\zeta}}D^{eff}\varphi\partial_1\hat{c}-\int_M H_m\hat{c}(1+\beta_m\hat{c}). \tag{3.2.26}$$

Taking the shape derivative of equation (3.2.26) leads to

$$\begin{aligned}&\int_\Omega\varepsilon\left[\left(D^{eff}\nabla\varphi+\varphi\hat{\mathbf{u}}\right)\cdot\nabla\hat{c}'+\varphi\nabla\hat{c}\cdot\hat{\mathbf{u}}'\right]+\int_{\partial\Omega}\varepsilon\left(\xi\cdot\nu\right)\left(D^{eff}\nabla\hat{c}\cdot\nabla\varphi+\varphi\hat{\mathbf{u}}\cdot\nabla\hat{c}\right)\\ =\;&-\int_{\Gamma_i}D^{eff}\varphi\partial_1\hat{c}'-\int_{\partial\Gamma_i}\left(\nu_{\partial\Gamma_i}\cdot\xi\right)\left(D^{eff}\varphi\partial_1\hat{c}\right)-\int_M H_m\varphi(1+2\beta_m\hat{c})\hat{c}'.\end{aligned} \tag{3.2.27}$$

Note that the above equation is derived using (3.1.19) in Theorem 3.1.10 by considering both Ω_ζ and $\Gamma_{i,\zeta}$ as volume domains. Since $\xi\cdot\nu=0$ on $\partial\Omega\backslash\overline{\Gamma}$ and $\varphi=0$ on Γ_i and $\hat{\mathbf{u}}=\mathbf{0}$ on Γ, (3.2.27) reduces to

$$\begin{aligned}&\int_\Omega\varepsilon[\left(D^{eff}\nabla\varphi+\varphi\hat{\mathbf{u}}\right)\cdot\nabla\hat{c}'+\varphi\nabla\hat{c}\cdot\hat{\mathbf{u}}']\\ =\;&-\int_M H_m\varphi(1+2\beta_m\hat{c})\hat{c}'-\int_\Gamma\left(\xi\cdot\nu\right)\left(D^{eff}\nabla\hat{c}\cdot\nabla\varphi\right).\end{aligned} \tag{3.2.28}$$

Integrating the volume term involving $\hat{c}'$ in (3.2.28) gives

$$\begin{aligned}\int_\Omega\varepsilon\left(D^{eff}\nabla\varphi+\varphi\hat{\mathbf{u}}\right)\cdot\nabla\hat{c}' \;=\;&-\int_\Omega\nabla\cdot\left(\varepsilon D^{eff}\nabla\varphi+\varepsilon\varphi\hat{\mathbf{u}}\right)\hat{c}'\\ &+\int_{\partial\Omega}\varepsilon\left(D^{eff}\partial_\nu\varphi+\varphi\hat{\mathbf{u}}\cdot\nu\right)\hat{c}'.\end{aligned} \tag{3.2.29}$$

Since $\hat{c}$ is constant and $\xi \cdot \nu = 0$ on Γ_i, it follows from Lemma 3.1.9 that $\hat{c}' = 0$ on Γ_i. Since also $\hat{\mathbf{u}} \cdot \nu = 0$ on $\Gamma \cup \Gamma_w$, the boundary integral in (3.2.29) simplifies to

$$\begin{aligned}\int_{\partial\Omega} \varepsilon \left(D^{eff}\nabla\varphi + \varphi\hat{\mathbf{u}}\right) \cdot \nu \hat{c}' &= \int_{\Gamma\cup\Gamma_w} \varepsilon \left(D^{eff}\partial_\nu\varphi\right) \hat{c}' \\ &\quad + \int_{\Gamma_o\cup M} \varepsilon \left(D^{eff}\partial_\nu\varphi + \varphi\hat{\mathbf{u}}\cdot\nu\right) \hat{c}'. \quad (3.2.30)\end{aligned}$$

Using (3.2.29), (3.2.30) and (2.1.64), which gives $\varepsilon\hat{u}_2 = -\frac{\beta_m H_m \hat{c}}{\varepsilon}$ on M, (3.2.28) is written as

$$\begin{aligned}&-\int_\Omega \nabla\cdot\left(\varepsilon D^{eff}\nabla\varphi + \varepsilon\varphi\hat{\mathbf{u}}\right)\hat{c}' + \int_\Omega \varepsilon\varphi\nabla\hat{c}\cdot\hat{\mathbf{u}}' \\ &= \int_M \left[-\varepsilon D^{eff}\partial_2\varphi + \varphi H_m\left(3\beta_m\hat{c}+1\right)\right]\hat{c}' - \int_{\Gamma_o}\left(D^{eff}\partial_\nu\varphi + \varphi\hat{\mathbf{u}}\cdot\nu\right)\hat{c}' \\ &\quad - \int_{\Gamma\cup\Gamma_w} \varepsilon\left(D^{eff}\partial_\nu\varphi\right)\hat{c}' - \int_\Gamma (\xi\cdot\nu)\left(D\nabla\hat{c}\cdot\nabla\varphi\right). \quad (3.2.31)\end{aligned}$$

∎

Lemma 3.2.9 *Let $\mathbf{v} = (v_1, v_2) \in C^\infty(\mathbb{R}^2) \times C^\infty(\mathbb{R}^2)$ and $q \in C^\infty(\mathbb{R}^2)$ be test functions independent of ζ, such that*

$$\begin{aligned} v_2 &= 0, && \Gamma_i \cup \overline{\Gamma} \cup \Gamma_o \\ v_1 &= 0, && \overline{\Gamma} \cup \Sigma \cup \Gamma_w \\ [v_2] = [q] &= 0, && \Sigma \\ \nabla\cdot\mathbf{v} &= 0, && \overline{A} \cup G. \end{aligned} \quad (3.2.32)$$

Then the shape derivatives $(\hat{\mathbf{u}}', \hat{p}')$ satisfy

$$\int_A (-\mu\Delta\mathbf{v} + \nabla q)\cdot\hat{\mathbf{u}}' + \int_G \Big(\frac{\mu}{K}\mathbf{v} + \nabla q\Big)\cdot\hat{\mathbf{u}}'$$
$$= p_i' \int_{\Gamma_i} v_1 - \int_{\Gamma_i} q\hat{u}_1' + \int_{\Gamma_o} q\hat{u}_1'$$
$$- \int_M \left(v_2\hat{p}' + \frac{\beta_m H_m}{\varepsilon} q\hat{c}'\right) + \int_\Gamma (\xi\cdot\nu)\,(\mu\partial_\nu\mathbf{v}\cdot\partial_\nu\hat{\mathbf{u}})\,. \quad (3.2.33)$$

Proof:

Multiplying Stokes equation by $\mathbf{v}$, the divergence equation by q and integrating by parts lead to

$$\int_{A_\zeta} \mu\nabla\hat{\mathbf{u}}\cdot\nabla\mathbf{v} + \int_G \frac{\mu}{K}\hat{\mathbf{u}}\cdot\mathbf{v} - \int_{A_\zeta\cup G} (\hat{p}\nabla\cdot\mathbf{v} - \nabla q\cdot\hat{\mathbf{u}})$$
$$= \int_{\partial A_\zeta} \mu\mathbf{v}\cdot\partial_{\nu_A}\hat{\mathbf{u}} - \int_{\partial A_\zeta} (\hat{p}\mathbf{v} - q\hat{\mathbf{u}})\cdot\nu_A - \int_{\partial G} (\hat{p}\mathbf{v} - q\hat{\mathbf{u}})\cdot\nu_G$$
$$= \int_{\partial A_\zeta} \mu\mathbf{v}\cdot\partial_{\nu_A}\hat{\mathbf{u}} - \int_{\partial\left(A_\zeta\cup G\right)\setminus\Sigma} (\hat{p}\mathbf{v} - q\hat{\mathbf{u}})\cdot\nu. \quad (3.2.34)$$

Here we used $[v_2] = [\hat{p}] = [\hat{u}_2] = [q] = 0$ on Σ. From (3.2.32), $v_1 = \hat{u}_1 = 0$ on Σ. Hence, $\partial_1\hat{u}_1 = 0$ on Σ. Then, using the divergence free condition on $\hat{\mathbf{u}}$ yields

$$\mathbf{v}\cdot\partial_{\nu_A}\hat{\mathbf{u}} = v_2\partial_2 u_2 = -v_2\partial_1 u_1 = 0 \qquad on\ \ \Sigma. \quad (3.2.35)$$

Using (3.2.32) and (3.2.35), (3.2.34) is written as

$$\int_{A_\zeta} \mu\nabla\hat{\mathbf{u}}\cdot\nabla\mathbf{v} + \int_G \frac{\mu}{K}\hat{\mathbf{u}}\cdot\mathbf{v} - \int_{A_\zeta\cup G} (\hat{p}\nabla\cdot\mathbf{v} - \nabla q\cdot\hat{\mathbf{u}})$$
$$= -\int_{\Gamma_{i,\zeta}} \mu v_2\partial_1\hat{u}_2 + \int_{\Gamma_\zeta} \mu\mathbf{v}\cdot\partial_\nu\hat{\mathbf{u}} + \int_{\Gamma_{o,\zeta}} \mu v_2\partial_1\hat{u}_2 + \int_{\Gamma_{i,\zeta}} (p_i v_1 - q\hat{u}_1)$$
$$- \int_{\Gamma_\zeta} (\hat{p}\mathbf{v} - q\hat{\mathbf{u}})\cdot\nu - \int_{\Gamma_{o,\zeta}} (p_o v_1 - q\hat{u}_1) - \int_M \left(\hat{p}v_2 + \frac{\beta_m H_m}{\varepsilon} q\hat{c}\right), \quad (3.2.36)$$

as $\hat{\mathbf{u}} = 0$ on Γ_ζ and $\hat{u}_2 = -\frac{\beta_m H_m}{\varepsilon}\hat{c}$ on M.

Before taking the shape derivative of the above equation, note that

$$\begin{aligned}
&\left(\int_{A_\zeta \cup G} (\hat{p}\nabla\cdot\mathbf{v} - \nabla q\cdot\hat{\mathbf{u}})\right)' \\
&= \int_{A\cup G} (\hat{p}'\nabla\cdot\mathbf{v} - \nabla q\cdot\hat{\mathbf{u}}') + \int_{\Gamma_i\cup\Gamma\cup\Gamma_o} (\xi\cdot\nu)\,(\hat{p}\nabla\cdot\mathbf{v} - \nabla q\cdot\hat{\mathbf{u}}) \\
&= -\int_{A\cup G} \nabla q\cdot\hat{\mathbf{u}}', \qquad (3.2.37)
\end{aligned}$$

where the last equality follows from $\nabla\cdot\mathbf{v}=0$ on $\overline{A}\cup G$, $\xi\cdot\nu=0$ on $\Gamma_i\cup\Gamma_o\cup\Sigma$ and $\hat{\mathbf{u}}=\mathbf{0}$ on Γ.

Also, the shape derivative of the boundary integral over Γ

$$\left(\int_{\Gamma_\zeta} (\hat{p}\mathbf{v} - q\hat{\mathbf{u}})\cdot\nu\right)' = 0. \qquad (3.2.38)$$

To see this, note that

$$\begin{aligned}
\left(\int_{\Gamma_\zeta} (\hat{p}\mathbf{v} - q\hat{\mathbf{u}})\cdot\nu\right)' &= \int_\Gamma \left\{\mathbf{v}\cdot(\hat{p}\nu)' - q\,(\hat{\mathbf{u}}\cdot\nu)' + div_\Gamma[\xi\,(\hat{p}\mathbf{v} - q\hat{\mathbf{u}})\cdot\nu]\right\} \\
&\quad + \int_\Gamma (\xi\cdot\nu)\,\partial_\nu[(\hat{p}\mathbf{v} - q\hat{\mathbf{u}})\cdot\nu], \qquad (3.2.39)
\end{aligned}$$

where $\mathbf{v}\cdot(\hat{p}\nu)' = 0$ and $div_\Gamma[\xi\,(\hat{p}\mathbf{v} - q\hat{\mathbf{u}})\cdot\nu] = 0$ on Γ as $\hat{\mathbf{u}} = \mathbf{v} = \mathbf{0}$ on Γ. Since also $\hat{\mathbf{u}} = \mathbf{0}$ on Γ_ζ, it follows from Lemma 3.1.9 that $\hat{\mathbf{u}}' = -(\xi\cdot\nu)\,\partial_\nu\hat{\mathbf{u}}$ on Γ. These simplify (3.2.39) to

$$\begin{aligned}
\left(\int_{\Gamma_\zeta} (\hat{p}\mathbf{v} - q\hat{\mathbf{u}})\cdot\nu\right)' &= \int_\Gamma (\xi\cdot\nu)\,\nu\cdot[q\partial_\nu\hat{\mathbf{u}} + \hat{p}\partial_\nu\mathbf{v} - q\partial_\nu\hat{\mathbf{u}}] \\
&= \int_\Gamma (\xi\cdot\nu)\,\hat{p}\nabla\cdot\mathbf{v} \\
&= 0, \qquad (3.2.40)
\end{aligned}$$

as $\nu\cdot\partial_\nu\mathbf{v} = \tau\cdot\partial_\tau\mathbf{v} + \nu\cdot\partial_\nu\mathbf{v} = \nabla\cdot\mathbf{v} = 0$ on Γ.

Similarly,

$$\left(\int_{\Gamma_\zeta} \mu \mathbf{v}\cdot\partial_\nu\hat{\mathbf{u}}\right)' = \int_\Gamma [\mu\mathbf{v}\cdot(\partial_\nu\hat{\mathbf{u}})' + div_\Gamma(\xi\mu\mathbf{v}\cdot\partial_\nu\hat{\mathbf{u}}) + (\xi\cdot\nu)\,\mu\partial_\nu\mathbf{v}\cdot\partial_\nu\hat{\mathbf{u}}]$$
$$= \int_\Gamma (\xi\cdot\nu)\,\mu\partial_\nu\mathbf{v}\cdot\partial_\nu\hat{\mathbf{u}}. \tag{3.2.41}$$

Using (3.2.37), (3.2.40), (3.2.41) and taking the shape derivative of (3.2.36) gives

$$\begin{aligned}
&\int_A \mu\nabla\mathbf{v}\cdot\nabla\hat{\mathbf{u}}' + \int_{\partial A}(\xi\cdot\nu_A)(\mu\nabla\mathbf{v}\cdot\nabla\hat{\mathbf{u}}) + \int_G \frac{\mu}{K}\mathbf{v}\cdot\hat{\mathbf{u}}' + \int_{A\cup G}\nabla q\cdot\hat{\mathbf{u}}'\\
&= -\int_{\Gamma_i}\mu v_2\partial_1 u_2' - \int_{\partial\Gamma_i}(\nu_{\partial\Gamma_i}\cdot\xi)(\mu v_2\partial_1 u_2)\\
&\quad + \int_\Gamma (\xi\cdot\nu)\,\mu\partial_\nu\mathbf{v}\cdot\partial_\nu\hat{\mathbf{u}}\\
&\quad + \int_{\Gamma_o}\mu v_2\partial_1 u_2' + \int_{\partial\Gamma_o}(\nu_{\partial\Gamma_o}\cdot\xi)(\mu v_2\partial_1 u_2)\\
&\quad + \int_{\Gamma_i}(p_i' v_1 - q\hat{u}_1') + \int_{\partial\Gamma_i}(\nu_{\partial\Gamma_i}\cdot\xi)(p_i v_1 - q\hat{u}_1)\\
&\quad - \int_{\Gamma_o}(p_o' v_1 - q\hat{u}_1') - \int_{\partial\Gamma_o}(\nu_{\partial\Gamma_o}\cdot\xi)(p_o v_1 - q\hat{u}_1)\\
&\quad - \int_M \left(v_2\hat{p}' + \frac{\beta_m H_m}{\varepsilon}q\hat{c}'\right).
\end{aligned} \tag{3.2.42}$$

Since $\xi\cdot\nu_A = 0$ on $\partial A\backslash\overline{\Gamma}$, $v_2 = 0$ on $\Gamma_i\cup\Gamma_o$, $\mathbf{v} = 0$ on $\overline{\Gamma}$ and $p_o' = \xi_2\partial_2 p_o = 0$ on Γ_o (as p_o is constant on Γ_o), equation (3.2.42) reduces to

$$\begin{aligned}
&\int_A \mu\nabla\mathbf{v}\cdot\nabla\hat{\mathbf{u}}' + \int_G \frac{\mu}{K}\mathbf{v}\cdot\hat{\mathbf{u}}' + \int_{A\cup G}\nabla q\cdot\hat{\mathbf{u}}'\\
&\qquad = p_i'\int_{\Gamma_i} v_1 - \int_{\Gamma_i} q\hat{u}_1' + \int_{\Gamma_o} q\hat{u}_1'\\
&\qquad\quad - \int_M \left(v_2\hat{p}' + \frac{\beta_m H_m}{\varepsilon}q\hat{c}'\right).
\end{aligned} \tag{3.2.43}$$

The first term of the above equation is integrated by parts:

$$\int_A \mu\nabla\mathbf{v}\cdot\nabla\hat{\mathbf{u}}' = -\int_A \mu\Delta\mathbf{v}\cdot\hat{\mathbf{u}}' + \int_{\partial A}\mu\partial_\nu\mathbf{v}\cdot\hat{\mathbf{u}}'. \tag{3.2.44}$$

Since $\hat{\mathbf{u}}' = -(\xi \cdot \nu)\,\partial_\nu \hat{\mathbf{u}}$ on Γ, $\hat{u}_1' = 0$ on Σ, $\hat{u}_2' = 0$ on $\Gamma_i \cup \Gamma_o$ and $\nabla \cdot \mathbf{v} = 0$ in A, the above equation is simplified to

$$\int_A \mu \nabla \mathbf{v} \cdot \nabla \hat{\mathbf{u}}' \;=\; -\int_A \mu \Delta \mathbf{v} \cdot \hat{\mathbf{u}}' - \int_\Gamma (\xi \cdot \nu)\,(\mu \partial_\nu \mathbf{v} \cdot \partial_\nu \hat{\mathbf{u}})\,. \tag{3.2.45}$$

Substituting (3.2.45) in (3.2.43) leads to the result:

$$\begin{aligned}\int_A (-\mu\Delta \mathbf{v} + \nabla q) \cdot \hat{\mathbf{u}}' + \int_G \left(\frac{\mu}{K}\mathbf{v} + \nabla q\right) \cdot \hat{\mathbf{u}}' \\ = p_i' \int_{\Gamma_i} v_1 - \int_{\Gamma_i} q\hat{u}_1' + \int_{\Gamma_o} q\hat{u}_1' \\ - \int_M \left(v_2 \hat{p}' + \frac{\beta_m H_m}{\varepsilon} q\hat{c}'\right) + \int_\Gamma (\xi \cdot \nu)\,(\mu \partial_\nu \mathbf{v} \cdot \partial_\nu \hat{\mathbf{u}})\,. \end{aligned} \tag{3.2.46}$$

∎

The following lemmas introduces an adjoint system with appropriate boundary conditions for the computation of the shape gradient of E.

Lemma 3.2.10 *Consider the following adjoint system*

$$\begin{aligned} -\nabla \cdot \left(\varepsilon D^{eff} \nabla \varphi + \varepsilon \varphi \hat{\mathbf{u}}\right) &= 0 \quad \Omega \\ (-\mu\Delta \mathbf{v} + \nabla q + \varphi \nabla \hat{c})\,\chi(A) + \left(\frac{\mu}{K}\mathbf{v} + \nabla q + \varepsilon\varphi\nabla\hat{c}\right)\chi(G) &= 0 \quad A \cup G, \\ \nabla \cdot \mathbf{v} &= 0 \quad A \cup G. \end{aligned} \tag{3.2.47}$$

Then the shape derivatives $(\hat{c}', \hat{\mathbf{u}}', \hat{p}')$ satisfy the following identity:

$$\begin{aligned} 0 = \quad & \int_M \left[-\varepsilon D^{eff} \partial_2 \varphi + H_m\,(3\beta_m \hat{c} + 1)\,\varphi - \frac{\beta_m H_m}{\varepsilon} q\right] \hat{c}' - \int_{\Gamma_o} \left(D^{eff} \partial_\nu \varphi + \varphi \hat{\mathbf{u}} \cdot \nu\right) \hat{c}' \\ & - \int_{\Gamma \cup \Gamma_w} \varepsilon \left(D^{eff} \partial_\nu \varphi\right) \hat{c}' - \int_\Gamma \xi_2 \nu_2 \left(D^{eff} \nabla \hat{c} \cdot \nabla \varphi\right) + p_i' \int_{\Gamma_i} v_1 - \int_{\Gamma_i} q\hat{u}_1' \\ & + \int_{\Gamma_o} q\hat{u}_1' - \int_M v_2 \hat{p}' + \int_\Gamma (\xi \cdot \nu)\,(\mu \partial_\nu \mathbf{v} \cdot \partial_\nu \hat{\mathbf{u}})\,. \end{aligned} \tag{3.2.48}$$

Proof:

The adjoint system is motivated from Lemma 3.2.8 and Lemma 3.2.9: summing up the equations (3.2.23) and (3.2.33), and equating the left side to zero, one obtains (3.2.48). ∎

The boundary conditions of the adjoint system are chosen so that the shape gradient of E is easily computed.

Lemma 3.2.11 *Consider the following boundary conditions for the adjoint system. For the variable φ, the boundary conditions are*

$$\begin{aligned} \varphi &= 0 \quad on \quad \Gamma_i \\ \partial_\nu \varphi &= 0 \quad on \quad \Gamma \cup \Gamma_w \\ D^{eff}\partial_1\varphi + u_1\varphi &= 0 \quad on \quad \Gamma_o \\ -\varepsilon D^{eff}\partial_2\varphi + H_m\left(3\beta_m\hat{c} - 1\right)\varphi - \frac{\beta_m H_m}{\varepsilon} q &= -g \quad on \quad M, \end{aligned} \tag{3.2.49}$$

and for $(\mathbf{v}, q)$

$$\begin{aligned} q - \frac{1}{|\Gamma_i|}\int_{\Gamma_i} q = \int_{\Gamma_i} v_1 + \sigma &= 0 \quad on \quad \Gamma_i \\ q &= 0 \quad on \quad \Gamma_o \\ v_1 &= 0 \quad on \quad \Gamma \cup \Sigma \cup \Gamma_w \\ v_2 &= 0 \quad on \quad \Gamma_i \cup \Gamma \cup \Gamma_o \cup M, \end{aligned} \tag{3.2.50}$$

where g is given by (3.2.22). Then the shape gradient E' is given by

$$E'(\mathbf{0})\xi = \int_\Gamma (\xi \cdot \nu)\left(\mu \partial_\nu \mathbf{v} \cdot \partial_\nu \hat{\mathbf{u}} - D\nabla\hat{c} \cdot \nabla\varphi\right). \tag{3.2.51}$$

Proof:

Using Lemma 3.2.7 and 3.2.10, namely combining similar terms of the identity (3.2.48)

to those of E' given in Lemma 3.2.7, leads to

$$\begin{aligned} E' = \int_M \left(g - \varepsilon D^{eff} \partial_2 \varphi + H_m \left(3\beta_m \hat{c} + 1\right) \varphi - \frac{\beta_m H_m}{\varepsilon} q \right) \hat{c}' + \int_{\Gamma_o} \left(-D^{eff} \partial_1 \varphi - \varphi \hat{u}_1 \right) \hat{c}' \\ + \left(\sigma + \int_{\Gamma_i} v_1 \right) \hat{p}_i' + \int_{\Gamma} \left(\xi \cdot \nu\right) \left(\mu \partial_\nu \mathbf{v} \cdot \partial_\nu \hat{\mathbf{u}} - D \nabla \varphi \cdot \nabla \hat{c} \right) \\ - \int_{\Gamma \cup \Gamma_w} \varepsilon \left(D^{eff} \partial_\nu \varphi \right) \hat{c}' - \int_{\Gamma_i} q \hat{u}_1' + \int_{\Gamma_o} q \hat{u}_1' - \int_M v_2 \hat{p}' \end{aligned} \tag{3.2.52}$$

Note that since

$$\int_{\Gamma_i} \hat{u}_1 \;=\; u \tag{3.2.53}$$

and $\hat{u}_1 = 0$ on $\partial\Gamma_i$, it follows that

$$\int_{\Gamma_i} \hat{u}_1' \;=\; 0. \tag{3.2.54}$$

Hence, the integral in (3.2.52),

$$\int_{\Gamma_i} q \hat{u}_1' \;=\; 0 \tag{3.2.55}$$

when q is constant. Then, the boundary condition

$$q \;=\; \frac{1}{|\Gamma_i|} \int_{\Gamma_i} q \tag{3.2.56}$$

is suitable.

The other boundary integrals involving the shape derivatives $\hat{c}', \hat{\mathbf{u}}'$, and $\hat{p}'$ are expensive to compute since they depend on the direction ξ. To overcome this problem, the coefficients of these derivatives are set to be zero:

$$\begin{aligned} M: &\quad g - \varepsilon D^{eff} \partial_2 \varphi + H_m \left(3\beta_m \hat{c} + 1\right) \varphi - \tfrac{\beta_m H_m}{\varepsilon} q = v_2 = 0, \\ \Gamma_o: &\quad -D^{eff} \partial_1 \varphi - \varphi \hat{u}_1 = q = 0, \\ \Gamma_i: &\quad \sigma + \textstyle\int_{\Gamma_i} v_1 = 0, \\ \Gamma \cup \Gamma_w: &\quad \partial_\nu \varphi = 0. \end{aligned}$$

The remaining boundary conditions were already considered in lemma (3.2.8) and lemma (3.2.9). Then the shape gradient of E at $\zeta = \mathbf{0}$ in the direction ξ is given by:

$$E'(\mathbf{0})\xi \quad = \quad \int_\Gamma (\xi \cdot \nu) \left(\mu \partial_\nu \mathbf{v} \cdot \partial_\nu \hat{\mathbf{u}} - D \nabla \hat{c} \cdot \nabla \varphi\right). \tag{3.2.57}$$

∎

3.3 Existence of the shape derivative of the state variables

The goal of this section is to analyze the existence of the shape derivative of the state variables: $c(\zeta)$, $\mathbf{u}(\zeta)$ and $p(\zeta)$, which are defined on $\Omega(\zeta) := (I+\zeta)(\Omega)$. Denote by

$$W(\zeta) \;:=\; (c(\zeta), \mathbf{u}(\zeta), p(\zeta))\,. \tag{3.3.1}$$

The state variables, given by $W(\zeta)$, satisfy state equations, written as

$$F(\zeta, W(\zeta)) \;=\; 0. \tag{3.3.2}$$

Assuming that $W(\zeta)$ is regular, then the shape derivative of $W(\zeta)$ at $\zeta = 0$ in the direction ξ is given by

$$\frac{\partial W(\zeta)}{\partial \zeta}(\mathbf{0})\xi \;=\; \frac{\partial W(\zeta)\circ(I+\zeta)}{\partial \zeta}(\mathbf{0})\xi - \xi\cdot\nabla W(\mathbf{0}). \tag{3.3.3}$$

Hence, the above equation (3.3.3) implies that the existence of the shape derivative $\frac{\partial W(\zeta)}{\partial \zeta}(\mathbf{0})\xi$ reduces to the existence of the shape derivative $\frac{\partial W(\zeta)\circ(I+\zeta)}{\partial \zeta}(\mathbf{0})\xi$ and the regularity of $\nabla W(\mathbf{0})$.

The goal of this section is to prove the existence of the shape derivative $\frac{\partial W(\zeta)\circ(I+\zeta)}{\partial \zeta}(\mathbf{0})\xi$. This is going to be achieved using the Implicit Mapping Theorem and Fixed Point Theorem. For this, the state equations represented by equation (3.3.2) is reformulated as

$$G(\zeta, W(\zeta)\circ(I+\zeta)) \;=\; 0, \tag{3.3.4}$$

where $W(\zeta\circ(I+\zeta)$ is defined on the fixed domain Ω. To prove the differentiability of $W(\zeta)\circ(I+\zeta)$, the Implicit Mapping Theorem is implemented on G; namely the following requirements are verified:

1. G is Fréchet differentiable near $\zeta = \mathbf{0}$,

2. $G(\zeta, W(\zeta) \circ (I + \zeta)) = 0$ near $\zeta = \mathbf{0}$,

3. $V \longmapsto \frac{\partial}{\partial W} G(\mathbf{0}, W(\mathbf{0}))[V]$ is an isomorphism.

When the above requirements are met, then the Implicit Mapping Theorem gives the existence and uniqueness of a Fréchet differentiable map f satisfying

$$G(\zeta, f(\zeta)) \;=\; 0, \tag{3.3.5}$$

where ζ is in a neighborhood of $\zeta = \mathbf{0}$. The uniqueness of such f and the second requirement imply that

$$f(\zeta) \;=\; W(\zeta) \circ (I + \zeta), \tag{3.3.6}$$

and hence the shape differentiability of $W(\zeta) \circ (I + \zeta)$. The second and the third requirements will be shown using a Fixed Point Theorem.

This section will be divided into subsections as follows. The first subsection introduces the main results needed to write weak formulations of the steady state and adjoint problems (see Section 3.2), and the results needed to implement the Fixed Point Theorem. The second subsection defines a weak formulation for the steady state problem. The third subsection investigates the differentiability of the steady state variables and the shape differentiability of the cost functional E, given in (2.2.4).

3.3.1 Preliminaries

Lemma 3.3.1 ([34], page 32) *Let A be a bounded open set of $\mathbb{R}^n$ with a Lipschitz continuous boundary ∂A. Define*

$$L^2(A)/\mathbb{R} \;:=\; \left\{ h \in L^2(A) : \int_A h = 0 \right\}. \tag{3.3.7}$$

Then the gradient operator,

$$grad : L^2(A) \;\longrightarrow\; \mathbf{H}^{-1}(A), \tag{3.3.8}$$

is an isomorphism from $L^2(A)/\mathbb{R}$ *onto its range,* $Range(grad)$*. Also, by transposition, its adjoint* $grad^* = -div$*,*

$$-div : \mathbf{H}_0^1(A) \longrightarrow L^2(A), \tag{3.3.9}$$

is an isomorphism from the subspace orthogonal to $Range(grad)$ *onto* $L^2(A)/\mathbb{R}$*.*

Remark 3.3.2 From the above lemma 3.3.1, it follows that for every $h \in L^2(A)/\mathbb{R}$, there exists $z(h) := div^{-1}(h) \in \mathbf{H}_0^1(A)$ such that

$$\begin{aligned} \nabla \cdot z(h) &= h, \\ C_1\|h\|_{L^2(A)/\mathbb{R}} &\leq \|z(h)\|_{\mathbf{H}_0^1(A)} \leq C_2\|h\|_{L^2(A)/\mathbb{R}}, \end{aligned} \tag{3.3.10}$$

where C_1, C_2 are constants independent of h.

Definition 3.3.3 *Let* $\mathbf{D}$ *be the subspace orthogonal to* $Range(grad)$*, given in lemma 3.3.1. We define* div_0 *by*

$$div_0 := -grad^* : \mathbf{D} \subset \mathbf{H}_0^1(A) \longrightarrow L^2(A)/\mathbb{R}. \tag{3.3.11}$$

Hence, div_0 *is an isomorphism.*

Theorem 3.3.4 (Trace Theorem, [24], page 10) *Let* A *be a bounded open set of* $\mathbb{R}^n$ *with Lipschitz continuous boundary* ∂A*, and let* $s > 1/2$*.*

1. *There exists a unique linear continuous map* γ*, called the trace operator,*

$$\gamma : H^s(A) \longrightarrow H^{s-1/2}(\partial A), \tag{3.3.12}$$

such that

$$\gamma(v) := v|_{\partial A}, \quad \forall \ v \in H^s(A) \cap C^0(\overline{A}). \tag{3.3.13}$$

2. There exists a linear continuous map γ_l, called the lifting operator,

$$\gamma_l : H^{s-1/2}(\partial A) \longrightarrow H^s(A), \tag{3.3.14}$$

such that

$$\gamma(\gamma_l(\varphi)) = \varphi, \quad \forall \quad \varphi \in H^{s-1/2}(\partial A). \tag{3.3.15}$$

Remark 3.3.5 Theorem 3.3.4 implies that for every given $\Phi \in \mathbf{H}^{1/2}(\partial A)$, there exists $z(\Phi) := \gamma_l(\Phi) \in \mathbf{H}^1(A)$, such that

$$\begin{aligned} \gamma(z(\Phi)) &= \Phi, \\ C_1\|\Phi\|_{\mathbf{H}^{1/2}(\partial A)} &\leq \|z(\Phi)\|_{\mathbf{H}^1(A)} \leq C_2\|\Phi\|_{\mathbf{H}^{1/2}(\partial A)}, \end{aligned} \tag{3.3.16}$$

for some constants C_1, C_2 independent from Φ.

The following definition and theorem, [34], will be used to prove Proposition 3.4.4. Let $(\cdot,\cdot)$ denote the L^2 inner product.

Definition 3.3.6 ([34], page 5) *Let $\mathbf{H}(div;\Omega)$ be the following linear space*

$$\mathbf{H}(div;\Omega) = \left\{\mathbf{u} \in \mathbf{L}^2(\Omega) : div\ \mathbf{u} \in L^2(\Omega)\right\}. \tag{3.3.17}$$

Then $\mathbf{H}(div;\Omega)$ is a Hilbert space when equipped with the scalar product

$$(\mathbf{u},\mathbf{v})_{\mathbf{H}(div;\Omega)} = (\mathbf{u},\mathbf{v}) + (div\ \mathbf{u}, div\ \mathbf{v}), \tag{3.3.18}$$

and the associated norm on $\mathbf{H}(div;\Omega)$ is defined as

$$\|\mathbf{u}\|_{\mathbf{H}(div,\Omega)} = (\mathbf{u},\mathbf{u})^{1/2}_{\mathbf{H}(div;\Omega)}. \tag{3.3.19}$$

Theorem 3.3.7 ([34], page 9) *Let Ω be an open set of class C^2. Then there exists a linear continuous operator $\gamma_\nu \in \mathcal{L}(\mathbf{H}(div;\Omega), H^{-1/2}(\partial\Omega))$ such that*

$$\gamma_\nu(\mathbf{u}) := \mathbf{u}\cdot\nu|_{\partial\Omega}, \quad \forall \mathbf{u} \in \mathcal{D}(\overline{\Omega}). \tag{3.3.20}$$

The following generalized Stokes formula is true for all $\mathbf{u} \in \mathbf{H}(div;\Omega)$ *and* $w \in H^1(\Omega)$

$$< \gamma_\nu \mathbf{u}, \gamma_0 w >_{H^{-1/2}(\Omega)\times H^{1/2}(\Omega)} \;=\; (\mathbf{u}, grad\ w) + (div\ \mathbf{u}, w). \tag{3.3.21}$$

The above theorem is still valid for domain Ω with Lipschitz boundary, see [34, page 13]. In the above theorem, γ_0 denotes the usual trace operator.

Definition 3.3.8 ([8], page 5) *Let* Ω *be a Lipschitz domain with boundary* $\partial\Omega$ *and* $\Gamma \subset \partial\Omega$. *Then, the restriction* $\gamma_\nu \mathbf{u}|_\Gamma$ *of* $\gamma_\nu \mathbf{u}$ *to* Γ *is defined as follows:*

$$< \gamma_{\nu,\Gamma} \mathbf{u}, \gamma_0 \varphi >_{H^{-1/2}(\Gamma)\times H^{1/2}(\Gamma)} := < \gamma_\nu \mathbf{u}, \gamma_0 \varphi >_{H^{-1/2}(\partial\Omega)\times H^{1/2}(\partial\Omega)}, \tag{3.3.22}$$

for all $\varphi \in H^1(\Omega)$ *with* $\varphi|_{\partial\Omega/\Gamma} := \gamma_0\varphi|_{\partial\Omega/\Gamma} = 0$.

Remark 3.3.9 The above definition uses the generalized Stokes formula (3.3.21) to "recover" $\gamma_\nu \mathbf{u}$ on Γ through functions $\varphi \in H^1(\Omega)$ with $\varphi = 0$ on $\partial\Omega/\Gamma$.

Lemma 3.3.10 *Let* $\Phi \in \mathbf{H}^{1/2}(\partial A)$ *and* $h \in L^2(A)$ *be such that*

$$\int_{\partial A} \Phi \cdot \nu \;=\; \int_A h. \tag{3.3.23}$$

Then there exists $z(\Phi, h)$ *given by*

$$z(\Phi, h) \;:=\; \gamma_l(\Phi) - div_0^{-1}(\nabla \cdot \gamma_l(\Phi) - h), \tag{3.3.24}$$

where

$$\begin{aligned} \nabla \cdot z(\Phi, h) &= h, \quad \gamma(z(\Phi, h)) = \Phi, \\ \|z(\Phi, h)\|_{\mathbf{H}^1(A)} &\leq C(\|\Phi\|_{\mathbf{H}^{1/2}(\partial A)} + \|h\|_{L^2(A)}), \end{aligned} \tag{3.3.25}$$

for some constant C.

Proof: The result follows from Remark 3.3.2 and 3.3.5. Note that equation (3.3.23) gives

$$\int_A (\nabla \cdot \gamma_l(\Phi) - h) \;=\; \int_{\partial A} \Phi \cdot \nu - \int_A h = 0. \tag{3.3.26}$$

Hence $\nabla \cdot \gamma_l(\Phi) - h \in L^2(A)/\mathbb{R}$. ∎

Lemma 3.3.11 *Consider the domain G with boundaries M, Σ and Γ_w shown in Figure 2.1. Let $g|_M \in H^{1/2}(M)$, $g|_\Sigma \in H^{1/2}(\Sigma)$ and $g|_{\Gamma_w} = 0$. Then there exists $z(g) := \nabla p$, where p is uniquely determined by the solution of the following problem: find $p \in H^2(G) \cap \left\{\int_G p = 0\right\}$ satisfying*

$$\begin{aligned} -\Delta p &= 0 \;\; in \;\; G, \\ \partial_{\nu_G} p &= g \;\; on \;\; \partial G. \end{aligned} \tag{3.3.27}$$

Hence, $\nabla \cdot z(g) = 0$ in G. Moreover,

$$\|z(g)\|_{\mathbf{H}^1(G)} \;\leq\; C\left(\|g\|_{H^{1/2}(M)} + \|g\|_{H^{1/2}(\Sigma)}\right), \tag{3.3.28}$$

for some constant C.

Proof:

Let

$$H \;:=\; \left\{ p \in H^1(G),\; \int_G p = 0 \right\}. \tag{3.3.29}$$

We first show that there exists a unique $p \in H$ satisfying

$$\begin{aligned} -\Delta p &= 0 \;\; in \;\; G, \;\; in \;\; the \;\; sense \;\; of \;\; distribution \\ \partial_{\nu_G} p &= g \;\; on \;\; \partial G. \end{aligned} \tag{3.3.30}$$

Note that for $p \in H^1(G)$ a solution of the first equation of (3.3.30), the boundary condition $\partial_{\nu_G} p = g$ is defined in $H^{-1/2}(\partial G)$. Existence and uniqueness is derived from

a variational formulation of (3.3.30). The variational formulation reads: find $p \in H$ such that

$$\int_G \nabla p \cdot \nabla w \;=\; -\int_\Sigma gw + \int_M gw, \quad \forall\, w \in H. \tag{3.3.31}$$

The Poincare-Friedrich's inequality, [34],

$$\|p\|_H \;\leq\; C\|\nabla p\|_{L^2(G)}, \tag{3.3.32}$$

for some constant C, gives the coercivity of the continuous bilinear form $a(.,.) : H \times H \longrightarrow \mathbb{R}$,

$$a(p,w) \;=\; \int_G \nabla p \cdot \nabla w. \tag{3.3.33}$$

The continuity of the linear functional $l(.) : H \longrightarrow \mathbb{R}$,

$$l(w) \;=\; -\int_\Sigma gw + \int_M gw, \tag{3.3.34}$$

follows because $g \in H^{-1/2}(M)$ and $g \in H^{-1/2}(\Sigma)$. The existence and uniqueness of $p \in H$ follow from Lax-Milgram Lemma, [25].

Now to obtain more regularity of the solution p, we follow the approach used in [9] for solutions of Neuman problems. Let $G := [0, L_x] \times [0, L_y]$, $\tilde{G} := G + ([-L_x, L_x], 0) = [-L_x, 2L_x] \times [0, L_y]$, and $\partial\tilde{G} = \tilde{\Sigma} \cup \tilde{\Gamma}_w \cup \tilde{M}$, where $\tilde{\Sigma} = [-L_x, 2L_x] \times \{0\}$, etc.

To show that $p \in H^2(G)$, p is first extended to a harmonic function $\tilde{p}$ in $\tilde{G}$ by even reflection across Γ_w. This extension is possible due to the boundary condition $\partial_\nu p = 0$ on Γ_w. Similarly, on $M \cup \Sigma$ the function g is extended to $\tilde{g}$ on $\tilde{M} \cup \tilde{\Sigma}$ by even reflection. Then $\tilde{p} \in H^1(\tilde{G})$ satisfies

$$\begin{aligned} -\Delta\tilde{p} \;&=\; 0 \;\; in \;\; \tilde{G}, \quad in \;\; the \;\; sense \;\; of \;\; distribution \\ \partial_{\nu_{\tilde{G}}}\tilde{p} \;&=\; \tilde{g} \;\; on \;\; \partial\tilde{G}. \end{aligned} \tag{3.3.35}$$

Now, let $\eta \in \mathcal{D}(\mathbb{R}^2)$ be such that $\eta \equiv 1$ in G, and $supp\{\eta\} \cap \tilde{\Gamma}_w = \emptyset$. Setting $q = \eta\tilde{p}$, it follows that

$$\Delta q \;=\; \tilde{p}\Delta\eta + 2\nabla\tilde{p} \cdot \nabla\eta \in L^2(\tilde{G})$$

$$\partial_{\nu_{\tilde{G}}} q \;=\; \eta\tilde{g} + \tilde{p}\partial_{\nu_{\tilde{G}}}\eta \in H^{1/2}(\partial\tilde{G}). \tag{3.3.36}$$

Hence from [9], $q \in H^2(\tilde{G})$. Since also $q|_G = p$, this shows that $p \in H^2(G)$. Moreover, it follows from [17] that

$$\|\nabla p\|_{H^1(G)} \;\leq\; C\left(\|g\|_{H^{1/2}(\partial G)} + \|\nabla p\|_{L^2(G)}\right). \tag{3.3.37}$$

On the other hand, substituting $w = p$ in (3.3.31) gives

$$\begin{aligned} \|\nabla p\|^2_{\mathbf{L}^2(G)} &\leq \|g\|_{L^2(\Sigma)}\|p\|_{L^2(\Sigma)} + \|g\|_{L^2(M)}\|p\|_{L^2(M)} \\ &\leq C_1\|g\|_{L^2(M\cup\Sigma)}\|\nabla p\|_{\mathbf{L}^2(G)}, \end{aligned} \tag{3.3.38}$$

which follows from Theorem 3.3.4 and Poincare-Friedrich inequality (3.3.32). Hence,

$$\|\nabla p\|_{\mathbf{L}^2(G)} \;\leq\; C_1\|g\|_{L^2(M\cup\Sigma)}. \tag{3.3.39}$$

Now writing $z(g) := \nabla p$ and using the two estimates (3.3.37) and (3.3.39) together with the embedding $H^{1/2}(.) \hookrightarrow L^2(.)$, this proves the required estimate (3.3.28):

$$\begin{aligned} \|z(g)\|_{\mathbf{H}^1(G)} &= \|\nabla p\|_{\mathbf{H}^1(G)} \\ &\leq C\left(\|g\|_{H^{1/2}(M)} + \|g\|_{H^{1/2}(\Sigma)}\right), \end{aligned} \tag{3.3.40}$$

for some constant C. ∎

Proposition 3.3.12 *Let $g \in H^{1/2}(M)$, $\phi \in \mathbb{R}$, and $h \in L^2(A)$ be given. Then there exists $\hat{\mathbf{z}} = \hat{\mathbf{z}}(g,\phi,h) \in \mathbf{H}^1(A\cup G)$, satisfying the following:*

$$\begin{aligned} \nabla\cdot\hat{\mathbf{z}} &= h \quad in \quad A, \\ \hat{\mathbf{z}} &= \nabla p \quad in \quad G, \\ \nabla\cdot\hat{\mathbf{z}} &= 0 \quad in \quad G, \end{aligned} \tag{3.3.41}$$

for some $p \in H^2(G)$, and

$$\begin{aligned}
&\hat{\mathbf{z}} \cdot \nu_G = -g && \text{on } M,\\
&\hat{\mathbf{z}} \cdot \nu_G = 0 && \text{on } \Gamma_w,\\
&\hat{\mathbf{z}} \cdot \tau = 0 && \text{on } \Sigma \cup \Gamma_i \cup \Gamma_o,\\
&\textstyle\int_{\Gamma_i} \hat{\mathbf{z}} \cdot \nu_A = -\phi && \text{on } \Gamma_i,\\
&\hat{\mathbf{z}} = \mathbf{0} && \text{on } \Gamma,
\end{aligned} \tag{3.3.42}$$

where τ denotes the unit tangential vector to $\partial A \cup \partial G$, and ν_A, ν_G respectively denote the exterior unit normal vector to $\partial A, \partial G$. Moreover,

$$\begin{aligned}
\|\hat{\mathbf{z}}\|_{\mathbf{H}^1(A)} + \|\hat{\mathbf{z}}\|_{\mathbf{L}^2(G)} &\leq C(|\phi| + \|h\|_{L^2(A)} + \|g\|_{L^2(M)}),\\
\|\hat{\mathbf{z}}\|_{\mathbf{H}^1(A)} + \|\hat{\mathbf{z}}\|_{\mathbf{H}^1(G)} &\leq C(|\phi| + \|h\|_{L^2(A)} + \|g\|_{H^{1/2}(M)}),
\end{aligned} \tag{3.3.43}$$

for some constant C.

Proof: Since it is required that $\nabla \cdot \hat{\mathbf{z}} = 0$ in G, it follows that

$$0 = \int_G \nabla \cdot \hat{\mathbf{z}} = \int_{\partial G} \hat{\mathbf{z}} \cdot \nu_G = -\int_M g + \int_\Sigma \hat{\mathbf{z}} \cdot \nu_G. \tag{3.3.44}$$

Then,

$$\int_\Sigma \hat{\mathbf{z}} \cdot \nu_G = \int_M g. \tag{3.3.45}$$

Since also $\nabla \cdot \hat{\mathbf{z}} = h$ in A, the boundary conditions (3.3.42) give

$$\int_A h = \int_A \nabla \cdot \hat{\mathbf{z}} = \int_{\partial A} \hat{\mathbf{z}} \cdot \nu_A = -\phi - \int_M g + \int_{\Gamma_o} \hat{\mathbf{z}} \cdot \nu_A, \tag{3.3.46}$$

which results in

$$\int_{\Gamma_o} \hat{\mathbf{z}} \cdot \nu_A = \phi + \int_M g + \int_A h. \tag{3.3.47}$$

Equations (3.3.45), (3.3.47) help to prescribe suitable boundary conditions for $\hat{\mathbf{z}} \cdot \nu_A$ on $\Gamma_i \cup \Sigma \cup \Gamma_o$. For this, choose $\varphi \in \mathcal{D}(\mathbb{R}^2)$, $\varphi|_{\Gamma_i} \in \mathcal{D}(\Gamma_i)$, $\varphi|_\Sigma \in \mathcal{D}(\Sigma)$, and $\varphi|_{\Gamma_o} \in \mathcal{D}(\Gamma_o)$ such that

$$\int_{\Gamma_i} \varphi = \int_\Sigma \varphi = \int_{\Gamma_o} \varphi = 1. \tag{3.3.48}$$

Then the following boundary conditions can be written:

$$\begin{aligned} \hat{\mathbf{z}} \cdot \nu_G &= \varphi \textstyle\int_M g && on \quad \Sigma, \\ \hat{\mathbf{z}} \cdot \nu_A &= -\phi\varphi && on \quad \Gamma_i, \\ \hat{\mathbf{z}} \cdot \nu_A &= \left(\phi + \textstyle\int_M g + \int_A h\right)\varphi && on \quad \Gamma_o. \end{aligned} \tag{3.3.49}$$

Let

$$\begin{aligned} \Phi_A &:= \hat{\mathbf{z}}|_{\partial A}, \\ \Phi_G &:= \hat{\mathbf{z}} \cdot \nu_G|_{\partial G}, \end{aligned} \tag{3.3.50}$$

where $\hat{\mathbf{z}}$ is substituted from the boundary conditions (3.3.42) and (3.3.49). Then according to Lemma 3.3.10 and 3.3.11, there exists an extension $\hat{\mathbf{z}} \in \mathbf{H}^1(A \cup G)$ given by

$$\hat{\mathbf{z}} := \begin{cases} \gamma_l(\Phi_A) - div_0^{-1}(\nabla \cdot \gamma_l(\Phi_A) - h) & in \quad A, \\ \nabla p(\Phi_G) & in \quad G, \end{cases} \tag{3.3.51}$$

where $p = p(\Phi_G) \in H^2(G)$ satisfies, as in Lemma 3.3.11:

$$\begin{aligned} -\Delta p &= 0 && in \quad G \\ \partial_{\nu_G} p &= \Phi_G && on \quad \partial G. \end{aligned} \tag{3.3.52}$$

Also using Lemma 3.3.10, 3.3.11 and inequality (3.3.39), it follows that

$$\begin{aligned} \|\hat{\mathbf{z}}\|_{\mathbf{H}^1(A)} &\leq C\left(\|\Phi_A\|_{\mathbf{H}^{1/2}(\partial A)} + \|h\|_{L^2(A)}\right), \\ \|\hat{\mathbf{z}}\|_{\mathbf{L}^2(G)} &\leq C\|\Phi_G\|_{L^2(\Sigma \cup M)}, \quad and \quad \|\hat{\mathbf{z}}\|_{\mathbf{H}^1(G)} \leq C\|\Phi_G\|_{\mathbf{H}^{1/2}(\Sigma \cup M)}. \end{aligned} \tag{3.3.53}$$

The above estimates in (3.3.53), the boundary conditions (3.3.49) and basic properties of Sobolev spaces result in the required estimates (3.3.43):

$$\begin{aligned} \|\hat{\mathbf{z}}\|_{\mathbf{H}^1(A)} + \|\hat{\mathbf{z}}\|_{\mathbf{L}^2(G)} &\leq C(|\phi| + \|h\|_{L^2(A)} + \|g\|_{L^2(M)}), \\ \|\hat{\mathbf{z}}\|_{\mathbf{H}^1(A)} + \|\hat{\mathbf{z}}\|_{\mathbf{H}^1(G)} &\leq C(|\phi| + \|h\|_{L^2(A)} + \|g\|_{H^{1/2}(M)}). \end{aligned} \tag{3.3.54}$$

∎

Remark 3.3.13 Let us consider the extension $\hat{\mathbf{z}}$ defined in (3.3.51), and take $h = 0$. Then $\hat{z} = \hat{z}(\Phi_A, \Phi_G)$ is bilinear, which follows from the linearity of γ_l, div_0^{-1}, div, and $p = p(\Phi_G)$ being a linear function of Φ_G.

The following remark is going to be used in the subsections 3.3.2 and 3.3.3.

Remark 3.3.14 1. Let β_m, H_m, ϕ and ε be given positive constants. Consider $\hat{c} \in H^{1/2}(M)$, and set

$$\hat{u}_2(\hat{c}) \;=\; -\frac{\beta_m H_m \hat{c}}{\varepsilon} \;\; on \;\; M. \tag{3.3.55}$$

Using Proposition 3.3.12 with $g = \hat{u}_2(\hat{c})$ and $h = 0$, then we obtain the extension $\hat{\mathbf{z}} = \hat{\mathbf{z}}(\hat{c})$ as in (3.3.51),

$$\hat{\mathbf{z}}(\hat{c}) \;:=\; \begin{cases} \gamma_l(\Phi_A(\hat{c})) - div_0^{-1}(\nabla \cdot \gamma_l(\Phi_A(\hat{c})) & in \;\; A, \\ \nabla p(\Phi_G(\hat{c})) & in \;\; G, \end{cases} \tag{3.3.56}$$

where

$$\Phi_A(\hat{c}) \;=\; \begin{cases} (\phi\varphi, 0) & on \;\; \Gamma_i \\ (0,0) & on \;\; \Gamma \\ ((\phi + \int_M \hat{u}_2(\hat{c}))\varphi, 0) & on \;\; \Gamma_o \\ (0, -\varphi \int_M \hat{u}_2(\hat{c})) & on \;\; \Sigma \end{cases} \tag{3.3.57}$$

and

$$\Phi_G(\hat{c}) \;=\; \begin{cases} -\varphi \int_M \hat{u}_2(\hat{c}) & on \;\; \Sigma \\ 0 & on \;\; \Gamma_w \\ -\hat{u}_2(\hat{c}) & on \;\; M \end{cases} \tag{3.3.58}$$

Also, the following estimates hold

$$\begin{aligned} \|\hat{\mathbf{z}}(\hat{c})\|_{\mathbf{H}^1(A)} + \|\hat{\mathbf{z}}(\hat{c})\|_{\mathbf{L}^1(G)} &\leq C\left(|\phi| + \|\hat{c}\|_{L^2(M)}\right), \\ \|\hat{\mathbf{z}}(\hat{c})\|_{\mathbf{H}^1(A)} + \|\hat{\mathbf{z}}(\hat{c})\|_{\mathbf{H}^1(G)} &\leq C\left(|\phi| + \|\hat{c}\|_{H^{1/2}(M)}\right), \end{aligned} \tag{3.3.59}$$

where C is a constant independent of $\hat{c}$.

2. The mapping $(\hat{c},\phi) \longmapsto \hat{\mathbf{z}}(\hat{c},\phi)$ is continuous from $H^{1/2}(M)\times\mathbb{R}$ into $\mathbf{H}^1(A\cup G)$. Note that from (3.3.57) and (3.3.58), $\Phi_A(\hat{c})$ and $\Phi_G(\hat{c})$ are linear functions of $\hat{c}$ and ϕ. This and Remark 3.3.13 implies that $\hat{\mathbf{z}}(\hat{c},\phi)$ is a linear function of $\hat{c}$ and ϕ. Hence, the second estimate of (3.3.59) results in the continuity of the mapping

$$\begin{aligned} H^{1/2}(M)\times\mathbb{R} &\longrightarrow \mathbf{H}^1(A\cup G) \\ (\hat{c},\phi) &\longmapsto \hat{\mathbf{z}}(\hat{c},\phi) \end{aligned} \tag{3.3.60}$$

3. The mapping $\hat{c}\longmapsto\hat{\mathbf{z}}(\hat{c})$ is C^1 from $H^{1/2}(M)$ into $\mathbf{H}^1(A\cup G)$.
This follows from the fact that this mapping is continuous and affine. Taking the derivative of $\hat{\mathbf{z}}(\hat{c})$ at $\hat{c}_0\in H^{1/2}(M)$ in the direction $c\in H^{1/2}(M)$ yields

$$\hat{\mathbf{z}}'(\hat{c}_0)c = \quad = \quad \begin{cases} \gamma_l(\Phi'_A(\hat{c}_0)[c]) - div_0^{-1}(\nabla\cdot\gamma_l(\Phi'_A(\hat{c}_0)[c]) & in \quad A, \\ \nabla p(\Phi'_G(\hat{c}_0)[c]) & in \quad G, \end{cases} \tag{3.3.61}$$

where

$$\Phi'_A(\hat{c}_0)[c] \quad = \quad \begin{cases} (0,0) & on \quad \Gamma_i \\ (0,0) & on \quad \Gamma \\ (\varphi\int_M \hat{u}_2(c),0) & on \quad \Gamma_o \\ (0,-\varphi\int_M \hat{u}_2(c)) & on \quad \Sigma \end{cases} \tag{3.3.62}$$

and

$$\Phi'_G(\hat{c}_0)[c] \quad = \quad \begin{cases} -\varphi\int_M \hat{u}_2(c) & on \quad \Sigma \\ 0 & on \quad \Gamma_w \\ -\hat{u}_2(c) & on \quad M \end{cases} \tag{3.3.63}$$

This shows that $\hat{\mathbf{z}}'(\hat{c}_0)c\in\mathbf{H}^1(A\cup G)$, and the following estimates hold

$$\begin{aligned} \|\hat{\mathbf{z}}'(\hat{c}_0)c\|_{\mathbf{H}^1(A)} + \|\hat{\mathbf{z}}'(\hat{c}_0)c\|_{\mathbf{L}^2(G)} &\leq C\|c\|_{L^2(M)}, \\ \|\hat{\mathbf{z}}'(\hat{c}_0)c\|_{\mathbf{H}^1(A)} + \|\hat{\mathbf{z}}'(\hat{c}_0)c\|_{\mathbf{H}^1(G)} &\leq C\|c\|_{H^{1/2}(M)}, \end{aligned} \tag{3.3.64}$$

where C is a constant independent from $\hat{c}_0$ and c.

4. In subsections 3.3.2 and 3.3.3, the extension $\hat{\mathbf{z}}(\hat{c})$ will be considered in $A_\zeta \cup G$, where $A_\zeta = (I+\zeta)(A)$ is a varying domain as a result of varying the boundary $\Gamma_\zeta = (I+\zeta)(\Gamma)$ with ζ near zero. To avoid the dependency on Γ_ζ and for differentiating $\hat{\mathbf{z}}(\hat{c})$ with respect to ζ, $\hat{\mathbf{z}}(\hat{c})$ is constructed independently from ζ as follows. Let $\epsilon > 0$ and A_ϵ be an open rectangle such that for all ζ near zero

$$A_\epsilon \;:=\; \Sigma \times (0,-\epsilon) \subset A_\zeta, \quad A_\epsilon \cap \Gamma_\zeta = \emptyset, \quad A_\zeta \subset A_\delta, \tag{3.3.65}$$

for some positive δ. Next, the extension $\hat{\mathbf{z}}(\hat{c})$ is obtained in $A_\epsilon \cup G$ using Proposition 3.3.12. Then, $\hat{\mathbf{z}}(\hat{c})$ is extended by zero in the set $\overline{A}_\epsilon^{\,c} \cap A_\delta$.

∎

In order to write the variational formulation of the steady state problem, (2.1.59)-(2.1.69), appropriate spaces are defined by considering the boundary conditions (2.1.59). For the oxygen mass fraction $\hat{c}$, consider the following spaces

$$\hat{C}_\zeta = \{\hat{c} \in \mathcal{C}^\infty(\Omega_\zeta) : \hat{c} = c_{in} \;\; on \;\; \Gamma_{i,\zeta}\}, \qquad C_\zeta = \{c \in \mathcal{C}^\infty(\Omega_\zeta), c = 0 \;\; on \;\; \Gamma_{i,\zeta}\}, \tag{3.3.66}$$

and their closure in $H^1(\Omega_\zeta)$:

$$\hat{\mathbf{C}}_\zeta = \overline{\hat{C}}_\zeta, \qquad \mathbf{C}_\zeta = \overline{C}_\zeta, \tag{3.3.67}$$

For the velocity variable $\hat{\mathbf{u}}$,

$$\begin{aligned}
\hat{U}_\zeta \;&=\; \big\{\hat{\mathbf{u}} = (\hat{u}_1, \hat{u}_2) \in \mathcal{C}^\infty(\Omega_\zeta)^2, \hat{u}_1|_{\Gamma_\zeta \cup \Sigma \cup \Gamma_w} = 0, \hat{u}_2|_{\Gamma_{i,\zeta} \cup \Gamma_\zeta \cup \Gamma_{o,\zeta}} = 0, \\
&\qquad\qquad [\hat{u}_2]_\Sigma = 0, \nabla \cdot \hat{\mathbf{u}} = 0, \hat{\mathbf{u}} = \nabla \hat{p} \; in \;\; G, \; for \; some \; \hat{p} \in \mathcal{C}^\infty(\Omega_\zeta)\big\}, \\
U_\zeta \;&=\; \Big\{\mathbf{u} = (u_1, u_2) \in \hat{U}_\zeta : u_2 = 0 \;\; on \;\; M\Big\},
\end{aligned} \tag{3.3.68}$$

and their closure for the norm $\|.\|_{\mathbf{H}^1(A_\zeta)} + \|.\|_{\mathbf{L}^2(G)}$ in $\mathbf{H}^1(A_\zeta) \otimes \mathbf{L}^2(G)$:

$$\hat{\mathbf{U}}_\zeta = \overline{\hat{U}}_\zeta, \qquad \mathbf{U}_\zeta = \overline{U}_\zeta. \tag{3.3.69}$$

For the pressure variable $\hat{p}$, we have

$$P_{A_\zeta} \;=\; \left\{\mathbf{p}=(p,p_{in})\in L^2(A_\zeta)\times\mathbb{R}\right\}, \tag{3.3.70}$$

with the following inner product:

$$<\mathbf{p},\mathbf{q}>_{P_{A_\zeta}\times P_{A_\zeta}} \;:=\; <p,q>_{L^2(A_\zeta)\times L^2(A_\zeta)} + p_{in}q_{in}. \tag{3.3.71}$$

Hence P_{A_ζ} is a Hilbert space, and its norms is defined by means of the inner product:

$$\|\mathbf{p}\|^2_{P_{A_\zeta}} \;=\; <\mathbf{p},\mathbf{p}>_{P_{A_\zeta}\times P_{A_\zeta}} = \|p\|^2_{L^2(A)} + p_{in}^2. \tag{3.3.72}$$

When $\zeta=\mathbf{0}$, the above spaces are written simply as $\mathbf{U}$, $\mathbf{C}$, P_A, etc.

Lemma 3.3.15 *$\mathbf{U}_\zeta$ is a closed Hilbert space. In fact, every $\mathbf{u}\in\mathbf{U}_\zeta$ satisfies*

1. *$\nabla\cdot\mathbf{u}=0$ in $H^{-1}(G)$, $\mathbf{u}=\nabla p$ in $L^2(G)$ for some $p\in H^1(G)$.*
2. *$\mathbf{u}\cdot\nu\in H^{-1/2}(\partial G)$, $\mathbf{u}\cdot\nu=0$ on $M\cup\Gamma_w$, and $u_2(.,0^+)=\lim_{y\to 0^+}u_2(.,y)\in H^{1/2}(\Sigma)$.*
3. *$\mathbf{u}\in\mathbf{H}^1(G)$ and $\|\mathbf{u}\|_{\mathbf{H}^1(G)}\le C\|\mathbf{u}\|_{\mathbf{H}^1(A)}$, for some constant C independent from $\mathbf{u}$.*

Proof:

1. Let $\{\mathbf{u}_n\}\subset U_\zeta$, $\mathbf{u}_n\to\mathbf{u}\in\mathbf{U}_\zeta$. Then, $\nabla\cdot\mathbf{u}_n=0$ in G, and $\forall\Phi\in H^1_0(G)$,

$$\begin{aligned} <\nabla\cdot\mathbf{u},\Phi>_{H^{-1}(G)\times H^1_0(G)} &= -\int_G \mathbf{u}\cdot\nabla\Phi = -\lim_{n\to\infty}\int_G \mathbf{u}_n\cdot\nabla\Phi \\ &= \lim_{n\to\infty}\int_G(\nabla\cdot\mathbf{u}_n)\,\Phi = 0. \end{aligned} \tag{3.3.73}$$

   Hence $\nabla\cdot\mathbf{u}=0$ in $H^{-1}(G)$.

   Also, for every $\mathbf{u}_n\in U_\zeta$, $\mathbf{u}_n=\nabla p_n$ for some $p_n\in H^1(G)$. Let $\mathbf{w}\in\mathcal{D}(G)^2\cap\{\nabla\cdot\mathbf{w}=0\}$. Then,

$$\int_G\mathbf{u}\cdot\mathbf{w} \;=\; \lim_{n\to\infty}\int_G\mathbf{u}_n\cdot\mathbf{w} = \lim_{n\to\infty}\int_G\nabla p_n\cdot\mathbf{w}$$

$$= \quad - \lim_{n\to\infty} \int_G p_n \nabla \cdot \mathbf{w} = 0. \tag{3.3.74}$$

Hence, from [34] there exists $p \in H^1(G)$ such that $\mathbf{u} = \nabla p$ in G.

2. For every $\mathbf{u} \in \mathbf{U}_\zeta$, $\mathbf{u} \in L^2(G) \cap \{\nabla \cdot \mathbf{u} = 0\}$. Then from [34], there exists a continuous linear map (the normal component of the trace operator), $\gamma_\nu : \mathbf{U}_\zeta \to H^{-1/2}(\partial G)$ such that

$$\gamma_\nu(\mathbf{u}) = \mathbf{u} \cdot \nu, \quad a.e \quad on \quad \partial G, \quad \forall \mathbf{u} \in U_\zeta. \tag{3.3.75}$$

Since $\mathbf{u} \cdot \nu = 0$ for every $\mathbf{u} \in U_\zeta$, the continuity of γ_ν gives $\gamma_\nu(\mathbf{u}) = \mathbf{u} \cdot \nu = 0$ on $\Gamma_w \cup M$ for every $\mathbf{u} \in \mathbf{U}_\zeta$.

To show that $u_2 \in H^{1/2}(\Sigma)$, let $\mathbf{u}_n \to \mathbf{u} \in \mathbf{U}_\zeta$. Then from the continuity of the trace, it follows that $u_2^n(., 0^+) \to u_2(., 0^+)$ in $H^{-1/2}(\Sigma)$, and $u_2^n(., 0^-) \to u_2(., 0^-)$ in $H^{1/2}(\Sigma)$. Since $u_2^n(., 0^-) = u_2^n(., 0^+)$ for all n, we obtain $u_2(., 0^-) = u_2(., 0^+)$ in $H^{-1/2}(\Sigma)$. But, since $u_2(., 0^-) \in H^{1/2}(\Sigma)$, it follows that $u_2(., 0^+) = u_2(., 0^-) \in H^{1/2}(\Sigma)$.

3. From items 1 and 2, every $\mathbf{u} \in \mathbf{U}_\zeta$ satisfies

$$\begin{aligned} \mathbf{u} = \nabla p, \quad \nabla \cdot \mathbf{u} &= 0 \quad in \quad G, \\ \partial_\nu p &= 0 \quad on \quad \Gamma_w \cup M, \\ \partial_\nu p &= u_2(., 0^-) \quad on \quad \Sigma. \end{aligned} \tag{3.3.76}$$

Then from Lemma 3.3.11, it follows that $\mathbf{u} \in \mathbf{H^1(G)}$ and

$$\|\mathbf{u}\|_{\mathbf{H^1(G)}} \quad \leq \quad C_1 \|u_2\|_{H^{1/2}(\Sigma)} \leq C \|\mathbf{u}\|_{\mathbf{H^1(A_\zeta)}} \tag{3.3.77}$$

∎

Proposition 3.3.16 *For every* $\mathbf{q} = (q, q_{in}) \in P_A$, *there exists* $\mathbf{z}(\mathbf{q}) \in \mathbf{H}^1(A \cup G)$ *such that*

$$\begin{aligned} \nabla \cdot \mathbf{z}(\mathbf{q}) &= -q \quad in \quad A, \\ \int_{\Gamma_i} \mathbf{z}(\mathbf{q}) \cdot \nu_A &= -q_{in}, \\ \|\mathbf{z}(\mathbf{q})\|_{\mathbf{H}^1(A)} + \|\mathbf{z}(\mathbf{q})\|_{\mathbf{H}^1(G)} &\leq C\left(|q_{in}| + \|q\|_{L^2(A)}\right), \end{aligned} \tag{3.3.78}$$

where C *is a constant independent from* $\mathbf{q}$.

Proof: Using Lemma 3.3.12, and taking $g = 0$ on M, $h = -q$ in A, and $\phi = q_{in}$, it follows from estimate (3.3.43) that

$$\|\mathbf{z}(\mathbf{q})\|_{\mathbf{H}^1(A)} + \|\mathbf{z}(\mathbf{q})\|_{\mathbf{H}^1(G)} \leq C\left(|q_{in}| + \|q\|_{L^2(A)}\right), \tag{3.3.79}$$

where C is independent from $\mathbf{q}$. ∎

Definition 3.3.17 *Define the bilinear mappings*

$$\begin{aligned} \alpha(.,.) : \mathbf{U} \times \mathbf{U} &\longrightarrow \mathbb{R}, \\ \beta(.,.) : \mathbf{U} \times P_A &\longrightarrow \mathbb{R}, \end{aligned} \tag{3.3.80}$$

given by

$$\begin{aligned} \alpha(\mathbf{u}, \mathbf{v}) &= \int_A \mu \nabla \mathbf{u} \cdot \nabla \mathbf{v} + \int_G \frac{\mu}{K} \mathbf{u} \cdot \mathbf{v}, \\ \beta(\mathbf{u}, \mathbf{q}) &= -\int_A q \nabla \cdot \mathbf{u} - q_{in} \int_{\Gamma_i} \mathbf{u} \cdot \nu_A. \end{aligned} \tag{3.3.81}$$

Lemma 3.3.18 *The mapping* $\beta(.,.)$, *defined above, is continuous. Also, it satisfies the compatibility condition: there exists a constant* C_β *such that for every* $\mathbf{q} \in P_A$, *there exists a nonzero* $\mathbf{z}(\mathbf{q}) \in \mathbf{U}$ *such that*

$$\beta(\mathbf{z}(\mathbf{q}), \mathbf{q}) \geq C_\beta \|\mathbf{z}(\mathbf{q})\|_{\mathbf{U}} \|\mathbf{q}\|_{P_A}. \tag{3.3.82}$$

Proof: The continuity of β results from

$$\begin{aligned} |\beta(\mathbf{u},\mathbf{q})| &\leq \|\nabla\cdot\mathbf{u}\|_{L^2(A)}\|q\|_{L^2(A)} + |q_{in}|\|\mathbf{u}\cdot\nu_A\|_{L^1(\Gamma_i)} \\ &\leq C\|\mathbf{u}\|_{\mathbf{H}^1(A)}\left(\|q\|_{L^2(A)} + |q_{in}|\right) \\ &\leq \sqrt{2}C\|\mathbf{u}\|_{\mathbf{U}}\|\mathbf{q}\|_{P_A}, \end{aligned} \tag{3.3.83}$$

where the second inequality follows from the embeddings $\mathbf{H}^1(A) \hookrightarrow H^{1/2}(\Gamma_i) \hookrightarrow L^1(\Gamma_i)$.

For the compatibility, Proposition 3.3.16 gives: for every $\mathbf{q} \in P_A$, there exists $\mathbf{z}(\mathbf{q}) \in \mathbf{U}$ such that

$$\begin{aligned} \nabla\cdot\mathbf{z}(\mathbf{q}) &= -q \ \ in \ \ A, \\ \int_{\Gamma_i} \mathbf{z}(\mathbf{q})\cdot\nu_A &= -q_{in}, \\ \|\mathbf{z}(\mathbf{q})\|_{\mathbf{U}} &\leq C\|\mathbf{q}\|_{P_A}, \end{aligned} \tag{3.3.84}$$

where C is independent from $\mathbf{q}$. Hence, there exists a constant $C_\beta := \frac{1}{C}$ for every $\mathbf{q} \in P_A$ such that

$$\begin{aligned} \beta(\mathbf{z}(\mathbf{q}),\mathbf{q}) &= \int_A q^2 + q_{in}^2 = \|\mathbf{q}\|_{P_A}^2 \\ &\geq C_\beta\|\mathbf{z}(\mathbf{q})\|_{\mathbf{U}}\|\mathbf{q}\|_{P_A}. \end{aligned} \tag{3.3.85}$$

∎

The following lemma, [24], is going to be used to prove the existence and uniqueness of the solution for Stokes problem.

Lemma 3.3.19 ([24], page 249) *Let* $\mathbf{X}$ *and* Y *be Banach spaces, and*

$$\begin{aligned} a(.,.) : \mathbf{X}\times\mathbf{X} &\longrightarrow \mathbb{R}, \\ b(.,.) : \mathbf{X}\times Y &\longrightarrow \mathbb{R}. \end{aligned} \tag{3.3.86}$$

be bilinear mappings. Consider the following problem: find $(\mathbf{u}, p) \in \mathbf{X} \times Y$ *such that*

$$\begin{aligned} a(\mathbf{u}, \mathbf{v}) + b(\mathbf{v}, p) &= < f, \mathbf{v} >_{\mathbf{X}^* \times \mathbf{X}} \quad \forall\ \mathbf{v} \in \mathbf{X}, \\ b(\mathbf{u}, q) &= < g, q >_{Y^* \times Y} \quad \forall\ q \in Y. \end{aligned} \tag{3.3.87}$$

Suppose also that there exist $\gamma, \delta, \omega,$ *and* β^* *positive constants such that*

1. $|a(\mathbf{u}, \mathbf{u})| \geq \omega \|\mathbf{u}\|^2_{\mathbf{X}}$, *for all* $\mathbf{u} \in \mathbf{X^0} := \mathbf{X} \cap \{\mathbf{u} | b(\mathbf{u}, q) = 0, \forall q \in Y\}$;

2. $|a(\mathbf{u}, \mathbf{v})| \leq \gamma \|\mathbf{u}\|_{\mathbf{X}} \|\mathbf{v}\|_{\mathbf{X}}$, *for all* $\mathbf{u}, \mathbf{v} \in \mathbf{X}$;

3. $|b(\mathbf{v}, q)| \leq \delta \|\mathbf{v}\|_{\mathbf{X}} \|q\|_Y$, *for all* $\mathbf{v} \in \mathbf{X},\ q \in Y$;

4. *for every* $q \in Y$ *there exists* $\mathbf{v} \neq \mathbf{0}$:

$$b(\mathbf{v}, q) \geq \beta^* \|\mathbf{v}\|_{\mathbf{X}} \|q\|_Y. \tag{3.3.88}$$

Then for every $f \in \mathbf{X}^*$ *and* $g \in Y^*$, *there exists a unique solution* $(\mathbf{u}, p) \in \mathbf{X} \times Y$ *satisfying (3.3.87), and the map*

$$(f, g) \longmapsto (\mathbf{u}, p) \tag{3.3.89}$$

is an isomorphism from $\mathbf{X}^* \times Y^*$ *onto* $\mathbf{X} \times Y$. *Also,*

$$\begin{aligned} \|\mathbf{u}\|_{\mathbf{X}} &\leq \frac{1}{\omega} \left(\|f\|_{\mathbf{X}^*} + \frac{\omega + \gamma}{\beta^*} \|g\|_{Y^*} \right), \\ \|q\|_Y &\leq \frac{1}{\beta^*} \left[\left(1 + \frac{\gamma}{\omega} \right) \|f\|_{\mathbf{X}^*} + \frac{\gamma(\omega + \gamma)}{\omega \beta^*} \|g\|_{Y^*} \right]. \end{aligned} \tag{3.3.90}$$

Lemma 3.3.20 *Let* $f \in \mathbf{U}^*$ *and* $g \in P_A^*$, *and* $\alpha(.,.)$ *and* $\beta(.,.)$ *be defined as in Definition 3.3.17. Then the following problem has a unique solution: find* $(\mathbf{u}, \mathbf{p}) \in \mathbf{U} \times P_A$ *such that*

$$\alpha(\mathbf{u}, \mathbf{v}) + \beta(\mathbf{v}, \mathbf{p}) = < f, \mathbf{v} >_{\mathbf{U}^* \times \mathbf{U}}, \quad \forall \mathbf{v} \in \mathbf{U},$$

$$\beta(\mathbf{u},\mathbf{q}) \;=\; <g,\mathbf{q}>_{P_A^*\times P_A},\quad \forall \mathbf{q}\in P_A, \tag{3.3.91}$$

with

$$\begin{aligned}\|\mathbf{u}\|_{\mathbf{U}} &\le C_1\left(\|f\|_{\mathbf{U}^*}+\|g\|_{P_A^*}\right),\\ \|\mathbf{p}\|_{P_A} &\le C_2\left(\|f\|_{\mathbf{U}^*}+\|g\|_{P_A^*}\right),\end{aligned} \tag{3.3.92}$$

where C_1 and C_2 are constants independent from $\mathbf{u}$, $\mathbf{p}$, f and g. Moreover,

$$\|\mathbf{u}\|_{\mathbf{H}^1(A)}+\|\mathbf{u}\|_{\mathbf{H}^1(G)} \;\le\; C\left(\|f\|_{\mathbf{U}^*}+\|g\|_{P_A^*}\right). \tag{3.3.93}$$

Proof: The bilinear mapping $\alpha(.,.)$ defines an inner-product on $\mathbf{U}_\zeta$, and hence it is a continuous, coercive bilinear form. Since also the mapping $\beta(.,.)$ is continuous and satisfies the compatibility condition, the existence and uniqueness of the solution for this problem as well as the first two estimates (3.3.92) follow from Lemma 3.3.19. The third estimate (3.3.93) is a result of Lemma 3.3.15, as for every $\mathbf{u}\in\mathbf{U}$,

$$\|\mathbf{u}\|_{\mathbf{H}^1(G)} \;\le\; C\|\mathbf{u}\|_{\mathbf{H}^1(A)}. \tag{3.3.94}$$

∎

Lemma 3.3.21 *Let $\hat{\mathbf{u}}\in\mathbf{L}^{\overline{p}}(\Omega)$ for some $\overline{p}>2$. Then the following problem: find $c\in\mathbf{C}$ such that*

$$\int_\Omega \varepsilon\left(D^{eff}\nabla c\cdot\nabla\varphi+\varphi\hat{\mathbf{u}}\cdot\nabla c\right)+\int_M H_m c\varphi \;=\; -\int_M H_m c_{in}\varphi, \forall\varphi\in\mathbf{C}, \tag{3.3.95}$$

has a unique solution $c\in\mathbf{C}\cap W^{1,p}(\Omega)$, for some $p>2$ satisfying $\frac{1}{\overline{p}}+\frac{1}{p}\le\frac{1}{2}$. Also,

$$\|\nabla c\|_{\mathbf{L}^2(\Omega)} \;\le\; c_{in}C_1\left(1+\|\hat{\mathbf{u}}\|_{\mathbf{L}^2(\Omega)}\right), \tag{3.3.96}$$

$$\|\nabla c\|_{\mathbf{L}^p(\Omega)} \;\le\; C_2\|\hat{\mathbf{u}}\|_{\mathbf{L}^{\overline{p}}(\Omega)}\|\nabla c\|_{\mathbf{L}^2(\Omega)}, \tag{3.3.97}$$

for some constants C_1 and C_2.

Proof: See [6] and [21]. ∎

3.3.2 Variational Formulation of the Steady State Problem

The goal of this subsection is to write a weak formulation of the steady state equations (2.1.69) coupled with the boundary conditions (2.1.59). This will be used to obtain the existence and uniqueness of the solution for the steady state problem. Let $\varphi \in C_\zeta$. Then from (2.1.69) and (2.1.59), it follows that the oxygen mass fraction $\hat{c}$ satisfies

$$\begin{aligned} 0 &= \int_{\Omega_\zeta} \varepsilon \left(D^{eff} \nabla \hat{c} \cdot \nabla \varphi + \varphi \hat{\mathbf{u}} \cdot \nabla \hat{c} \right) - \int_{\partial \Omega_\zeta} D \varphi \partial_\nu \hat{c} \\ &= \int_{\Omega_\zeta} \varepsilon \left(D^{eff} \nabla \hat{c} \cdot \nabla \varphi + \varphi \hat{\mathbf{u}} \cdot \nabla \hat{c} \right) + \int_M h_M(\hat{c}) \varphi, \end{aligned} \tag{3.3.98}$$

where

$$h_M(\hat{c}) = H_m \hat{c} \, (1 + \beta_m \hat{c}) \approx H_m \hat{c} \quad on \quad M, \tag{3.3.99}$$

since $\hat{c} << 1$ on M and $\beta_m < 1$. Writing $\hat{c} = c + c_i$, $c \in C_\zeta$, then (3.3.98) reduces to

$$\int_{\Omega_\zeta} \varepsilon \left(D^{eff} \nabla c \cdot \nabla \varphi + \varphi \hat{\mathbf{u}} \cdot \nabla c \right) + \int_M H_m \hat{c} \varphi = 0, \quad \forall \varphi \in C_\zeta. \tag{3.3.100}$$

The following boundary conditions:

$$\hat{p} = p_{out} \quad on \quad \Gamma_{o,\zeta}, \quad \hat{u}_2 = -\frac{\beta_m H_m \hat{c}}{\varepsilon} \quad on \quad M, \quad \int_{\Gamma_{i,\zeta}} \hat{u}_1 = \phi, \tag{3.3.101}$$

will be treated as follows. The pressure variable is written as $\hat{p} = p + p_{out}$. Then, $p = 0$ on $\Gamma_{o,\zeta}$. The velocity is written as $\hat{\mathbf{u}} = \mathbf{u} + \hat{\mathbf{z}}(\hat{c})$, where $\hat{\mathbf{z}}(\hat{c}) \in \mathbf{H}^1(A_\zeta \cup G)$ is the extension defined in Lemma 3.3.12 and Remark 3.3.14, with $g = \hat{z}_2 = -\frac{\beta_m H_m \hat{c}}{\varepsilon}$ *on* M, $h = 0$ in A and using the same ϕ given in (3.3.101). With this setting, it implies that $\mathbf{u} \in \mathbf{U}_\zeta$, and $u_2 = 0$ on M, and $\int_{\Gamma_i} u_1 = 0$. The extension $\hat{\mathbf{z}}(\hat{c})$ is constructed independently from ζ, see item 4 in Remark 3.3.14.

Now multiplying Stokes and Darcy equations in (2.1.69) by a test function $\mathbf{v} \in U_\zeta$, and using the divergence theorem gives

$$\begin{aligned} 0 &= \int_{A_\zeta} (-\mu\Delta\hat{\mathbf{u}} + \nabla\hat{p}) \cdot \mathbf{v} + \int_G \Big(\frac{\mu}{K}\hat{\mathbf{u}} + \nabla\hat{p}\Big) \cdot \mathbf{v} \\ &= \int_{A_\zeta} [\mu\nabla\left(\mathbf{u} + \hat{\mathbf{z}}(\hat{c})\right) \cdot \nabla\mathbf{v} - p\nabla\cdot\mathbf{v}] + \int_G \frac{\mu}{K}\left(\mathbf{u} + \hat{\mathbf{z}}(\hat{c})\right) \cdot \mathbf{v} \\ &\quad + \int_{\partial A_\zeta} -\mu\mathbf{v}\cdot\partial_\nu\left(\mathbf{u} + \hat{\mathbf{z}}(\hat{c})\right) + \int_{\partial A_\zeta \cup \partial G} p\mathbf{v}\cdot\nu, \quad \forall \mathbf{v} \in U_\zeta. \end{aligned} \tag{3.3.102}$$

Using the boundary conditions (2.1.59), (3.3.102) simplifies to

$$\int_{A_\zeta} \mu\nabla\mathbf{u}\cdot\nabla\mathbf{v} + \int_G \frac{\mu}{K}\mathbf{u}\cdot\mathbf{v} - \int_{A_\zeta} p\nabla\cdot\mathbf{v} - p_{in}\int_{\Gamma_{i,\zeta}} v_1 = l(\hat{\mathbf{z}}(\hat{c}))(\mathbf{v}), \tag{3.3.103}$$

for all $\mathbf{v} \in U_\zeta$, where $l : \mathbf{H}^1(A_\zeta) \otimes \mathbf{L}^2(G) \longrightarrow \mathbf{U}_\zeta^*$ is given by

$$l(\hat{\mathbf{z}}(\hat{c}))(\mathbf{v}) = -\int_{A_\zeta} \mu\nabla\hat{\mathbf{z}}(\hat{c})\cdot\nabla\mathbf{v} - \int_G \frac{\mu}{K}\hat{\mathbf{z}}(\hat{c})\cdot\mathbf{v}. \tag{3.3.104}$$

To enforce the conditions $\nabla\cdot\mathbf{u} = 0$ in A_ζ and $\int_{\Gamma_{i,\zeta}} u_1 = 0$, the velocity $\mathbf{u}$ must satisfy

$$-\int_{A_\zeta} q\nabla\cdot\mathbf{u} - q_{in}\int_{\Gamma_{i,\zeta}} u_1 = 0, \quad \forall\ \mathbf{q} = (q, q_{in}) \in P_{A_\zeta}. \tag{3.3.105}$$

Using equations (3.3.100), (3.3.103)-(3.3.105) and the mappings $\alpha(.,.)$ and $\beta(.,.)$ given in Definition 3.3.17, then the variational formulation of the state problem reads:
Find $(c, \mathbf{u}, p) \in \mathbf{C}_\zeta \times \mathbf{U}_\zeta \times P_A$ satisfying

$$\begin{aligned} \int_{\Omega_\zeta} \varepsilon\left(D^{eff}\nabla c\cdot\nabla\varphi + \varphi\hat{\mathbf{u}}\cdot\nabla c\right) + \int_M H_m\hat{c}\varphi &= 0, \quad \forall\varphi \in \mathbf{C}_\zeta, \\ \alpha(\mathbf{u}, \mathbf{v}) + \beta(\mathbf{v}, \mathbf{p}) &= l(\hat{\mathbf{z}}(\hat{c}))(\mathbf{v}), \quad \forall\ \mathbf{v} \in \mathbf{U}_\zeta, \\ \beta(\mathbf{u}, \mathbf{q}) &= 0, \quad \forall\ \mathbf{q} \in P_{A_\zeta}. \end{aligned} \tag{3.3.106}$$

The existence and uniqueness of the above problem is proved using a fixed point technique. The proof follows from Proposition 3.3.20 and Lemma 3.3.21 beside the work done by [21]. The proof is similar to the work presented in sections 3.3 and 3.4, so it will not be repeated.

3.3.3 Shape differentiability of the state variables

The goal of this section is to investigate the shape differentiability of the state variables. For this, the weak formulation (3.3.106) is first written in fixed domains: A, G and Ω, which results by taking $\zeta = \mathbf{0}$. Let us use the following notations:

$$\begin{aligned} c_\zeta &= c(\zeta) \circ (I + \zeta), \\ \mathbf{u}_\zeta &= (u_{\zeta,1}, u_{\zeta,2}) = \mathbf{u}(\zeta) \circ (I + \zeta), \\ p_\zeta &= p(\zeta) \circ (I + \zeta), \\ \mathbf{p}_\zeta &= (p_\zeta, p_{in}). \end{aligned} \tag{3.3.107}$$

Then c_ζ, $\mathbf{u}_\zeta$, and $\mathbf{p}_\zeta$ are defined in fixed domains A, G and Ω independent of ζ.
To prove the shape differentiability of $c_\zeta, \mathbf{u}_\zeta$ and $\mathbf{p}_\zeta$, the following implicit mapping theorem is implemented.

Theorem 3.3.22 ([20], page 352) *Let X, Y, Z be Banach spaces. Let the mapping*

$$K : X \times Y \longrightarrow Z \tag{3.3.108}$$

be Fréchet differentiable. If $(x_0, y_0) \in X \times Y$ satisfies

1. *$K(x_0, y_0) = 0$*
2. *$y \longrightarrow \partial_y K(x_0, y_0)$ is a Banach space isomorphism from Y onto Z,*

then there exist neighborhoods U_{x_0} of x_0, V_{y_0} of y_0, and a Fréchet differentiable function

$$f : U_{x_0} \longrightarrow V_{y_0} \tag{3.3.109}$$

such that $K(x, f(x)) = 0$, and

$$K(x, y) = 0 \ \textit{iff} \ y = f(x), \quad \forall (x, y) \in U_{x_0} \times V_{y_0}. \tag{3.3.110}$$

Now to write the weak formulation (3.3.106) in fixed domains, independent of ζ, some shape calculus results from section 3.1 are used.

For $x_\zeta \in \Omega_\zeta = (I+\zeta)(\Omega)$, then

$$\begin{aligned} x_\zeta &= (I+\zeta)(x), \\ dx_\zeta &= Jac(I+\zeta)dx, \\ \left(\nabla_{x_\zeta} u\right)(x_\zeta) &= M(\zeta)\nabla_x \left(u \circ (I+\zeta)\right)(x), \end{aligned} \tag{3.3.111}$$

where $M(\zeta) = \left[\nabla_x (I+\zeta)\right]^{-T}$, and T denotes the transpose operator. Hence,

$$\left(\nabla_{x_\zeta} \cdot \mathbf{u}(\zeta)\right)(x_\zeta) = \Sigma_{i,j=1}^2 M_{i,j}(\zeta)\partial_j \left(u_{\zeta,i}\right)(x). \tag{3.3.112}$$

Then the variational problem (3.3.106) is written as:

Find $(c_\zeta, \mathbf{u}_\zeta, \mathbf{p}_\zeta) \in \mathbf{C} \times \mathbf{U} \times P_A$ such that

$$\begin{aligned} 0 &= \int_\Omega \varepsilon \left(D^{eff} M(\zeta)\nabla c_\zeta \cdot M(\zeta)\nabla\varphi + \varphi \hat{\mathbf{u}}_\zeta \cdot M(\zeta)\nabla c_\zeta\right) Jac(I+\zeta) + \int_M H_m \hat{c}_\zeta \varphi, \quad \forall \varphi \in \mathbf{C}, \\ 0 &= \int_A \left(\mu M(\zeta)\nabla \mathbf{u}_\zeta \cdot M(\zeta)\nabla \mathbf{v}\right) Jac(I+\zeta) + \int_G \frac{\mu}{K}\mathbf{u}_\zeta \cdot \mathbf{v} \\ &\quad - \int_A \left(p_\zeta \Sigma_{i,j=1}^2 M_{i,j}(\zeta)\partial_j v_i\right) Jac(I+\zeta) - p_{in}\int_{\Gamma_i} v_1 |1+\partial_y \zeta_2| \\ &\quad + \int_A \left(\mu M(\zeta)\nabla \hat{\mathbf{u}}(\hat{c}_\zeta) \cdot M(\zeta)\nabla \mathbf{v}\right) Jac(I+\zeta) + \int_G \frac{\mu}{K}\hat{\mathbf{u}}(c_\zeta)\cdot \mathbf{v}, \qquad \forall \mathbf{v} \in \mathbf{U}, \\ 0 &= -\int_A \left(q \Sigma_{i,j=1}^2 M_{i,j}(\zeta)\partial_j u_{\zeta,i}\right) Jac(I+\zeta) \\ &\quad -q_{in}\int_{\Gamma_i} u_{1,\zeta}|1+\partial_y\zeta_2|, \qquad \forall\, \mathbf{q} = (q, q_{in}) \in P_A. \end{aligned} \tag{3.3.113}$$

Now the shape differentiability of $c_\zeta, \mathbf{u}_\zeta, \mathbf{p}_\zeta$ at $\zeta = 0$ is proved by using Theorem 3.3.22, in which we take

$$\begin{aligned} X &= C^2(\mathbb{R}^2;\mathbb{R}^2), \\ Y &= \mathbf{C} \times \mathbf{U} \times P_A, \\ Z &= Y^* := \mathbf{C}^* \times \mathbf{U}^* \times P_A^*. \end{aligned} \tag{3.3.114}$$

Definition 3.3.23 *Using (3.3.114) and setting* $\mathbf{y} = (c, \mathbf{u}, \mathbf{p}) \in Y$, $\tilde{\mathbf{y}} = (\varphi, \mathbf{v}, \mathbf{q}) \in Y$, *the mapping* F,

$$\mathbf{F} = (F_1, F_2, F_3) : C^2(\mathbb{R}^2; \mathbb{R}^2) \times Y \quad \rightarrow \quad Y^*, \tag{3.3.115}$$

is defined as

$$\begin{aligned}
F_1(\zeta, \mathbf{y})(\tilde{\mathbf{y}}) &= \int_\Omega \varepsilon \left(D^{eff} M(\zeta) \nabla c \cdot M(\zeta) \nabla \varphi + \varphi \hat{\mathbf{u}} \cdot M(\zeta) \nabla c \right) Jac(I + \zeta) \\
&\quad + \int_M H_m \hat{c} \varphi, \qquad (3.3.116) \\
F_2(\zeta, \mathbf{y})(\tilde{\mathbf{y}}) &= \int_A \left(\mu M(\zeta) \nabla \mathbf{u} \cdot M(\zeta) \nabla \mathbf{v} \right) Jac(I + \zeta) + \int_G \frac{\mu}{K} \mathbf{u} \cdot \mathbf{v} \\
&\quad - \int_A \left(p \Sigma_{i,j=1}^2 M_{i,j}(\zeta) \partial_j v_i \right) Jac(I + \zeta) - p_{in} \int_{\Gamma_i} v_1 |1 + \partial_y \zeta_2| \\
&\quad + \int_A \left(\mu M(\zeta) \nabla \hat{\mathbf{u}}(\hat{c}) \cdot M(\zeta) \nabla \mathbf{v} \right) Jac(I + \zeta) \\
&\quad + \int_G \frac{\mu}{K} \hat{\mathbf{u}}(\hat{c}) \cdot \mathbf{v}, \qquad (3.3.117) \\
F_3(\zeta, \mathbf{y})(\tilde{\mathbf{y}}) &= - \int_A \left(q \Sigma_{i,j=1}^2 M_{i,j}(\zeta) \partial_j u_i \right) Jac(I + \zeta) \\
&\quad - q_{in} \int_{\Gamma_i} u_1 |1 + \partial_y \zeta_2|. \qquad (3.3.118)
\end{aligned}$$

Now we verify the requirements of the Implicit Mapping Theorem 3.3.22.

Proposition 3.3.24 *There exists* $\mathbf{y}_\zeta = (c_\zeta, \mathbf{u}_\zeta, \mathbf{p}_\zeta) \in Y$ *that satisfies*

$$\mathbf{F}\left(\zeta, \mathbf{y}_\zeta\right) \tilde{\mathbf{y}} \quad = \quad 0, \quad \forall \tilde{\mathbf{y}} \in Y, \tag{3.3.119}$$

for ζ *near zero.*

Proof: This follows from existence and uniqueness of the solution for the weak formulation (3.3.106) which results from Proposition 3.3.20 and Lemma 3.3.21 beside the work done by [21]. ∎

Proposition 3.3.25 *The map* $\mathbf{F} : C^2(\mathbb{R}^2;\mathbb{R}^2)\times Y \longrightarrow Y^*$*, given in Definition 3.3.23, is Fréchet differentiable at* $(\mathbf{0},\mathbf{y_0})$*, where* $\mathbf{y_0} = (c_0, \mathbf{u}_0, \mathbf{p}_0)$ *is a solution of (3.3.119).*

Proof: Let us first note that the integrands appearing in the definition of $\mathbf{F}$ are continuously differentiable. This is a consequence of the continuity and differentiability of the mappings:

$$\begin{aligned} C_2(\mathbb{R}^2;\mathbb{R}^2) &\longrightarrow C_1(\mathbb{R}^2) \\ \zeta &\longmapsto Jac(I+\zeta), \qquad (3.3.120) \\ C_2(\mathbb{R}^2;\mathbb{R}^2) &\longrightarrow (C_1(\mathbb{R}^2,\mathbb{R}^2))^2 \\ \zeta &\longmapsto M(\zeta), \qquad (3.3.121) \\ H^{1/2}(M) &\longrightarrow \mathbf{H}^1(A\cup G) \\ \hat{c} &\longmapsto \hat{\mathbf{z}}(\hat{c}), \qquad (3.3.122) \\ \nabla : H^1 &\longrightarrow \mathbf{L}^2, \qquad (3.3.123) \\ \int : L^1 &\longrightarrow \mathbb{R} \qquad (3.3.124) \end{aligned}$$

Let $d\mathbf{F}(\mathbf{0},\mathbf{y_0})[\mathbf{y}]$ denote the derivative of $\mathbf{F}$ at $(\mathbf{0},\mathbf{y_0})$ in the direction $\mathbf{y}$. Then

$$d\mathbf{F}(\mathbf{0},\mathbf{y_0}) : Y \longrightarrow Y^* \qquad (3.3.125)$$

defines a continuous, linear map, given by:

$$\begin{aligned} &d\mathbf{F}(\mathbf{0},\mathbf{y_0})[\mathbf{y}]\tilde{\mathbf{y}} \\ &= \begin{cases} \int_\Omega \varepsilon\left\{D^{eff}\nabla c\cdot\nabla\varphi + [(\mathbf{u}+\hat{\mathbf{z}}'(c_0)c)\cdot\nabla c_0 + \hat{\mathbf{u}}_0\cdot\nabla c]\,\varphi\right\} + \int_M H_m c\varphi, \\ \alpha(\mathbf{u},\mathbf{v}) + \beta(\mathbf{v},p) - l(\hat{\mathbf{z}}'(c_0)c)\mathbf{v}, \\ \beta(\mathbf{u},q). \end{cases} \qquad (3.3.126) \end{aligned}$$

Hence, $\mathbf{F}$ is Fréchet differentiable. ∎

Now the second requirement of Theorem 3.3.22 is to show that the mapping $d\mathbf{F}(\mathbf{0},\mathbf{y_0})$ is an isomorphism from Y onto Y^*, that is a continuous bijection. The continuity follows from Proposition 3.3.25, in particular from the expression (3.3.126) for $d\mathbf{F}(\mathbf{0},\mathbf{y_0})$.

The bijectivity is proved by showing that the following problem has a unique solution:

Find $\mathbf{y} \in Y$ such that

$$d\mathbf{F}(\mathbf{0}, \mathbf{y_0})[\mathbf{y}]\tilde{\mathbf{y}} = (f(\varphi), g(\mathbf{v}), h(\mathbf{q}))^T, \tag{3.3.127}$$

where $(f, g, h) \in Y^*$, and $\tilde{\mathbf{y}} = (\varphi, \mathbf{v}, \mathbf{q}) \in Y$. This problem can be treated through a fixed point theorem. First, consider the following mappings.

Definition 3.3.26 *For every $\tilde{\mathbf{u}} \in \mathbf{L}^q(\Omega)$, $q > 2$, let*

$$\begin{aligned} T_c : L^q(\Omega) &\longrightarrow \mathbf{C}, \\ \tilde{\mathbf{u}} &\longmapsto c, \end{aligned} \tag{3.3.128}$$

where c is the solution of

$$\int_\Omega \varepsilon \left[D^{eff} \nabla c \cdot \nabla \varphi + (\tilde{\mathbf{u}} \cdot \nabla c_0 + \mathbf{u}_0 \cdot \nabla c)\, \varphi \right] + \int_M H_m c \varphi = f(\varphi), \tag{3.3.129}$$

for every $\varphi \in \mathbf{C}$.

This mapping is well-defined due to existence and uniqueness of c, which follows from Lemma 3.3.21.

Definition 3.3.27 *Let*

$$\begin{aligned} T_{\tilde{\mathbf{u}}} : \quad & \mathbf{C} \longrightarrow \mathbf{L}^q(\Omega), \quad q > 2 \\ & c \longmapsto \tilde{\mathbf{u}} := \mathbf{u} + \hat{\mathbf{z}}'(\hat{c}_0)c, \end{aligned} \tag{3.3.130}$$

where $\mathbf{u}$ is the solution of the following system:

$$\begin{aligned} \alpha(\mathbf{u}, \mathbf{v}) + \beta(\mathbf{v}, \mathbf{p}) &= g(\mathbf{v}) + l(\hat{\mathbf{z}}'(\hat{c}_0)c)\mathbf{v}, \\ \beta(\mathbf{u}, \mathbf{q}) &= h(\mathbf{q}) \end{aligned} \tag{3.3.131}$$

for every $\mathbf{v} \in \mathbf{U}$, $\mathbf{q} \in P_A$, and $(g, h) \in \mathbf{U}^* \times P_A^*$.

The mapping $T_{\tilde{\mathbf{u}}}$ is well-defined from Lemma 3.3.20. Note that $\tilde{\mathbf{u}} \in \mathbf{L}^q(\Omega)$ since $\tilde{\mathbf{u}} \in \mathbf{H}^1(A \cup G)$, and $\mathbf{L}^q(\Omega)$ is continuously embedded in $\mathbf{H}^1(A \cup G)$.

Definition 3.3.28 *Let*

$$T \;:=\; T_{\tilde{\mathbf{u}}} \circ T_c : \mathbf{L}^q(\Omega) \longrightarrow \mathbf{L}^q(\Omega). \tag{3.3.132}$$

Note that when T has a fixed point $\tilde{\mathbf{u}}_* \in \mathbf{L}^q(\Omega)$, then it follows that $\tilde{\mathbf{u}}_* = T\tilde{\mathbf{u}}_*$, and there exists $c_* \in \mathbf{C}$ such that

$$\begin{aligned} c_* &= T_c\tilde{\mathbf{u}}_*, \\ \tilde{\mathbf{u}}_* &= \mathbf{u}_* + \hat{\mathbf{z}}'(\hat{c}_0)c_*. \end{aligned} \tag{3.3.133}$$

Hence, when T has a fixed point, then $(c_*, \mathbf{u}_*, \mathbf{p}_*)$ is a solution of (3.3.127).

Now, let us show that T indeed has a fixed point by checking the requirements of the following definition and Fixed Point Theorem, [7].

Definition 3.3.29 *A continuous mapping between two Banach spaces is called compact if the images of bounded sets are precompact.*

Theorem 3.3.30 ([7], page 222) *Let T be a compact mapping of a Banach space B into itself, and suppose there exists a constant N such that*

$$\|x\|_B \;<\; N \tag{3.3.134}$$

for all $x \in B$ and $\epsilon \in [0,1]$ satisfying $x = \epsilon Tx$. Then T has a fixed point.

Theorem 3.3.31 *The mapping $T = T_{\tilde{\mathbf{u}}} \circ T_c$ is compact (that is, continuous and compact), and there exists a constant N such that*

$$\|\tilde{\mathbf{u}}\|_{\mathbf{L}^q(\Omega)} \;<\; N, \tag{3.3.135}$$

for all

$$\tilde{\mathbf{u}} \in \mathbf{L}^q(\Omega) \quad \cap \quad \{\tilde{\mathbf{u}} : \tilde{\mathbf{u}} = \epsilon T\tilde{\mathbf{u}}, \epsilon \in [0,1]\}\,. \tag{3.3.136}$$

In addition, T has a fixed point $\tilde{\mathbf{u}} \in \mathbf{L}^q(\Omega) \cap \mathbf{H}^1(A \cup G)$, and the fixed point is unique when the parameter c_{in} is sufficiently small.

Proof:

1. The mapping $T := T_{\tilde{\mathbf{u}}} \circ T_c$ is continuous. This results from $T_{\tilde{\mathbf{u}}}$ and T_c being continuous mappings. To prove this, let us first show that T_c is continuous. Let $\{\tilde{\mathbf{u}}_n\} \subset \mathbf{L}^q(\Omega)$, $\tilde{\mathbf{u}}_n \longrightarrow \tilde{\mathbf{u}} \in \mathbf{L}^q(\Omega)$, and set $c_n = T_c\tilde{\mathbf{u}}_n$, $\quad c = T_c\tilde{\mathbf{u}}$, $\delta\tilde{\mathbf{u}}_n = \tilde{\mathbf{u}}_n - \tilde{\mathbf{u}}$, and $\delta c_n = c_n - c$. Now define $L : \mathbf{C} \longrightarrow \mathbf{C}^*$ by

$$< L(c), \varphi > \;\; = \;\; \int_\Omega \varepsilon \left(D^{eff}\nabla c \cdot \nabla\varphi + \varphi\hat{\mathbf{u}}_0 \cdot \nabla c \right) \varphi + \int_M H_m c\varphi \tag{3.3.137}$$

   Then the mapping L is a continuous, invertible linear map, which follows from Lemma 3.3.21. Moreover, $L^{-1} : \mathbf{C}^* \longrightarrow \mathbf{C}$ is a continuous linear map. Also, from Definition 3.3.26, it follows that δc_n and $\delta\tilde{\mathbf{u}}_n$ satisfy

$$\begin{aligned} \int_\Omega \varepsilon\nabla\delta c_n \cdot \left(D^{eff}\nabla\varphi + \varphi\hat{\mathbf{u}}_0 \right) + \int_M H_m \; \varphi \; \delta c_n \;\; &= \;\; -\int_\Omega \varepsilon\varphi \; \delta\tilde{\mathbf{u}}_n \cdot \nabla c_0 \\ &=: \;\; G(\varphi). \end{aligned} \tag{3.3.138}$$

   Note that $G \in \mathbf{C}^*$ as

$$|G(\varphi)| \;\; \leq \;\; \|\varphi\|_{L^{\bar{q}}(\Omega)} \|\nabla c_0\|_{\mathbf{L}^2(\Omega)} \|\delta\tilde{\mathbf{u}}_n\|_{\mathbf{L}^q(\Omega)}, \tag{3.3.139}$$

   where $\frac{1}{\bar{q}} + \frac{1}{q} = \frac{1}{2}$. Also, from Sobolev embeddings, we obtain $\|\varphi\|_{L^{\bar{q}}(\Omega)} \leq C\|\varphi\|_{\mathbf{C}}$ for some constant C independent from φ. In turn,

$$\|G\|_{\mathbf{C}^*} \;\; \leq \;\; C\|\nabla c_0\|_{\mathbf{L}^2(\Omega)} \|\delta\tilde{\mathbf{u}}_n\|_{\mathbf{L}^q(\Omega)}. \tag{3.3.140}$$

   Hence,

$$\|\delta c_n\|_{\mathbf{C}} = \|L^{-1}G\|_{\mathbf{C}} \;\; \leq \;\; \|L^{-1}\| \|G\|_{\mathbf{C}^*}$$

$$\begin{aligned} &\leq C\|L^{-1}\|\|\nabla c_0\|_{\mathbf{L}^2(\Omega)}\|\delta\tilde{\mathbf{u}}_n\|_{\mathbf{L}^q(\Omega)} \\ &\longrightarrow 0 \quad as \quad n\to\infty. \end{aligned} \tag{3.3.141}$$

This shows that T_c is a continuous mapping.

Now we show that $T_{\tilde{\mathbf{u}}}$ is continuous. Let $c_n \longrightarrow c$ in $\mathbf{C}$, and write $\bar{\mathbf{u}}_n = T_{\tilde{\mathbf{u}}}c_n$ and $\bar{\mathbf{u}} = T_{\tilde{\mathbf{u}}}c$. Then from the definition of $T_{\tilde{\mathbf{u}}}$, Definition 3.3.27, it follows that δc_n and $\delta\bar{\mathbf{u}}_n$ satisfy

$$\begin{aligned} \alpha(\delta\bar{\mathbf{u}}_n,\mathbf{v})+\beta(\mathbf{v},\delta\mathbf{p}_n) &= l(\hat{\mathbf{z}}'(\hat{c}_0)\delta c_n)\mathbf{v}, \\ \beta(\delta\bar{\mathbf{u}}_n,\mathbf{q}) &= 0. \end{aligned} \tag{3.3.142}$$

Using Lemma 3.3.20,

$$\|\delta\bar{\mathbf{u}}_n\|_{\mathbf{H}^1(A)}+\|\delta\bar{\mathbf{u}}_n\|_{\mathbf{H}^1(G)} \leq C\|l(\hat{\mathbf{z}}'(\hat{c}_0)\delta c_n)\|_{\mathbf{U}^*}. \tag{3.3.143}$$

From Remark 3.3.14, it follows that $\hat{\mathbf{z}}'(\hat{c}_0)\delta c_n \in \mathbf{H}^1(A\cup G)$, and from estimate (3.3.64) we deduce

$$\begin{aligned} \|l(\hat{\mathbf{z}}'(\hat{c}_0)\delta c_n)\|_{\mathbf{U}^*} &\leq C_1\|\hat{\mathbf{z}}'(\hat{c}_0)\delta c_n\|_{\mathbf{H}^1(A\cup G)} \\ &\leq C_2\|\delta c_n\|_{H^{1/2}(M)} \\ &\leq C_3\|\delta c_n\|_{\mathbf{C}}, \end{aligned} \tag{3.3.144}$$

where the last inequality is deduced from the Trace Theorem 3.3.4. Therefore, the above equations give

$$\|\delta\bar{\mathbf{u}}_n\|_{\mathbf{H}^1(A)}+\|\delta\bar{\mathbf{u}}_n\|_{\mathbf{H}^1(G)} \leq C\|\delta c_n\|_{\mathbf{C}}, \tag{3.3.145}$$

where C is a constant independent form $\delta\bar{\mathbf{u}}_n$ and δc_n. Since also $\mathbf{H}^1(A\cup G)$ is continuously embedded in $\mathbf{L}^q(\Omega)$, $q>2$, there exists a constant C_1 such that

$$\begin{aligned} \|\delta\bar{\mathbf{u}}_n\|_{\mathbf{L}^q(\Omega)} &\leq C_1\left(\|\delta\bar{\mathbf{u}}_n\|_{\mathbf{H}^1(A)}+\|\delta\bar{\mathbf{u}}_n\|_{\mathbf{H}^1(G)}\right) \\ &\leq C_2\|\delta c_n\|_{\mathbf{C}} \longrightarrow 0 \quad as \quad n\to\infty. \end{aligned} \tag{3.3.146}$$

This proves the continuity of $T_{\tilde{\mathbf{u}}}$. The continuity of $T_{\tilde{\mathbf{u}}}$ and T_c result in the continuity of T.

2. There exists $N > 0$ such that

$$\|\tilde{\mathbf{u}}\|_{\mathbf{L}^q(\Omega)} \quad < \quad N, \tag{3.3.147}$$

for all

$$\tilde{\mathbf{u}} \in \mathbf{L}^q(\Omega) \cap \{\tilde{\mathbf{u}} : \tilde{\mathbf{u}} = \epsilon T\tilde{\mathbf{u}}, \quad \epsilon \in [0,1]\}. \tag{3.3.148}$$

For this, let $\tilde{\mathbf{u}} \in \mathbf{L}^q(\Omega)$ be such that $\tilde{\mathbf{u}} = \epsilon T\tilde{\mathbf{u}}$. If $\epsilon = 0$, then $\tilde{\mathbf{u}} = 0$ and any $N > 0$ would satisfy the inequality (3.3.147). Now if $\epsilon \neq 0$, then

$$\frac{\tilde{\mathbf{u}}}{\epsilon} \quad = \quad T\tilde{\mathbf{u}}. \tag{3.3.149}$$

Let $c = T_c\tilde{\mathbf{u}}$, then $\frac{\tilde{\mathbf{u}}}{\epsilon} = T_{\tilde{\mathbf{u}}}c$. Hence, c and $\tilde{\mathbf{u}}$ satisfy

$$\int_\Omega \varepsilon \left(D^{eff}\nabla c \cdot \nabla\varphi + \varphi\hat{\mathbf{u}}_0\nabla c\right) + \int_M H_m c\varphi = f(\varphi) - \int_\Omega \varepsilon\varphi\tilde{\mathbf{u}} \cdot \nabla c_0, \tag{3.3.150}$$

$$\alpha(\tilde{\mathbf{u}}, \mathbf{v}) + \beta(\mathbf{v}, \epsilon\mathbf{p}) = \epsilon\left[g(\mathbf{v}) + l(\hat{\mathbf{z}}'(\hat{c}_0)c)\mathbf{v}\right], \tag{3.3.151}$$

$$\beta(\tilde{\mathbf{u}}, \mathbf{q}) = \epsilon h(\mathbf{q}). \tag{3.3.152}$$

Using the Poincare inequality and the same argument made in (3.3.141), then (3.3.150) gives

$$\|\nabla c\|_{\mathbf{L}^2(\Omega)} \quad \leq \quad C_1\left(\|f\|_{\mathbf{C}^*} + \|\tilde{\mathbf{u}}\|_{\mathbf{L}^q(\Omega)}\|\nabla c_0\|_{\mathbf{L}^2(\Omega)}\right). \tag{3.3.153}$$

Using equations (3.3.151), (3.3.152) and Lemma 3.3.20, we obtain

$$\begin{aligned} \|\tilde{\mathbf{u}}\|_{\mathbf{L}^q(\Omega)} \quad &\leq \quad C\|\tilde{\mathbf{u}}\|_{\mathbf{H}^1(A\cup G)} \\ &\leq \quad \epsilon C_2\|g + l(\hat{\mathbf{z}}'(\hat{c}_0)c)\|_{\mathbf{U}^*}. \end{aligned} \tag{3.3.154}$$

Note also from the definition of $l(\cdot)$ that

$$\|l(\hat{\mathbf{z}}'(\hat{c}_0)c)\|_{\mathbf{U}^*} \quad \leq \quad C_3\left(\|\nabla\hat{\mathbf{z}}'(\hat{c}_0)c)\|_{\mathbf{L}^2(A)} + \|\hat{\mathbf{z}}'(\hat{c}_0)c)\|_{\mathbf{L}^2(G)}\right)$$

$$\leq \quad C_4\|c\|_{L^2(M)}, \tag{3.3.155}$$

where the last inequality follows from (3.3.64). The trace theorem and Poincare inequality result in $\|c\|_{L^2(M)} \leq C\|\nabla c\|_{\mathbf{L}^2(\Omega)}$. Then the above three inequalities give

$$\|\tilde{\mathbf{u}}\|_{\mathbf{L}^q(\Omega)} \quad \leq \quad \epsilon C_5 \left[\|g\|_{\mathbf{U}^*} + C_1 \left(\|f\|_{\mathbf{C}^*} + \|\tilde{\mathbf{u}}\|_{\mathbf{L}^q(\Omega)}\|\nabla c_0\|_{\mathbf{L}^2(\Omega)}\right)\right] \tag{3.3.156}$$

Hence,

$$\begin{aligned} \|\tilde{\mathbf{u}}\|_{\mathbf{L}^q(\Omega)} &\leq \frac{\epsilon C_5}{1-\epsilon C_1 C_5\|\nabla c_0\|_{\mathbf{L}^2(\Omega)}} \left(\|g\|_{\mathbf{U}^*} + C_1\|f\|_{\mathbf{C}^*}\right) \\ &< N, \end{aligned} \tag{3.3.157}$$

where

$$N \quad = \quad \frac{2\epsilon C_5 \left(\|g\|_{\mathbf{U}^*} + C_1\|f\|_{\mathbf{C}^*}\right)}{1-\epsilon C_1 C_5\|\nabla c_0\|_{\mathbf{L}^2(\Omega)}}. \tag{3.3.158}$$

Note that N can be made positive when $\|\nabla c_0\|_{\mathbf{L}^2(\Omega)}$ is small enough. However, it follows from Lemma 3.3.21 that

$$\|\nabla c_0\|_{\mathbf{L}^2(\Omega)} \quad \leq \quad c_{in} C \left(1 + \|\hat{\mathbf{u}}_0\|_{\mathbf{L}^2(\Omega)}\right). \tag{3.3.159}$$

Therefore N is positive when c_{in} is sufficiently small.

3. T is compact. For this, let $\{\tilde{\mathbf{u}}_n\}$ be a bounded sequence in $\mathbf{L}^q(\Omega)$. We show that $\{T\tilde{\mathbf{u}}_n\}$ has a convergent subsequence in $\mathbf{L}^q(\Omega)$. Let $c_n = T_c\tilde{\mathbf{u}}_n$ and $\bar{\mathbf{u}}_n = T\tilde{\mathbf{u}}_n = T_{\tilde{\mathbf{u}}}c_n$. Similar to the work done in equation (3.3.156), it follows that $\bar{\mathbf{u}}_n$ and $\tilde{\mathbf{u}}_n$ satisfy the following estimate:

$$\begin{aligned} \|\bar{\mathbf{u}}_n\|_{\mathbf{L}^q(\Omega)} &\leq C\|\bar{\mathbf{u}}_n\|_{\mathbf{H}^1(A\cup G)} \\ &\leq C_2 \left[\|g\|_{\mathbf{U}^*} + C_1 \left(\|f\|_{\mathbf{C}^*} + \|\tilde{\mathbf{u}}_n\|_{\mathbf{L}^q(\Omega)}\|\nabla c_0\|_{\mathbf{L}^2(\Omega)}\right)\right] \\ &< \infty, \quad \forall n, \end{aligned} \tag{3.3.160}$$

as $\|\tilde{\mathbf{u}}_n\|_{\mathbf{L}^q(\Omega)}$ is bounded. Hence, the sequence $\{\bar{\mathbf{u}}_n\}$ is bounded in $\mathbf{H}^1(A\cup G) \hookrightarrow^c \mathbf{L}^q(\Omega)$. Therefore, $\{\bar{\mathbf{u}}_n\}$ has a convergent subsequent in $\mathbf{L}^q(\Omega)$. This shows that T is compact.

4. T has a unique fixed point when c_{in} is sufficiently small. Existence of a fixed point results from items 1-3 and Theorem 3.3.30.

   For the uniqueness of the fixed point, let $(c_1, \tilde{\mathbf{u}}_1)$ and $(c_2, \tilde{\mathbf{u}}_2)$ be two fixed points, and set $\delta c = c_1 - c_2$ and $\delta\tilde{\mathbf{u}} = \tilde{\mathbf{u}}_1 - \tilde{\mathbf{u}}_2$. Then similar estimates to (3.3.141) and (3.3.146) are obtained:

$$\|\delta c\|_{\mathbf{C}} \leq C_1 \|\nabla c_0\|_{\mathbf{L}^2(\Omega)} \|\delta\tilde{\mathbf{u}}\|_{\mathbf{L}^q(\Omega)}, \tag{3.3.161}$$

   and

$$\|\delta\tilde{\mathbf{u}}\|_{\mathbf{L}^q(\Omega)} \leq C_2 \|\delta c\|_{\mathbf{C}}. \tag{3.3.162}$$

   Now the above two estimates yield

$$\left(1 - C_1 C_2 \|\nabla c_0\|_{\mathbf{L}^2(\Omega)}\right) \|\delta c\|_{\mathbf{C}} \leq 0, \tag{3.3.163}$$

   where $\|\nabla c_0\|_{\mathbf{L}^2(\Omega)}$ can be made as small as possible by choosing c_{in} small enough. In turn, the estimate (3.3.163) gives $\|\delta c\|_{\mathbf{C}} = 0$. Hence $c_1 = c_2$ and $\tilde{\mathbf{u}}_1 = \tilde{\mathbf{u}}_2$.

∎

Remark 3.3.32 From Propositions 3.3.24, 3.3.25 and Theorem 3.3.31, all the hypotheses of Theorem 3.3.22 are met; hence the shape differentiability of the transported state variables $c_\zeta, \mathbf{u}_\zeta$ and $\mathbf{p}_\zeta$ is defined, and

$$\frac{\partial c_\zeta}{\partial \zeta}(\mathbf{0})\xi \in \mathbf{C}; \quad \frac{\partial \mathbf{u}_\zeta}{\partial \zeta}(\mathbf{0})\xi \in \mathbf{U}; \quad \frac{\partial p_\zeta}{\partial \zeta}(\mathbf{0}) \in L^2(A) \otimes H^1(G). \tag{3.3.164}$$

On the other hand,

$$c(\mathbf{0}) \in \mathbf{C}; \quad \mathbf{u}(\mathbf{0}) \in \mathbf{H}^1(A) \otimes \mathbf{H}^1(G); \quad p(\mathbf{0}) \in L^2(A) \otimes H^2(G). \tag{3.3.165}$$

Hence the shape derivatives of the state variables exist and satisfy the following equations:

$$\frac{\partial c(\mathbf{0})}{\partial \zeta}\xi = \frac{\partial c_\zeta}{\partial \zeta}(\mathbf{0})\xi - \xi \cdot \nabla c(\mathbf{0}) \quad in \quad L^2(\Omega), \tag{3.3.166}$$

$$\frac{\partial \mathbf{u}(\mathbf{0})}{\partial \zeta}\xi = \frac{\partial \mathbf{u}_\zeta}{\partial \zeta}(\mathbf{0})\xi - \xi \cdot \nabla \mathbf{u}(\mathbf{0}) \quad in \quad \mathbf{L}^2(A) \otimes \mathbf{L}^2(G), \tag{3.3.167}$$

$$\frac{\partial p(\mathbf{0})}{\partial \zeta}\xi = \frac{\partial p_\zeta}{\partial \zeta}(\mathbf{0})\xi - \xi \cdot \nabla p(\mathbf{0}) \quad in \quad H^{-1}(A) \otimes H^1(G), \tag{3.3.168}$$

The last equation is valid in A because

$$-\mu\Delta(\mathbf{u} + \hat{\mathbf{z}}(\hat{c})) + \nabla p = \mathbf{0} \quad in \quad \mathbf{H}^{-1}(A), \tag{3.3.169}$$

and consequently $\xi \cdot \nabla p$ is defined in $H^{-1}(A)$ as follows

$$< \xi \cdot \nabla p, \varphi >_{H^{-1}(A)\times H_0^1(A)} = -\int_A \nabla\left(\mathbf{u} + \hat{\mathbf{z}}(\hat{c})\right) \cdot \nabla(\xi\varphi), \quad \forall \varphi \in H_0^1(A) \tag{3.3.170}$$

This shows the shape differentiability of the state variables.

Remark 3.3.33 Let us recall from (2.2.4) that the cost functional E is defined as

$$E(\zeta) = \frac{H_m^2}{2}\alpha \int_M \left(\hat{c} - \frac{1}{|M|}\int_M \hat{c}\right)^2 - H_m\beta \int_M \hat{c} + \sigma(p_{in} - p_{out}), \tag{3.3.171}$$

where H_m satisfies $N_{\hat{c}} \cdot \nu = H_m \hat{c}$ on M. In fact, $\zeta \longmapsto E(\zeta)$ is differentiable at $\zeta = \mathbf{0}$ from C_2 into $\mathbb{R}$. This follows from Theorem 3.1.10.

Note first that since $\zeta = \mathbf{0}$ on M, one obtains

$$c' := \frac{\partial c(\mathbf{0})}{\partial \zeta}\xi = \frac{\partial c_\zeta}{\partial \zeta}(\mathbf{0})\xi \quad in \quad H^{1/2}(M). \tag{3.3.172}$$

This implies the existence of the shape derivative H_m', given in (3.2.10). Also, the fact that $\partial_2 p_{in} = 0$ on $\Gamma_{i,\zeta}$ gives

$$\begin{aligned} p_{in}' = \frac{\partial p_{in}(0)}{\partial \zeta_2}\xi_2 &= \frac{\partial p_{in}(\zeta_2) \circ (1 + \zeta_2)}{\partial \zeta_2}(0)\xi_2 - \xi_2 \partial_2 p_{in}(0) \\ &= \frac{\partial p_{in}(\zeta_2) \circ (1 + \zeta_2)}{\partial \zeta_2}(0)\xi_2 \quad in \quad \mathbb{R}, \end{aligned} \tag{3.3.173}$$

where ζ_2 is the second component of ζ.

Since $\hat{c}(\zeta) \in H^{1/2}(M)$, the integrands, in (3.3.171), are differentiable at $\zeta = \mathbf{0}$ from C_2 into $L^1(M)$. This proves the differentiability of the cost functional E.

3.4 Existence and Uniqueness for the Adjoint Problem

The adjoint problem serves to calculate the gradient of the cost functional, E, see section 3.2. Therefore the study of existence and uniqueness of the solution for this problem is important. In this section, it will be shown that for small parameters c_{in}, ϕ, the adjoint problem has a unique solution.

3.4.1 The Adjoint Problem in Strong Form

Let $\hat{c}$, $\hat{\mathbf{u}}$, $\hat{p}$ be the solution of the steady state problem (3.3.106). Then from Section 3.2, the strong form of the adjoint problem reads:

Find φ, $\mathbf{v} = (v_1, v_2)$, $\mathbf{q}$ such that

$$\begin{aligned} &-\varepsilon D^{eff}\Delta\varphi + \varepsilon\hat{\mathbf{u}}\cdot\nabla\varphi = 0 && in\ \ \Omega \\ &(-\mu\Delta\mathbf{v} + \nabla q)\,\chi(A) + \left(\tfrac{\mu}{K}\mathbf{v} + \nabla q\right)\chi(G) = -\varphi\nabla\hat{c} && in\ \ A\cup G \\ &\nabla\cdot\mathbf{v} = 0 && in\ \ A\cup G, \end{aligned} \tag{3.4.1}$$

associated with the following boundary conditions:

$$\begin{aligned} \Gamma_i: \quad & \textstyle\int_{\Gamma_i} v_1 + \sigma &=\ & v_2 = \mu\partial_1 v_1 - (q - q_{in}) = \varphi = 0, \\ \Gamma_o: \quad & v_2 &=\ & -\mu\partial_1 v_1 + q = \varepsilon D^{eff}\partial_1\varphi + \varepsilon\hat{u}_1\varphi = 0, \\ \Gamma: \quad & v_1 &=\ & v_2 = \partial_\nu\varphi = 0, \\ \Sigma: \quad & v_1(.,0^-) &=\ & [v_2]_\Sigma = -\mu\partial_1 v_2 + [q]_\Sigma = 0, \\ \Gamma_w: \quad & v_1 &=\ & \partial_\nu\varphi = 0, \\ M: \quad & v_2 &=\ & \varepsilon D^{eff}\partial_\nu\varphi + (-\hat{u}_2 + H_m)\varphi + \tfrac{\beta_m H_m q}{\varepsilon} - g = 0, \end{aligned} \tag{3.4.2}$$

where $g = \alpha(\hat{c} - \frac{1}{|M|}\int_M \hat{c}) - \beta$, α, β, and σ are nonnegative given parameters considered in the definition of the cost functional E, (2.2.4).

3.4.2 Variational Formulation of the adjoint problem

To write a variational formulation of the adjoint system (3.4.1)-(3.4.2), consider the linear spaces defined in Section 3.3: $U, \mathbf{U}, \hat{\mathbf{U}}, C, \mathbf{C}$, and $P := P_A \otimes H^1(G)$.

Using (3.4.1)-(3.4.2), for every $\Phi \in C$

$$\begin{aligned} &\int_\Omega \varepsilon \left(D^{eff}\nabla\Phi + \Phi\hat{\mathbf{u}}\right)\cdot\nabla\varphi + \int_M \left(-\hat{u}_2 + H_m\right)\varphi\Phi + \int_{\Gamma_o} \hat{u}_1\varphi\Phi \\ &= \int_M h(q)\Phi, \end{aligned} \tag{3.4.3}$$

where

$$h(q) \;=\; g - \frac{\beta_m H_m q}{\varepsilon}. \tag{3.4.4}$$

Also, for every $\mathbf{w} \in U$ and $\mathbf{q}^* \in P_A$, (3.4.1)-(3.4.2) gives

$$\begin{aligned} \int_A \mu\nabla\mathbf{v}\cdot\nabla\mathbf{w} + \int_G \frac{\mu}{K}\mathbf{v}\cdot\mathbf{w} - \int_A q\nabla\cdot\mathbf{w} - q_{in}\int_{\Gamma_i} w_1 &= -\int_\Omega \varepsilon\varphi\nabla\hat{c}\cdot\mathbf{w}, \\ -\int_A q^*\nabla\cdot\mathbf{v} - q^*_{in}\int_{\Gamma_i} v_1 &= \sigma q^*_{in}, \end{aligned} \tag{3.4.5}$$

where the boundary integrals simplify as follows

$$\int_{\partial A} \mathbf{w}\cdot(\mu\partial_{\nu_A}\mathbf{v} + q\nu_A) + \int_{\partial G} q\nu_G\cdot\mathbf{w} \;=\; -q_{in}\int_{\Gamma_i} w_1. \tag{3.4.6}$$

Equations (3.4.3), (3.4.5) defines the following weak formulation of the adjoint problem: Find $(\varphi, \mathbf{v}, \mathbf{q}) \in \mathbf{C}\times\mathbf{U}\times\mathbf{P}$ such that

$$\begin{aligned} &\int_\Omega \varepsilon \left(D^{eff}\nabla\Phi + \Phi\hat{\mathbf{u}}\right)\cdot\nabla\varphi + \int_M \left(-\hat{u}_2 + H_m\right)\varphi\Phi + \int_{\Gamma_o} \hat{u}_1\varphi\Phi = \int_M h(q)\Phi, \\ &\alpha(\mathbf{v},\mathbf{w}) + \beta(q,\mathbf{w}) = -\int_\Omega \varphi\nabla\hat{c}\cdot\mathbf{w}, \\ &\beta(q^*,\mathbf{v}) = \sigma q^*_{in}, \end{aligned} \tag{3.4.7}$$

for all $\Phi \in \mathbf{C}$, $\mathbf{w} \in \mathbf{U}$ and $\mathbf{q}^* = (q^*, q^*_{in}) \in P_A$; where $\alpha(.,.)$ and $\beta(.,.)$ are defined in Definition 3.3.17, and $h(q)$ is given in (3.4.4).

Proposition 3.4.1 *: Let $\hat{c} \in W^{1,p}(\Omega)$ and $\varphi \in L^{\overline{p}}(\Omega)$ be given, where $\overline{p} = \frac{2p}{p-2}$, $p > 2$. Then the following problem has a unique solution:*
Find $(\mathbf{v}, \mathbf{q}) \in \boldsymbol{U} \times P_A$ such that

$$\begin{aligned} &\alpha(\mathbf{v}, \mathbf{w}) + \beta(q, \mathbf{w}) = -\int_\Omega \varphi \nabla \hat{c} \cdot \mathbf{w}, \quad \forall \mathbf{w} \in \mathbf{U}, \\ &\beta(q^*, \mathbf{v}) = \sigma q^*_{in}, \quad \forall \mathbf{q}^* = (q^*, q^*_{in}) \in P_A. \end{aligned} \tag{3.4.8}$$

Also,

$$\begin{aligned} \|\mathbf{v}\|_{\boldsymbol{U}} &\leq C\left(\sigma + \|\varphi\|_{L^{\overline{p}}(\Omega)} \|\nabla \hat{c}\|_{\mathbf{L}^p(\Omega)}\right), \\ \|\mathbf{q}\|_{P_A} &\leq C\left(\sigma + \|\varphi\|_{L^{\overline{p}}(\Omega)} \|\nabla \hat{c}\|_{\mathbf{L}^p(\Omega)}\right). \end{aligned} \tag{3.4.9}$$

Proof:

Note first that $\varphi \nabla \hat{c} \in \mathbf{U}^*$, which follows as $\varphi \nabla \hat{c} \in \mathbf{L}^2(\Omega)$: $\frac{1}{p} + \frac{1}{\overline{p}} = \frac{1}{2}$, and

$$\begin{aligned} \int_\Omega |\varphi \nabla \hat{c}|^2 &\leq \left(\int_\Omega |\varphi|^{\overline{p}}\right)^{2/\overline{p}} \left(\int_\Omega |\nabla \hat{c}|^p\right)^{2/p} \\ &= \|\varphi\|^2_{L^{\overline{p}}(\Omega)} \|\nabla \hat{c}\|^2_{L^p(\Omega)}. \end{aligned} \tag{3.4.10}$$

Since also $\sigma \in P_A^*$, Lemma 3.3.20 completes the proof. ∎

Remark 3.4.2 Let us consider equation (3.4.8) and take $\mathbf{w} \in \mathcal{D}(A \cup G) \cap \{\nabla \cdot \mathbf{w} = 0\} \subset \mathbf{U}$. Then, it follows that the solution $\mathbf{v} \in \mathbf{U}$ satisfies

$$\begin{aligned} < -\mu \Delta \mathbf{v} + \varphi \nabla \hat{c}, \mathbf{w} >_{\mathbf{H}^{-1}(A) \times \mathbf{H}^1_0(A)} &= 0, \\ < \frac{\mu}{K} \mathbf{v} + \varphi \nabla \hat{c}, \mathbf{w} >_{\mathbf{L}^2(G) \times \mathbf{L}^2(G)} &= 0. \end{aligned} \tag{3.4.11}$$

Then from [34, Remark 1.4, page 15], there exists $q \in L^2(A) \otimes H^1(G)$ such that

$$-\mu \Delta \mathbf{v} + \nabla q = -\varphi \nabla \hat{c} \quad in \ \mathbf{H}^{-1}(A), \tag{3.4.12}$$

$$\frac{\mu}{K}\mathbf{v} + \nabla q \;=\; -\varphi\nabla\hat{c} \quad in \;\; \mathbf{L}^2(G). \tag{3.4.13}$$

Lemma 3.4.3 *The solution* $(\mathbf{v}, \mathbf{q}) \in \mathbf{U} \times P_A$ *of (3.4.8) satisfies*

$$\begin{aligned} -\mu\partial_1 v_1 + q &= q_{in} \quad in \quad H^{-1/2}(\Gamma_i), \\ \mu\partial_1 v_1 - q &= 0 \quad\;\; in \quad H^{-1/2}(\Gamma_o), \\ \mu\partial_2 v_2 - q &= -q_G \quad in \quad H^{-1/2}(\Sigma), \end{aligned} \tag{3.4.14}$$

for some $q_G \in H^1(G)$.

Proof:

Let

$$S_1 \;:=\; -\mu\nabla v_1 + (q, 0)^T, \quad S_2 := -\mu\nabla v_2 + (0, q)^T, \tag{3.4.15}$$

where T denotes the transpose operator. From Remark 3.4.2,

$$S_i \;\in\; \mathbf{L}^2(A), \quad and \;\; \nabla \cdot S_i = -\varphi\partial_i\hat{c} \in L^2(A), \tag{3.4.16}$$

where $i = 1, 2$. Then from Theorem 3.3.7, the trace of $S_i \cdot \nu$ is defined in $H^{-1/2}(\partial A)$, and for every $\mathbf{w} \in \mathbf{U}$

$$\begin{aligned} &< \gamma_\nu S_1, \gamma_0 w_1 >_{H^{-1/2}(\partial A)\times H^{1/2}(\partial A)} \\ &\qquad = \int_A \left[-\mu\nabla v_1 \cdot \nabla w_1 + q\partial_1 w_1 - (\varphi\partial_1\hat{c})\, w_1\right]. \end{aligned} \tag{3.4.17}$$

Since $w_1 = 0$ on $\Sigma \cup \Gamma$, the above equation simplifies to

$$\begin{aligned} &< \gamma_\nu S_1, \gamma_0 w_1 >_{H^{-1/2}(\Gamma_i\cup\Gamma_o)\times H^{1/2}(\Gamma_i\cup\Gamma_o)} \\ &\qquad = \int_A \left[-\mu\nabla v_1 \cdot \nabla w_1 + q\partial_1 w_1 - (\varphi\partial_1\hat{c})\, w_1\right]. \end{aligned} \tag{3.4.18}$$

Similarly,

$$< \gamma_\nu S_2, \gamma_0 w_2 >_{H^{-1/2}(\partial A)\times H^{1/2}(\partial A)} = \int_A \left[-\mu \nabla v_2 \cdot \nabla w_2 + q\partial_2 w_2 - (\varphi \partial_2 \hat{c})\, w_2\right]. \quad (3.4.19)$$

Since $w_2 = 0$ on $\Gamma_i \cup \Gamma_o \cup \Gamma$, the above equation reduces to

$$< \gamma_\nu S_2, \gamma_0 w_2 >_{H^{-1/2}(\Sigma)\times H^{1/2}(\Sigma)} = \int_A \left[-\mu \nabla v_2 \cdot \nabla w_2 + q\partial_2 w_2 - (\varphi \partial_2 \hat{c})\, w_2\right]. \quad (3.4.20)$$

Adding equations (3.4.18) and (3.4.20) yields

$$\begin{aligned} &- < \gamma_\nu S_1, \gamma_0 w_1 >_{H^{-1/2}(\Gamma_i\cup\Gamma_o)\times H^{1/2}(\Gamma_i\cup\Gamma_o)} - < \gamma_\nu S_2, \gamma_0 w_2 >_{H^{-1/2}(\Sigma)\times H^{1/2}(\Sigma)} \\ &= \int_A \left[\mu \nabla \mathbf{v} \cdot \nabla \mathbf{w} - q \nabla \cdot \mathbf{w} + (\varphi \nabla \hat{c}) \cdot \mathbf{w}\right]. \end{aligned} \quad (3.4.21)$$

On the other hand, Remark 3.4.2 gives

$$-\nabla q_G \;=\; \frac{\mu}{K}\mathbf{v} + \varphi \nabla \hat{c} \quad in \;\; \mathbf{L}^2(G). \quad (3.4.22)$$

Since $w_1 = 0$ on Γ_w, $w_2 = 0$ on M and $\nabla \cdot \mathbf{w} = 0$ in G; multiplying the above equation by $\mathbf{w}$ and integrating the left side by parts result in

$$\int_\Sigma q_G w_2 \;=\; \int_G \Big(\frac{\mu}{K}\mathbf{v} + \varphi \nabla \hat{c}\Big) \cdot \mathbf{w}. \quad (3.4.23)$$

Now, adding (3.4.21) and (3.4.23) gives

$$\begin{aligned} &< -\gamma_\nu S_1, \gamma_0 w_1 >_{H^{-1/2}(\Gamma_i\cup\Gamma_o)\times H^{1/2}(\Gamma_i\cup\Gamma_o)} + < q_G - \gamma_\nu S_2, \gamma_0 w_2 >_{H^{-1/2}(\Sigma)\times H^{1/2}(\Sigma)} \\ &= \int_A \left[\mu \nabla \mathbf{v} \cdot \nabla \mathbf{w} - q \nabla \cdot \mathbf{w} + (\varphi \nabla \hat{c}) \cdot \mathbf{w}\right] + \int_G \Big(\frac{\mu}{K}\mathbf{v} + \varphi \nabla \hat{c}\Big) \cdot \mathbf{w}. \end{aligned} \quad (3.4.24)$$

However, from Proposition 3.4.1, the solution $\mathbf{v}$ satisfies

$$\begin{aligned} &q_{in} \int_{\Gamma_i} w_1 \\ &= \int_A \left[\mu \nabla \mathbf{v} \cdot \nabla \mathbf{w} - q \nabla \cdot \mathbf{w} + (\varphi \nabla \hat{c}) \cdot \mathbf{w}\right] + \int_G \Big(\frac{\mu}{K}\mathbf{v} + \varphi \nabla \hat{c}\Big) \cdot \mathbf{w}. \end{aligned} \quad (3.4.25)$$

Hence, the above two equations result in

$$\begin{aligned} 0 &= < -\gamma_\nu S_1, \gamma_0 w_1 >_{H^{-1/2}(\Gamma_i \cup \Gamma_o) \times H^{1/2}(\Gamma_i \cup \Gamma_o)} - q_{in} \int_{\Gamma_i} w_1 \\ &\quad + < q_G - \gamma_\nu S_2, \gamma_0 w_2 >_{H^{-1/2}(\Sigma) \times H^{1/2}(\Sigma)}, \end{aligned} \tag{3.4.26}$$

which implies that the solution $(\mathbf{v}, \mathbf{q}) \in \mathbf{U} \times P_A$ of (3.4.8) satisfies

$$\begin{aligned} -\gamma_\nu S_1 = -\mu \partial_1 v_1 + q &= q_{in} \quad in \;\; H^{-1/2}(\Gamma_i), \\ -\gamma_\nu S_1 = \mu \partial_1 v_1 - q &= 0 \quad in \;\; H^{-1/2}(\Gamma_o), \\ -\gamma_\nu S_2 = \mu \partial_2 v_2 - q &= -q_G \;\; in \;\; H^{-1/2}(\Sigma). \end{aligned} \tag{3.4.27}$$

∎

Proposition 3.4.4 *Let* $\mathbf{q}$, $\mathbf{v}$ *be the solution of (3.4.8). Let also* $\Phi \in \mathbf{C}$ *and* $\hat{\mathbf{z}} = \hat{\mathbf{z}}(\Phi) \in \mathbf{H}^1(A \cup G)$ *be the extension constructed in Proposition 3.3.12 by taking* $g = \Phi$, $h = 0$, *and* $\phi = 0$, *that is*

$$\begin{aligned} \hat{z}_2(\Phi) &= \Phi \;\; on \;\; M, \\ \nabla \cdot \hat{\mathbf{z}}(\Phi) &= 0 \;\; in \;\; A \\ \int_{\Gamma_i} \hat{z}_1(\Phi) &= 0. \end{aligned} \tag{3.4.28}$$

Then,

$$\begin{aligned} \int_M q_G \Phi &= -\int_A [\mu \nabla \mathbf{v} \cdot \nabla \hat{\mathbf{z}}(\Phi) + \varphi \nabla \hat{c} \cdot \hat{\mathbf{z}}(\Phi)] \\ &\quad - \int_G \left(\frac{\mu}{K} \mathbf{v} + \varphi \nabla \hat{c} \right) \cdot \hat{\mathbf{z}}(\Phi), \end{aligned} \tag{3.4.29}$$

where $q_G \in H^1(G)$ *satisfies*

$$-\nabla q_G = \frac{\mu}{K} \mathbf{v} + \varphi \nabla \hat{c} \;\; in \;\; \mathbf{L}^2(G). \tag{3.4.30}$$

In addition,

$$|\int_M q_G\Phi| \;\leq\; C\left(\|\mathbf{v}\|_{\mathbf{U}} + \|\varphi\|_{L^{\overline{p}}(\Omega)}\|\nabla\hat{c}\|_{\mathbf{L}^p(\Omega)}\right)\|\Phi\|_{L^2(M)}. \tag{3.4.31}$$

Proof:

The proof of this proposition follows from Lemma 3.4.3. Let us first note that the extension $\hat{\mathbf{z}}(\Phi)$, constructed in Proposition 3.3.12, satisfies as well the following

$$\begin{aligned} \hat{z}_1(\Phi) &= 0 \;\; on \;\; \Gamma_i \cup \Gamma \cup \Sigma \cup \Gamma_w, \\ \hat{z}_2(\Phi) &= 0 \;\; on \;\; \Gamma \cup \Gamma_i \cup \Gamma_o, \\ \nabla\cdot\hat{\mathbf{z}}(\Phi) &= 0 \;\; in \;\; G. \end{aligned} \tag{3.4.32}$$

Equation (3.4.21) in Lemma 3.4.3 gives

$$\begin{aligned} &- <\gamma_\nu S_1, \gamma_0\hat{z}_1(\Phi)>_{H^{-1/2}(\Gamma_i\cup\Gamma_o)\times H^{1/2}(\Gamma_i\cup\Gamma_o)} - <\gamma_\nu S_2, \gamma_0\hat{z}_2(\Phi)>_{H^{-1/2}(\Sigma)\times H^{1/2}(\Sigma)} \\ &= \int_A \left[\mu\nabla\mathbf{v}\cdot\nabla\hat{\mathbf{z}}(\Phi) - q\nabla\cdot\hat{\mathbf{z}}(\Phi) + (\varphi\nabla\hat{c})\cdot\hat{\mathbf{z}}(\Phi)\right]. \end{aligned} \tag{3.4.33}$$

Since $\hat{z}_1(\Phi) = 0$ on Γ_i, $\nabla\cdot\hat{\mathbf{z}}(\Phi) = 0$ in G, $\gamma_\nu S_1 = 0$ on Γ_o and $\gamma_\nu S_2 = q_G$ on Σ, the above equation reduces to

$$\begin{aligned} &<q_G, \gamma_0\hat{z}_2(\Phi)>_{H^{-1/2}(\Sigma)\times H^{1/2}(\Sigma)} \\ &\quad = \int_\Sigma q_G\hat{z}_2(\Phi) = -\int_A \left[\mu\nabla\mathbf{v}\cdot\nabla\hat{\mathbf{z}}(\Phi) + (\varphi\nabla\hat{c})\cdot\hat{\mathbf{z}}(\Phi)\right], \end{aligned} \tag{3.4.34}$$

where $q_G \in H^1(G)$ satisfies

$$-\nabla q_G \;=\; \frac{\mu}{k}\mathbf{v} + \varphi\nabla\hat{c} \;\; in \;\; \mathbf{L}^2(G). \tag{3.4.35}$$

Multiplying the above equation by $\hat{\mathbf{z}}(\Phi)$ and integrating the left side by parts give

$$\int_\Sigma q_G\hat{z}_2(\Phi) \;=\; \int_M q_G\Phi + \int_G \left(\frac{\mu}{K}\mathbf{v} + \varphi\nabla\hat{c}\right)\cdot\hat{\mathbf{z}}(\Phi). \tag{3.4.36}$$

Summing equations (3.4.34) and (3.4.36) results in

$$\begin{aligned}&\int_M q_G\Phi\\ &= -\int_A [\mu\nabla\mathbf{v}\cdot\nabla\hat{\mathbf{z}}(\Phi)+(\varphi\nabla\hat{c})\cdot\hat{\mathbf{z}}(\Phi)]-\int_G\left(\frac{\mu}{K}\mathbf{v}+\varphi\nabla\hat{c}\right)\cdot\hat{\mathbf{z}}(\Phi).\end{aligned}\tag{3.4.37}$$

Consequently,

$$\begin{aligned}&|\int_M q_G\Phi|\\ \leq\ & C_1\left(\|\mathbf{v}\|_{\mathbf{U}}+\|\varphi\|_{L^{\bar{p}}(\Omega)}\|\nabla\hat{c}\|_{\mathbf{L}^p(\Omega)}\right)\left(\|\hat{\mathbf{z}}(\Phi)\|_{\mathbf{H}^1(A)}+\|\hat{\mathbf{z}}(\Phi)\|_{\mathbf{L}^2(G)}\right),\end{aligned}\tag{3.4.38}$$

and from Proposition 3.3.12,

$$\|\hat{\mathbf{z}}(\Phi)\|_{\mathbf{H}^1(A)}+\|\hat{\mathbf{z}}(\Phi)\|_{\mathbf{L}^2(G)}\ \leq\ C\|\Phi\|_{L^2(M)}.\tag{3.4.39}$$

∎

Proposition 3.4.5 *: For any given* $\mathbf{v}\in\mathbf{U}$ *and small parameters* c_{in} *and* ϕ*, the problem: Find* $\varphi\in\mathbf{C}$ *such that*

$$\begin{aligned}&\int_\Omega \varepsilon\left(D^{eff}\nabla\Phi+\Phi\hat{\mathbf{u}}\right)\cdot\nabla\varphi+\int_M\left(-\hat{u}_2+H_m\right)\varphi\Phi+\int_{\Gamma_o}\hat{u}_1\varphi\Phi\\ &=\int_M h(q)\Phi,\quad\forall\Phi\in\mathbf{C},\end{aligned}\tag{3.4.40}$$

has a unique solution, where $h(q)=g-\frac{\beta_m H_m q}{\varepsilon}$*. Also,*

$$\|\varphi\|_{\mathbf{C}}\ \leq\ C\left(\|g\|_{L^2(M)}+\|\mathbf{v}\|_{\mathbf{U}}\right).\tag{3.4.41}$$

Proof: The existence and uniqueness of the solution of the above problem follows from the Lax-Milgram Lemma, [25, page 244]. Define the bilinear form $a(\cdot,\cdot):\mathbf{C}\times\mathbf{C}\longrightarrow\mathbb{R}$ as

$$\begin{aligned} a(\varphi,\Phi) &= \int_\Omega \varepsilon\left(D^{eff}\nabla\Phi + \Phi\hat{\mathbf{u}}\right)\cdot\nabla\varphi \\ &\quad + \int_M \left(-\hat{u}_2 + H_m\right)\varphi\Phi + \int_{\Gamma_o}\hat{u}_1\varphi\Phi, \end{aligned} \tag{3.4.42}$$

and the functional $l : \mathbf{C} \longrightarrow \mathbb{R}$ as

$$l(\Phi) = \int_M h(q)\Phi. \tag{3.4.43}$$

The functional l is continuous since $h(q) = g - \frac{\beta_m H_m q}{\varepsilon}$, where both $g,\ q \in H^{1/2}(M)$. Hence, $h(q) \in L^2(M)$. Also, the bilinear form $a(\cdot,\cdot)$ is continuous. This results from

$$\begin{aligned} |a(\varphi,\Phi)| &\leq C_1\left(\|\nabla\varphi\|_{L^2(\Omega)}\|\nabla\Phi\|_{L^2(\Omega)} + \|\Phi\|_{L^p(\Omega)}\|\hat{\mathbf{u}}\|_{L^{\overline{p}}(\Omega)}\|\nabla\varphi\|_{L^2(\Omega)}\right. \\ &\quad + \|\hat{u}_1\|_{L^2(\Gamma_o)}\|\varphi\|_{L^{\overline{p}}(\Gamma_o)}\|\Phi\|_{L^p(\Gamma_o)} \\ &\quad \left. + \|-\hat{u}_2 + H_m\|_{L^2(M)}\|\varphi\|_{L^{\overline{p}}(M)}\|\Phi\|_{L^p(M)}\right). \end{aligned} \tag{3.4.44}$$

Let us recall that $\hat{\mathbf{u}} := \mathbf{u} + \hat{\mathbf{z}}(\hat{c}) \in \mathbf{H}^1(A\cup G)$ as $\mathbf{u} \in \mathbf{H}^1(A\cup G)$ from Lemma 3.3.20, and $\hat{\mathbf{z}}(\hat{c}) \in \mathbf{H}^1(A\cup G)$ from Remark 3.3.14. Since also

$$H^{1/2}(\Gamma_o) \hookrightarrow L^p(\Gamma_o), \quad H^{1/2}(M) \hookrightarrow L^p(M), \quad p > 2, \tag{3.4.45}$$

estimate (3.4.44) reduces to

$$|a(\varphi,\Phi)| \leq C\left(1 + \|\hat{\mathbf{u}}\|_{\mathbf{H}^1(A\cup G)}\right)\|\varphi\|_{\mathbf{C}}\|\Phi\|_{\mathbf{C}}, \tag{3.4.46}$$

for some constant C. This proves the continuity of $a(\cdot,\cdot)$. For the coercivity of $a(\cdot,\cdot)$, note that

$$\begin{aligned} a(\varphi,\varphi) &= \left(\varepsilon D^{eff}\|\nabla\varphi\|^2_{L^2(\Omega)} + \int_\Omega \varphi\hat{\mathbf{u}}\cdot\nabla\varphi + \int_{\Gamma_o}\hat{u}_1\varphi^2 + \int_M\left(-\hat{u}_2 + H_m\right)\varphi^2\right) \\ &\geq \left(\varepsilon D^{eff}\|\nabla\varphi\|^2_{L^2(\Omega)} - \int_\Omega|\varphi\hat{\mathbf{u}}\cdot\nabla\varphi| - \int_{\Gamma_o}|\hat{u}_1\varphi^2|\right), \end{aligned} \tag{3.4.47}$$

noting that $-\hat{u}_2 = \beta_m H_m\hat{c} \geq 0$ on M. Also,

$$-\int_\Omega|\varphi\hat{\mathbf{u}}\cdot\nabla\varphi| \geq -\|\hat{\mathbf{u}}\|_{L^{\overline{p}}(\Omega)}\|\varphi\|_{L^p(\Omega)}\|\nabla\varphi\|_{L^2(\Omega)}$$

$$\geq \quad -C\|\hat{\mathbf{u}}\|_{\mathbf{H}^1(A\cup G)}\|\varphi\|^2_{\mathbf{C}}. \tag{3.4.48}$$

where the second inequality follows using the same argument as in (3.4.46). Also,

$$\begin{aligned} -\int_{\Gamma_o}|\hat{u}_1\varphi^2| &\geq -C_1\|\hat{u}_1\|_{L^2(\Gamma_o)}\|\varphi\|_{L^p(\Gamma_o)}\|\varphi\|_{L^{\overline{p}}(\Gamma_o)} \\ &\geq -C_2\|\hat{\mathbf{u}}\|_{\mathbf{H}^1(A)}\|\varphi\|^2_{\mathbf{C}}, \end{aligned} \tag{3.4.49}$$

where the second inequality follows from the continuity of the trace operator γ_0 and the Sobolev embedding $\gamma_0(H^1(\Omega)) = H^{1/2}(\partial\Omega) \hookrightarrow L^r(\partial\Omega)$, $r \geq 2$. However, from (3.3.59) and Lemma 3.3.20 (by taking $f = l(\hat{\mathbf{z}}(\hat{c}))$ in this lemma), one obtains

$$\begin{aligned} \|\hat{\mathbf{u}}\|_{\mathbf{H}^1(A)} &\leq \|\mathbf{u}\|_{\mathbf{H}^1(A)} + \|\hat{\mathbf{z}}(\hat{c})\|_{\mathbf{H}^1(A)} \\ &\leq C\left(\|\hat{\mathbf{z}}(\hat{c})\|_{\mathbf{H}^1(A)} + \|\hat{\mathbf{z}}(\hat{c})\|_{\mathbf{L}^2(G)}\right) \\ &\leq C_1\left(\phi + \|\hat{c}\|_{L^2(M)}\right) \\ &\leq C_2\left(\phi + \|\nabla\hat{c}\|_{\mathbf{L}^2(\Omega)}\right). \end{aligned} \tag{3.4.50}$$

This and estimate (3.3.96) imply that $\|\hat{\mathbf{u}}\|_{\mathbf{H}^1(A)}$ can be made small by choosing small parameters c_{in} and ϕ. Hence (3.4.47), (3.4.48), (3.4.49) and (3.4.50) as well as the Poincare inequality yield

$$a(\varphi,\varphi) \quad \geq \quad \lambda\|\varphi\|^2_{\mathbf{C}}, \tag{3.4.51}$$

for some positive constant λ. Hence, the requirements of Lax-Milgram Lemma are met, and therefore there exists a unique solution $\varphi \in \mathbf{C}$.

For the estimate (3.4.41), note that $a(\varphi,\varphi) = \int_M h(q)\varphi$ gives

$$\begin{aligned} \|\nabla\varphi\|^2_{\mathbf{L}^2(\Omega)} &\leq C_1\left(|\int_M h(q)\varphi| + \|\hat{\mathbf{u}}\|_{\mathbf{H}^1(A\cup G)}\|\nabla\varphi\|^2_{L^2(\Omega)}\right) \\ &\leq C_2\left[\|g\|_{L^2(M)}\|\varphi\|_{L^2(M)} + \left(\|\mathbf{v}\|_{\mathbf{U}} + \|\varphi\|_{L^{\overline{p}}(\Omega)}\|\nabla\hat{c}\|_{\mathbf{L}^p(\Omega)}\right)\|\varphi\|_{L^2(M)}\right] \\ &\quad + C_1\|\hat{\mathbf{u}}\|_{\mathbf{H}^1(A\cup G)}\|\nabla\varphi\|^2_{L^2(\Omega)} \\ &\leq C_3\left(\|g\|_{L^2(M)} + \|\mathbf{v}\|_{\mathbf{U}}\right)\|\nabla\varphi\|_{\mathbf{L}^2(\Omega)} \\ &\quad + C_4\left(\|\nabla\hat{c}\|_{\mathbf{L}^p(\Omega)} + \|\hat{\mathbf{u}}\|_{\mathbf{H}^1(A\cup G)}\right)\|\nabla\varphi\|^2_{L^2(\Omega)}, \end{aligned} \tag{3.4.52}$$

where the first inequality follows using the same argument as in (3.4.46), and the second from the estimate (3.4.31) and $\|\varphi\|_{L^r(M)} \leq G\|\nabla\varphi\|^2_{\mathbf{L}^2(\Omega)}$ for $r \geq 2$ (which follows from the Sobolev embeddings and Poincare inequality). Again, $\|\hat{\mathbf{u}}\|_{\mathbf{H}^1(A\cup G)}$ and $\|\nabla\hat{c}\|_{\mathbf{L}^p(\Omega)}$ can be made small by taking small parameters c_{in} and ϕ, the last two terms of inequality (3.4.52) can be combined with the left side to give

$$\|\nabla\varphi\|_{\mathbf{L}^2(\Omega)} \leq C\left(\|g\|_{L^2(M)} + \|\mathbf{v}\|_{\mathbf{U}}\right). \tag{3.4.53}$$

∎

3.4.3 Fixed Point Formulation of the Adjoint Problem

In this section, the existence and uniqueness of the adjoint problem is proved using the Fixed Point Theorem 3.3.30, assuming small parameters c_{in} and ϕ. For this, the following mappings are defined.

Definition 3.4.6 *Let*

$$\begin{aligned} T_{\mathbf{v}} : L^{\overline{p}}(\Omega) &\longrightarrow \mathbf{U} \\ \varphi &\longmapsto \mathbf{v}, \end{aligned} \tag{3.4.54}$$

where $\mathbf{v}$ *is given by the solution of the problem in Proposition 3.4.1. Also, let*

$$\begin{aligned} T_{\varphi} : \mathbf{U} &\longrightarrow L^{\overline{p}}(\Omega) \\ \mathbf{v} &\longmapsto \varphi, \end{aligned} \tag{3.4.55}$$

where φ *is given by the solution of the problem in (3.4.40). Finally, define*

$$T := T_{\varphi} \circ T_{\mathbf{v}} : L^{\overline{p}}(\Omega) \longrightarrow L^{\overline{p}}(\Omega). \tag{3.4.56}$$

Then the mapping T *is well-defined.*

The Fixed Point Theorem 3.3.30 is implemented to show that the mapping T has a fixed point, which proves the existence of a solution to the adjoint problem (3.4.7). The uniqueness of the solution is proved under the assumption of small parameters c_{in} and ϕ.

Theorem 3.4.7 *The mapping $T = T_\varphi \circ T_{\mathbf{v}}$ has the following properties:*

1. *T is continuous*

2. *T is compact*

3. *there exists a constant N such that*

$$\|\varphi\|_{L^{\overline{p}}(\Omega)} \quad < \quad N, \tag{3.4.57}$$

for all

$$\varphi \in L^{\overline{p}}(\Omega) \quad \cap \quad \{\varphi : \varphi = \epsilon T\varphi, \ \textit{for some } \epsilon \in [0,1]\}. \tag{3.4.58}$$

Then from Theorem 3.3.30, T has a fixed point $\varphi \in L^{\overline{p}}(\Omega) \cap \mathbf{C}$. Moreover,

4. *the fixed point is unique when the parameters c_{in} and ϕ are sufficiently small.*

Proof:

1. T is continuous: let $\{\varphi_n\} \subset L^{\overline{p}}(\Omega)$, $\varphi_n \longrightarrow \varphi$ in $L^{\overline{p}}(\Omega)$, and set $\delta\varphi_n = \varphi_n - \varphi$, $\mathbf{v}_n = T_{\mathbf{v}}\varphi_n$, $\mathbf{v} = T_{\mathbf{v}}\varphi$, $\delta\mathbf{v}_n = \mathbf{v}_n - \mathbf{v}$ and $\delta\mathbf{q}_n = \mathbf{q}_n - \mathbf{q}$, where $\mathbf{q}_n$ and $\mathbf{q}$ are associated with $\mathbf{v}_n$ and $\mathbf{v}$, respectively. Then $\delta\mathbf{v}_n$ satisfies

$$\begin{aligned} \alpha(\delta\mathbf{v}_n, \mathbf{w}) + \beta(\delta\mathbf{q}_n, \mathbf{w}) &= -\int_\Omega \delta\varphi_n \nabla\hat{c} \cdot \mathbf{w}, \\ \beta(\mathbf{q}^*, \delta\mathbf{v}_n) &= 0, \end{aligned} \tag{3.4.59}$$

for all $(\mathbf{w}, \mathbf{q}^*) \in \mathbf{U} \times P_A$. Hence from Proposition 3.4.1,

$$\|\delta\mathbf{v}_n\|_{\mathbf{U}} \quad \leq \quad C_1 \|\delta\varphi_n\|_{L^{\overline{p}}} \|\nabla\hat{c}\|_{\mathbf{L}^p(\Omega)}. \tag{3.4.60}$$

Now let $\overline{\varphi}_n = T_\varphi \mathbf{v}_n$ and $\overline{\varphi} = T_\varphi \mathbf{v}$, then $\delta\overline{\varphi}_n$ satisfies

$$\int_\Omega \varepsilon \left(D^{eff}\nabla\Phi + \Phi\hat{\mathbf{u}}\right)\cdot\nabla\delta\overline{\varphi}_n + \int_M \left(-\hat{u}_2 + H_m\right)\delta\overline{\varphi}_n\Phi + \\ + \int_{\Gamma_o} \hat{u}_1\delta\overline{\varphi}_n\Phi = \int_M \left(h(q_n) - h(q)\right)\Phi. \tag{3.4.61}$$

Then it follows from $H^1(\Omega) \hookrightarrow L^{\overline{p}}(\Omega)$ and Proposition 3.4.5 that

$$\begin{aligned} \|\delta\overline{\varphi}_n\|_{L^{\overline{p}}(\Omega)} \le C_2\|\delta\overline{\varphi}_n\|_{\mathbf{C}} &\le C_3\|\delta\mathbf{v}_n\|_{\mathbf{U}} \\ &\le C_4\|\delta\varphi_n\|_{L^{\overline{p}}(\Omega)}\|\nabla\hat{c}\|_{\mathbf{L}^p(\Omega)}, \end{aligned} \tag{3.4.62}$$

where the last inequality follows from the estimate (3.4.60). Hence, the last estimate (3.4.62) gives $\delta\overline{\varphi}_n = T\delta\varphi_n \to 0$ in $L^{\overline{p}}(\Omega)$ as $\delta\varphi_n \to 0$ in $L^{\overline{p}}(\Omega)$, which proves the continuity of T.

2. T is compact: let $\{\varphi_n\}$ be a bounded sequence in $L^{\overline{p}}(\Omega)$. Then it is required to show that $\{T\varphi_n\}$ has a convergent subsequence in $L^{\overline{p}}(\Omega)$. Note that for $\mathbf{v}_n = T_{\mathbf{v}}\varphi_n$, Proposition 3.4.1 gives

$$\|\mathbf{v}_n\|_{\mathbf{U}} \le C_1\left(\sigma + \|\varphi_n\|_{L^{\overline{p}}(\Omega)}\|\nabla\hat{c}\|_{\mathbf{L}^p(\Omega)}\right). \tag{3.4.63}$$

Also for $\overline{\varphi}_n = T_\varphi\mathbf{v}_n = T\varphi_n$, Proposition 3.4.5 gives

$$\|\overline{\varphi}_n\|_{\mathbf{C}} \le C_2\left(\|g\|_{L^2(M)} + \sigma + \|\varphi_n\|_{L^{\overline{p}}(\Omega)}\|\nabla\hat{c}\|_{\mathbf{L}^p(\Omega)}\right), \tag{3.4.64}$$

which implies that $\{\overline{\varphi}_n\}$ is bounded in $H^1(\Omega)$. Since $H^1(\Omega) \hookrightarrow^c L^{\overline{p}}(\Omega)$, the sequence $\{\overline{\varphi}_n\}$ has a convergent subsequence in $L^{\overline{p}}(\Omega) \cap \mathbf{C}$.

3. Repeating the work done in item 2, it follows that for every $\varphi \in L^{\overline{p}}(\Omega)$ satisfying $\varphi = \epsilon T\varphi$ for some $\epsilon \neq 0$ that

$$\|\varphi\|_{L^{\overline{p}}(\Omega)} \le \epsilon C_1\left(\|g\|_{L^2(M)} + \sigma + \|\varphi\|_{L^{\overline{p}}(\Omega)}\|\nabla\hat{c}\|_{\mathbf{L}^p(\Omega)}\right). \tag{3.4.65}$$

Taking c_{in} sufficiently small, the factor $\|\nabla\hat{c}\|_{\mathbf{L}^p(\Omega)}$ can be made small. Consequently, the last term of the above inequality can be grouped with the left side

to give

$$\|\varphi\|_{L^{\overline{p}}(\Omega)} \leq C\left(\|g\|_{L^2(M)} + \sigma\right), \tag{3.4.66}$$

which implies the existence of $N < \infty$.

4. Let φ_1 and φ_2 be two fixed points for the mapping T, and set $\delta\varphi = \varphi_1 - \varphi_2$. Then following the same work done in estimate (3.4.62), it follows that

$$\|\delta\varphi\|_{L^{\overline{p}}(\Omega)} \leq C\|\delta\varphi\|_{L^{\overline{p}}(\Omega)}\|\nabla\hat{c}\|_{\mathbf{L}^p(\Omega)}. \tag{3.4.67}$$

Since also the factor $\|\nabla\hat{c}\|_{\mathbf{L}^p(\Omega)}$ can be made small by taking c_{in} small enough, the right side is combined with the left side to give $\delta\varphi = 0$.

∎

The existence and uniqueness of the solution for the adjoint problem is proved under the assumption c_{in} and ϕ being sufficiently small. Let us remark that ϕ was assumed to be small only in Proposition 3.4.5 to prove the coercivity of the bilinear form $a(\cdot,\cdot)$ defined in (3.4.42). Elsewhere, only c_{in} is assumed to be small enough.

Chapter 4

Numerical Methods

The goal of this chapter is to present the numerical methods used to solve the two FC models and the shape optimization problem. These involve the finite element formulation of the steady state problem and the adjoint problem (presented below), and calculating the shape gradient of the objective functional E as well as perturbing the air channel. In this chapter, the simplified model will be considered, but the derivation for the general model is similar.

4.1 The steady state problem

Let us first consider the steady state problem and show how to obtain its finite element formulation. The strong form of this problem reads: Find $\hat{c}$, $\hat{\mathbf{u}}$, p_A, and p_G such that

$$-\varepsilon D^{eff}\Delta\hat{c} + \varepsilon\hat{\mathbf{u}}\cdot\nabla\hat{c} = 0 \quad on \quad \Omega, \tag{4.1.1}$$

$$-\mu\Delta\hat{\mathbf{u}} + \nabla p_A = 0 \quad on \quad A, \tag{4.1.2}$$

$$\nabla\cdot\hat{\mathbf{u}} = 0 \quad on \quad A\cup G, \tag{4.1.3}$$

$$\hat{\mathbf{u}} + \frac{K}{\mu}\nabla p_G = 0 \quad on \quad G. \tag{4.1.4}$$

Equations (4.1.4) can be simplified by taking the divergence on both sides and using equation (4.1.3), which results in

$$-\nabla \cdot \left(\frac{K}{\mu} \nabla p_G \right) \quad = \quad 0 \quad on \quad G. \tag{4.1.5}$$

Hence the variable $\hat{\mathbf{u}}$ is eliminated on G, yet can be recovered using equation (4.1.4) while required in equation (4.1.1).

The boundary conditions are as follows (see Fig. 2.1 for the definition of boundaries):

$$\begin{array}{lll}
\Gamma_i: & \hat{c} = c_{in}, & \mu \partial_1 \hat{u}_1 - p_A = -\frac{1}{|\Gamma_i|} \int_{\Gamma_i} p_A, \\
& \int_{\Gamma_i} \hat{u}_1 = \phi, & \hat{u}_2 = 0 \\
\Gamma_o: & -\varepsilon D^{eff} \partial_\nu \hat{c} = 0, & -\mu \partial_1 \hat{u}_1 + p_A = 0, \\
& \hat{u}_2 = 0 & \\
\Gamma: & \varepsilon D^{eff} \partial_\nu \hat{c} = 0, & \\
& \hat{u}_1 = 0, & \hat{u}_2 = 0 \\
\Sigma: & \hat{u}_1 = -\mu \partial_1 \hat{u}_1 + p_A - p_G = 0, & -\frac{K}{\mu} \partial_2 p_G = \hat{u}_2 \\
\Gamma_w: & -\varepsilon D^{eff} \partial_\nu \hat{c} = 0 & -\frac{K}{\mu} \partial_1 p_G = 0 \\
M: & -\varepsilon D^{eff} \partial_\nu \hat{c} = (H_m + \beta_m H_m \hat{c})\, \hat{c}, & -\frac{K}{\mu} \partial_2 p_G = -\frac{\beta_m H_m \hat{c}}{\varepsilon},
\end{array} \tag{4.1.6}$$

Let

$$\hat{c} = c + c_{in}, \tag{4.1.7}$$

then $c = 0$ on Γ_i. Therefore, the variables for the steady state problem are c in Ω, $\hat{\mathbf{u}}$ and p_A in A, and p_G in G.

4.2 The adjoint problem

The adjoint problem serves to compute the shape gradient of the cost functional E. The strong form of the adjoint problem reads: Given the solution $\hat{\mathbf{u}}$, c of the steady state problem, find c^*, $\mathbf{u}^*$, p_A^*, p_G^* such that

$$\begin{aligned} -\varepsilon D^{eff}\Delta c^* - \varepsilon\hat{\mathbf{u}}\cdot\nabla c^* &= 0 && on \quad \Omega, && (4.2.1)\\ -\mu\Delta\mathbf{u}^* + \nabla p_A^* &= -c^*\nabla c && on \quad A, && (4.2.2)\\ \nabla\cdot\mathbf{u}^* &= 0 && on \quad A\cup G, && (4.2.3)\\ \mathbf{u}^* &= -\frac{K}{\mu}\left(\nabla P_G^* + \varepsilon c^*\nabla c\right) && on \quad G. && (4.2.4) \end{aligned}$$

The variable $\mathbf{u}^*$ in G can be eliminated by using equations (4.2.3) and (4.2.4), which gives

$$-\nabla\cdot\left[\frac{K}{\mu}\left(\nabla p_G^* + \varepsilon c^*\nabla c\right)\right] = 0 \quad on \quad G. \qquad (4.2.5)$$

The variable $\mathbf{u}^*$ in G can be recovered with equation (4.2.4) for using equation (4.2.1) in domain G. Then the main variables of the adjoint problem are c^* in Ω, $\mathbf{u}^*$ and p_A^* in A, and p_G^* in G.

The associated boundary conditions are:

$$\begin{array}{lll} \Gamma_i: & c^* = 0, & \mu\partial_1 v_1 - p_A^* = -\frac{1}{|\Gamma_i|}\int_{\Gamma_i} p_A^*,\\ & \int_{\Gamma_i} u_1^* = -\sigma, & u_2^* = 0\\ \Gamma_o: & -\varepsilon D^{eff}\partial_\nu c^* = \varepsilon\hat{u}_1 c^*, & -\mu\partial_1 v_1 + p_A^* = 0,\\ & u_2^* = 0 & \\ \Gamma: & \varepsilon D^{eff}\partial_\nu c^* = 0, & \\ & u_1^* = 0, & u_2^* = 0\\ \Sigma: & u_1^* = -\mu\partial_1 v_1 + p_A^* - p_G^* = 0, & -\frac{K}{\mu}\left(\partial_2 p_G^* + \varepsilon c^*\partial_2 c\right) = u_2^*\\ \Gamma_w: & -\varepsilon D^{eff}\partial_\nu c^* = 0 & -\frac{K}{\mu}\partial_1 p_G^* = 0\\ M: & -\varepsilon D^{eff}\partial_\nu c^* = \left(H_m - 3\beta_m H_m\hat{c}\right)c^* + \frac{\beta_m H_m p_G^*}{\varepsilon} - g, & -\frac{K}{\mu}\left(\partial_2 p_G^* + \varepsilon c^*\partial_2 c\right) = 0, \end{array} \qquad (4.2.6)$$

where

$$g = \alpha\left(\hat{c} - \frac{1}{|M|}\int_M \hat{c}\right) - \beta, \tag{4.2.7}$$

α, β and σ are nonnegative parameters appearing in the definition of the cost functional E,

$$E = \alpha\int_M \left(\hat{c} - \frac{1}{|M|}\int_M \hat{c}\right)^2 - \beta\int_M \hat{c} + \sigma p_{in}, \tag{4.2.8}$$

and $p_{in} = p_A|_{\Gamma_i}$ is the pressure at the inlet.

4.3 Finite element formulations of the steady state and the adjoint problems

Let $\mathcal{T}_h(A)$, $\mathcal{T}_h(G)$, and $\mathcal{T}_h(\Omega) = \mathcal{T}_h(A) \cup \mathcal{T}_h(G)$ be triangulations of A, G and Ω, respectively, where h represents the size of the largest element of the triangulation $\mathcal{T}_h(\Omega)$.

To define the finite element spaces, let

$$V_h^l(\Omega) := \left\{v \in C_0(\overline{\Omega}) : v|_K \in P_l(K), \forall K \in \mathcal{T}_h(\Omega)\right\}, \tag{4.3.1}$$

where $V_h^l(A)$ and $V_h^l(G)$ are defined similarly, and $P_l(K)$ is the space of polynomials of degree l on the triangle K. Then using the boundary conditions (4.1.6) and (4.2.6), the following finite element spaces are considered:

$$C_h = \left\{c \in V_h^2(\Omega) : c|_{\Gamma_i} = 0\right\}, \tag{4.3.2}$$

$$P_{G,h} = V_h^2(G), \tag{4.3.3}$$

$$\hat{\mathbf{U}}_{A,h} = \left\{\hat{\mathbf{u}} = (\hat{u}_1, \hat{u}_2) \in V_h^2(A) \times V_h^2(A) : \hat{u}_1|_{\Gamma\cup\Sigma} = 0, \hat{u}_2|_{\Gamma_i\cup\Gamma\cup\Gamma_o} = 0\right\}, \tag{4.3.4}$$

$$P_{A,h} = V_h^1(A). \tag{4.3.5}$$

These discrete spaces are used to write the finite element formulation of the steady state and the adjoint problems.

To derive a finite element formulation, we multiply equation (4.1.1) by φ, equation (4.1.2) by $\mathbf{v}$, equation (4.1.3) by q_A, equation (4.1.4) by q_G; integrate by parts and use boundary conditions (4.1.6). This results in the following finite element formulation of the steady state problem:

For any given H_m, find $c \in C_h$, $\hat{\mathbf{u}} \in \hat{\mathbf{U}}_h$, $p_A \in P_{A,h}$, and $p_G \in P_{G,h}$ such that for all $\varphi \in C_h$, $\mathbf{v} \in \hat{\mathbf{U}}_{A,h}$, $q_A \in P_{A,h}$ and $q_G \in P_{G,h}$,

$$\int_\Omega \left(\varepsilon D^{eff} \nabla c \cdot \nabla \varphi + \varepsilon(\hat{\mathbf{u}} \cdot \nabla c)\varphi\right) + \int_M \left(H_m + \varepsilon \beta_m H_m \hat{c}\right) \hat{c}\varphi = 0, \quad (4.3.6)$$

$$\int_A \left(\mu \nabla \hat{\mathbf{u}} \cdot \nabla \mathbf{v} - p_A \nabla \cdot \mathbf{v}\right) - \int_{\Gamma_i} \overline{p}_A v_1 + \int_\Sigma p_G v_2 = 0, \quad (4.3.7)$$

$$- \int_A \left(\nabla \cdot \hat{\mathbf{u}}\right) q_A - \int_{\Gamma_i} \left(\phi - \int_{\Gamma_i} \hat{u}_1\right) q_A = 0, \quad (4.3.8)$$

$$\int_G \frac{K}{\mu} \nabla p_G \cdot \nabla q_G - \int_\Sigma \hat{u}_{2,A} q_G - \int_M (\beta_m H_m \hat{c}) q_G = 0, \quad (4.3.9)$$

where $\overline{p}_A$ is the average pressure on Γ_i.

Note that the Dirichlet boundary conditions are included in the finite element spaces. The other boundary conditions are recovered, in the weak sense, from the above formulation when the solution is regular either at the continuous level or as $h \to 0$:

1. Integrating equation (4.3.6) by parts gives

$$\int_{\Gamma \cup \Gamma_o \cup \Gamma_w} \left(\varepsilon D^{eff} \partial_\nu c\right) \varphi ds + \int_M \left[\varepsilon D^{eff} \partial_\nu \hat{c} + \left(H_m + \beta_m H_m \hat{c}\right) \hat{c}\right] \varphi ds = 0. \quad (4.3.10)$$

   Hence, $-\varepsilon D^{eff} \partial_\nu \hat{c} = 0$ on $\Gamma \cup \Gamma_o \cup \Gamma_w$ and $-\varepsilon D^{eff} \partial_\nu \hat{c} = \left(H_m + \varepsilon \beta_m H_m \hat{c}\right) \hat{c}$ on M, almost everywhere.

2. Integrating equation (4.3.7) by parts gives

$$\int_{\partial A} \left(\mu \partial_\nu \hat{\mathbf{u}} \cdot \mathbf{v} - p_A \mathbf{v} \cdot \nu\right) ds - \int_{\Gamma_i} \overline{p}_A v_1 ds + \int_\Sigma p_G v_2 ds = 0. \quad (4.3.11)$$

   Substituting $\mathbf{v} = (v_1, 0)^T$ in the above equation gives

$$\int_{\Gamma_i} \left(-\mu \partial_1 \hat{u}_1 + p_A - \overline{p}_A\right) v_1 ds + \int_{\Gamma_o} \left(\mu \partial_1 \hat{u}_1 - p_A\right) v_1 ds = 0, \quad (4.3.12)$$

which implies that $\mu\partial_1\hat{u}_1 - p_A = -\overline{p}_A$ on Γ_i and $-\mu\partial_1\hat{u}_1 + p_A = 0$ on Γ_o, almost everywhere. Similarly, substituting $\mathbf{v} = (0, v_2)^T$ results in

$$\int_\Sigma \left(\mu\partial_2\hat{u}_2 - p_A + p_G\right) v_2 ds \;=\; 0, \tag{4.3.13}$$

which brings $-\mu\partial_1\hat{u}_1 + p_A = p_G$ almost everywhere on Σ.

3. Equation (4.3.8) implies that

$$\int_A \left(\nabla\cdot\hat{\mathbf{u}}\right) q_A \;=\; 0, \tag{4.3.14}$$

$$\int_{\Gamma_i} \left(\phi - \int_{\Gamma_i} \hat{u}_1\right) q_A \;=\; 0. \tag{4.3.15}$$

This leads to $\nabla\cdot\hat{\mathbf{u}} = 0$ in A and $\int_{\Gamma_i}\hat{u}_1 = \phi$ on Γ_i almost everywhere.

4. Integrating equation (4.3.9) by parts gives

$$\begin{aligned}&\int_\Sigma \left(\frac{K}{\mu}\partial_2 p_G + \hat{u}_2\right) q_G ds + \int_{\Gamma_w}\left(\frac{K}{\mu}\partial_\nu p_G\right) q_G ds\\ &+ \int_M \left(\frac{K}{\mu}\partial_2 p_G - \frac{\beta_m H_m \hat{c}}{\varepsilon}\right) q_G ds = 0,\end{aligned} \tag{4.3.16}$$

which results in $-\frac{K}{\mu}\partial_2 p_G = \hat{u}_2$ on Σ, $-\frac{K}{\mu}\partial_\nu p_G = 0$ on Γ_w and $\frac{K}{\mu}\partial_2 p_G = \frac{\beta_m H_m \hat{c}}{\varepsilon}$ on M, almost everywhere.

Similarly, the finite element formulation of the adjoint problem reads:
For given H_m, $\hat{c}$ and $\hat{\mathbf{u}}$, find $c^* \in C_h$, $\mathbf{u}^* \in \hat{\mathbf{U}}_h$, $p_A^* \in P_{A,h}$, and $p_G^* \in P_{G,h}$ such that for every $\varphi^* \in C_h$, $\mathbf{v}^* \in \hat{\mathbf{U}}_{A,h}$, $q_A^* \in P_{A,h}$ and $q_G^* \in P_{G,h}$,

$$\int_\Omega \left(\varepsilon D^{eff}\nabla c^*\cdot\nabla\varphi^* - \varepsilon(\hat{\mathbf{u}}\cdot\nabla c^*)\varphi^*\right) + \int_{\Gamma_o}(\varepsilon\hat{u}_1 c^*)\varphi^* \tag{4.3.17}$$

$$+ \int_M \left[\left(H_m - 3\beta_m H_m\hat{c}\right) c^* + \frac{\beta_m H_m p_G^*}{\varepsilon} - g\right]\varphi^* \;=\; 0, \tag{4.3.18}$$

$$\int_A \left(\mu\nabla\mathbf{u}^*\cdot\nabla\mathbf{v}^* - p_A^*\nabla\cdot\mathbf{v}^* + c^*\nabla c\cdot\mathbf{v}^*\right) - \int_{\Gamma_i}\overline{p}_A^* v_1^* + \int_\Sigma p_G^* v_2^* \;=\; 0, \tag{4.3.19}$$

$$-\int_A (\nabla \cdot \mathbf{u}^*)\, q_A^* - \int_{\Gamma_i} \left(\sigma + \int_{\Gamma_i} \hat{u}_1^*\right) q_A^* = 0, \quad (4.3.20)$$

$$\int_G \frac{K}{\mu} (\nabla p_G^* + \varepsilon c^* \nabla c) \cdot \nabla q_G^* - \int_\Sigma \hat{u}_{2,A}^* q_G^* = 0, \quad (4.3.21)$$

where $\overline{p}_A^*$ denotes the average of p_A^* on Γ_i.

The above finite element formulations, for the steady state and the adjoint problems, are solved by means of a commercial software, FemLab, which uses Newton's method to solve nonlinear systems. In our case, the linear system is solved using the direct solver, UMFPACK.

The parameter H_m, however, needs to be determined. In fact, H_m is a function of η (the catalyst layer activation over-potential, see chapter 2), where $H_m(\eta)$ and η satisfy the following equations:

$$0 = E_{rev} - E_{cell} - \eta - rI_{av}(\eta), \quad (4.3.22)$$

$$I_{av}(\eta) = \frac{1}{|M|} \int_M \frac{4F}{M_o} H_m(\eta) \hat{c}, \quad (4.3.23)$$

$$H_m(\eta) = \frac{M_o i_0}{4F\hat{c}_{ref}} \left(e^{\frac{\alpha_c F}{RT}\eta} - e^{-\frac{\alpha_c F}{RT}\eta}\right). \quad (4.3.24)$$

Hence H_m is determined once η is known. For this, set

$$\delta(\eta) = E_{rev} - E_{cell} - \eta - rI_{av}(\eta). \quad (4.3.25)$$

Then according to equation (4.3.22), the solution η must satisfy $\delta(\eta) = 0$. Note also that

$$\delta(0) = E_{rev} - E_{cell} > 0, \quad (4.3.26)$$

$$\delta(E_{rev}) = -E_{cell} - rI_{av}(E_{rev}) < 0, \quad (4.3.27)$$

which implies that the solution η satisfies

$$0 < \eta < E_{rev}. \quad (4.3.28)$$

The fact that the function $\delta(\eta)$ changes sings in the interval $[0, E_{rev}]$ makes it possible to implement the Bisection method to determine the zero of $\delta(\eta)$.

Another approach to find η is by using a fixed point technique. Note that η must satisfy

$$\eta = E_{rev} - E_{cell} - rI_{av}(\eta). \tag{4.3.29}$$

Setting $f(\eta) = E_{rev} - E_{cell} - rI_{av}(\eta)$, then η is a fixed point of the following formulation:

$$\eta = f(\eta). \tag{4.3.30}$$

Finding η using this approach requires iterations between η and $f(\eta)$, which is obtained after solving the state problem to find $I_{av}(\eta)$. However, this technique was attempted, but did not converge when $I_{av}(\eta)$ is large. In turn, the whole polarization curve could not be obtained using this technique. This situation is expected as the fixed point approach does not guarantee convergence when the derivative of f at some η is greater than one in absolute value. In fact, this occurs when η is large enough to make the derivative of $I_{av}(\eta)$ be greater than one in absolute value.

4.4 Algorithm

The goal of this section is to present the main steps involved to get the numerical results. The algorithm is divided into three main parts for solving the optimal shape problem:

1. solving the steady state problem,
2. solving the adjoint problem for computing the shape gradient ∇E,
3. perturbing the geometry to get the optimal shape design.

For this, let us set the following parameters: $\eta_a = 0$, $\eta_b = E_{rev}$, $N_{steps} = 200$, TOL(H_m)=1e-4, TOL(Γ)=$h_A/100$, where h_A denotes the thickness of the air channel.

- For $n = 1 : N_{steps}$
- Solve the steady state problem
  - while $\frac{|H_m^n - H_m^{n+1}|}{|H_m^n|} \geq \text{TOL}(H_m)$, $\eta_c = \frac{\eta_a + \eta_b}{2}$.
  - compute $H_m(\eta_c)$
  - solve the steady state problem
  - update η_a as follows:

$$\begin{aligned} if \quad & \delta(\eta_a) * \delta(\eta_c) < 0, \quad then \quad \eta_b = \eta_c; \\ else \quad & \eta_a = \eta_c. \\ end \quad & \end{aligned} \tag{4.4.1}$$

  - end of the while statement
- Use the H_m obtained to solve the adjoint problem
- Compute the cost functional $E^n := E(\Gamma^n)$ and the derivative of the cost functional $\nabla E(\Gamma^n)$ from equation (3.2.57), and get $DE^n_{max} := \|\nabla E(\Gamma^n)\|_\infty$

- Stop if $n = N_{steps}$, $DE^n_{max} = 0$, or $\|\Gamma^{n+1} - \Gamma^n\|_\infty < TOL(\Gamma)$.
- Else perturb Γ_n as follows:

$$\Gamma^{n+1} = \Gamma^n - \lambda_n \nabla E(\Gamma_n), \tag{4.4.2}$$

  where

$$\lambda_n := \frac{0.5 * h_A}{DE^n_{max}} \tag{4.4.3}$$

- Repeat the main loop.

Note that with this choice of λ_n, the maximum perturbation $\|\Gamma^{n+1} - \Gamma^n\|_\infty \leq 0.5 * h_A$. This choice is suitable to ensure that Γ^{n+1} stays, for some steps, within the lower and upper limits set for Γ.

Chapter 5

Numerical Results

The goal of this chapter is to present and discuss the numerical results of the steady state problem for the simplified and general models of the cathode presented in Chapter 2, and the solution of the shape optimization problem (2.2.5).

In the first section, computational requirements are assessed in terms of mesh resolution for the numerical solution using the simplified model. In the second section, the numerical solutions of the simplified and general models will be compared and shown to be close enough. This will be useful since it is much easier to deal with the simplified model to solve the optimization problem. In the third section, the simplified model is validated by comparing the polarization curve obtained with experimental data from [15]. In the last section, the solution of the optimization problem (2.2.5) will be presented for a long channel geometry and the short channel geometry considered in [15].

5.1 Description of the test cases

Two types of geometries will be considered to solve our optimization problem: long and short air channel geometries. The short geometry was studied experimentally in [15] while a longer channel and larger MEA (membrane electrode assembly) tends to produce a larger current.

Table 5.1 lists the values of the parameters used to set the optimization problem for both geometries. The values used for the short geometry are taken from [15]. For the long geometry, the values for ε, K, $\hat{c}_{o,in}$, $\hat{c}_{n,in}$ are used in [14] and [22]. Figure 5.1 shows the domains with the main geometrical parameters.

The two constants, $h_{A,min}$ and $h_{A,max}$, set lower and upper limits for the widths of the optimized air channel geometries. Any optimized air channel geometry will be required to have a minimum width not less that $h_{A,min}$ and a maximum width not greater than $h_{A,max}$.

Table 5.2 lists standard parameters used for both geometries. These parameters are documented in [35].

5.2 Verifying the numerical solution of the simplified model

The numerical solution is obtained using the finite element method presented in Chapter 4. In this section, the long geometry is considered. To show that the numerical solution is reliable, it must be verified that the solution is relatively independent from the mesh used. Two meshes are considered: a coarser mesh (Mesh 1) and a mesh obtained by refining Mesh 1 (Mesh 2), see Figure 5.2 and Table 5.3.

The numerical solutions corresponding to the two meshes are compared on the cross-section $x = 0.2m$, see Figure 5.1. It is enough to compare the main variables: the oxygen mass fraction $\hat{c}_o$, the gas pressure drop $\hat{p} - p_{in}$, and the two velocity

Table 5.1: Primary parameters used to solve the simplified and general models

Parameter	Long Geometry	Short Geometry	Description
l	$0.4m$	$0.02m$	length of the air channel and GDL
h_A	$6 \times 10^{-3}m$	$10^{-3}m$	width of the air channel
h_G	$3 \times 10^{-3}m$	$3.8 \times 10^{-4}m$	width of GDL
ε	0.74	0.4	porosity of GDL
K	$10^{-12}m^2$	$1.76 \times 10^{-11}m^2$	permeability of GDL
$\hat{c}_{o,in}$	0.24	0.96	oxygen mass fraction at the inlet Γ_i
$\hat{c}_{n,in}$	0.69	0	nitrogen mass fraction at the inlet Γ_i
p_{out}	$10^5 Pa$	$10^5 Pa$	gas pressure at the outlet Γ_o
ϕ	$3.8 \times 10^{-3}m^2/s$	$6.4 \times 10^{-4}m^2/s$	volumetric flow rate at the inlet Γ_i
$h_{A,min}$	$h_A/5$	$h_A/5$	minimum width of the air channel
$h_{A,max}$	$3h_A$	$3h_A$	maximum width of the air channel
E_{rev}	$1.115V$	$1.115V$	reversible cell voltage
r	$3.65 \times 10^{-5}\Omega m^2$	$3.65 \times 10^{-5}\Omega m^2$	ohmic resistance of the fuel cell
$\hat{c}_{o,ref}$	$\hat{c}_{in}$	$\hat{c}_{in}$	oxygen reference mass fraction
α_m	0.3	0.3	net transported water across M

components $(\hat{u}_1, \hat{u}_2)$. Figure 5.3 shows that the graphs of the two solutions coincide. In conclusion, the numerical solution obtained using Mesh 1 is acceptable. All the subsequent results will be computed with Mesh 1.

Table 5.2: Standard parameters used to solve the simplified and general models

Parameter	Value	Description
μ_{air}	$2.0721 \times 10^{-5}\ kg/(m \cdot s)$	dynamic viscosity of air at $T = 348K$
μ_w	$1.0585 \times 10^{-4}\ kg/(m.s)$	dynamic viscosity of water at $T = 348K$
μ_{sv}	$1.688 \times 10^{-5}\ kg/(m.s)$	dynamic viscosity of the gas at the saturation point
T	$348\ K$	gas temperature
M_o	$32 \times 10^{-3}\ kg/mol$	molar mass of oxygen
M_n	$28 \times 10^{-3}\ kg/mol$	molar mass of nitrogen
M_w	$18 \times 10^{-3}\ kg/mol$	molar mass of water
R	$8.314\ J/(mol.K)$	universal ideal gas constant
F	$96,485\ A \cdot s/mol$	Faraday's constant

5.3 Comparing the numerical solutions of the simplified and general models

The goal of this section is to compare the numerical solutions of the simplified and general models. The two solutions are compared on the cross-section $x = 0.2m$. Provided the two solutions are close enough, the simplified model can be used to solve the optimal shape problem (2.2.5).

The simplified model makes the following assumptions: the gas density and the nitrogen mass fraction are constant in both domains A and G. Figures 5.4 and 5.5 show these assumptions are reasonable since the oxygen mass fraction, $\hat{c}_o$, the gas pressure drop, $\hat{p} - p_{in}$, and the gas velocity components,$(\hat{u}_1, \hat{u}_2)$, are close for both models. These are the main variables that must match for the optimization problem to be set with the simplified model.

Figure 5.5 also shows that both the gas density,ρ_g, and the nitrogen mass fraction,

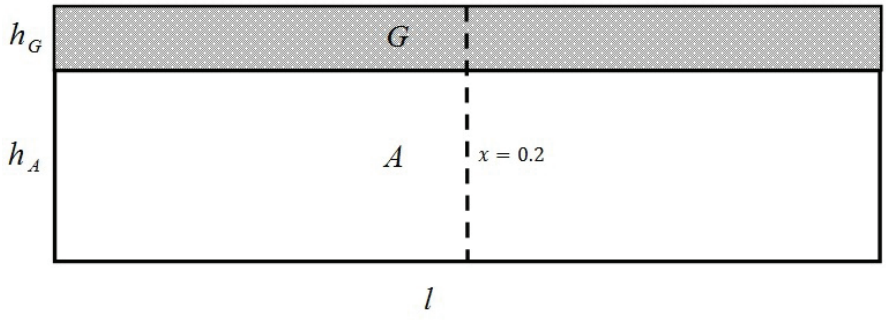

Figure 5.1: Domains with the air channel and GDL, and the cross-section $x = 0.2m$ at which two numerical solutions are compared.

$\hat{c}_n$, gradually deviate along the cross-section toward the membrane. Note that the simplified model is derived assuming ρ_g is constant, while the density in Figure 5.5 is recovered from the solution of the simplified model using the ideal gas law. The general model gives slightly smaller nitrogen mass fraction and gas density in domain G than the ones assumed in the simplified model. Domain G is to a large extent occupied by the water vapor, which reduces the relative mass fraction of nitrogen and oxygen. Since also the molar mass of water is less than those of oxygen and nitrogen, the gas density in domain G must decrease. This difference, however, has a minor effect on the main variables $\hat{c}_o$, $\hat{p}$, and $(\hat{\mathbf{u}}_1, \hat{\mathbf{u}}_2)$ when compared to the simplified model. Therefore, the simplified model well approximates the general model.

5.4 Validating the simplified model

The main objective of this section is to proceed with some validation of the numerical solution of the simplified model by comparing it with experimental results. The comparison is made on the short air channel. First, the simplified model is solved as binary system involving oxygen and water vapor. The numerical solution of this problem is shown in Figure 5.6.

A similar model has been considered in [15] to describe the fluid dynamics in

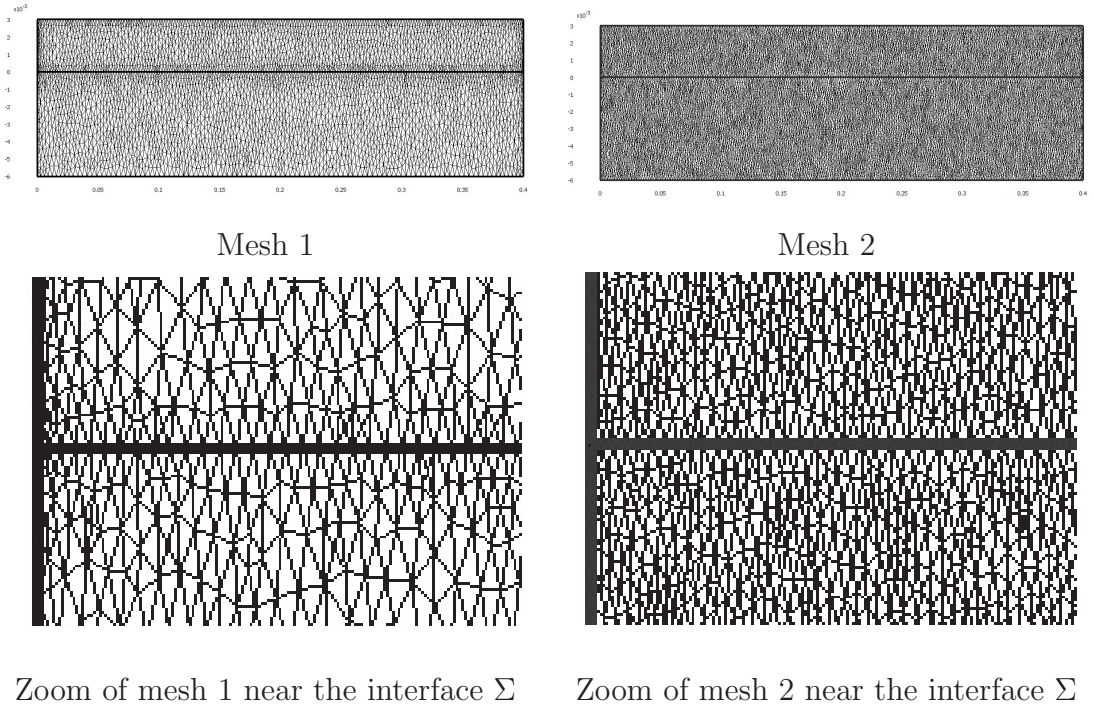

Figure 5.2: The two meshes used to verify relative mesh independence of the solution.

the cathode part of the fuel cell, where the "polarization curve" has been found experimentally. The polarization curve presets the fuel cell's voltage (E_{cell}) versus its averaged current density (I). The polarization curve is used to evaluate the performance of the fuel cell.

Using the same parameters as in [15], the simplified model is solved at different cell voltages, E_{cell}, and the polarization curve is then obtained. The polarization curve obtained with the simplified model was compared with the experimental curve found in [15]. As shown in Figure 5.7, the two curves are found to be close to each other except for small mismatch at high current density. Hence, our model can produce a valid polarization curve for a wide range of fuel cell voltage.

Table 5.3: Properties of Mesh 1 and Mesh 2

Number of elements of	**Mesh 1**	**Mesh 2**
domain A (air channel)	3811	12967
domain G (GDL)	2686	6594
domains A and G	6497	19561
each of channel inlet and outlet	11	16
channel wall (Γ)	104	200
the channel and GDL interface	193	207
GDL walls	10	10
membrane	193	207

5.5 Optimal Shape Design of the Air Channel

The goal of this section is to present and discuss the solution of the shape optimization problem (2.2.5). To recall, this problem consists in finding the optimal shape design of the air channel's wall, Γ, such that the following cost functional $E(\Gamma)$ is minimized:

$$E(\Gamma) = \frac{1}{2}a\int_M \left(N_{\hat{c}_o}\cdot\nu - \frac{1}{|M|}\int_M N_{\hat{c}_o}\cdot\nu\right)^2 - b\int_M N_{\hat{c}_o}\cdot\nu + e\left(p_{in}-p_{out}\right), \quad (5.5.1)$$

where a, b, and e are some given nonnegative parameters. The cost functional $E(\Gamma)$ has three objectives or terms: the first represents the total variance of the oxygen mass flux on the membrane, the second term the total oxygen mass flux on the membrane, and the last term the pressure drop between the inlet and the outlet (see chapter 2 for more details). The optimization problem is going to be solved first by considering one objective by setting one parameter, say $a = 1$, and the others to be zero. Next, mixed objectives will be considered. In this case, the parameters a, b, and e are chosen such that the considered terms of $E(\Gamma)$ have the same order.

This optimization problem is going to be solved first for the long air channel with

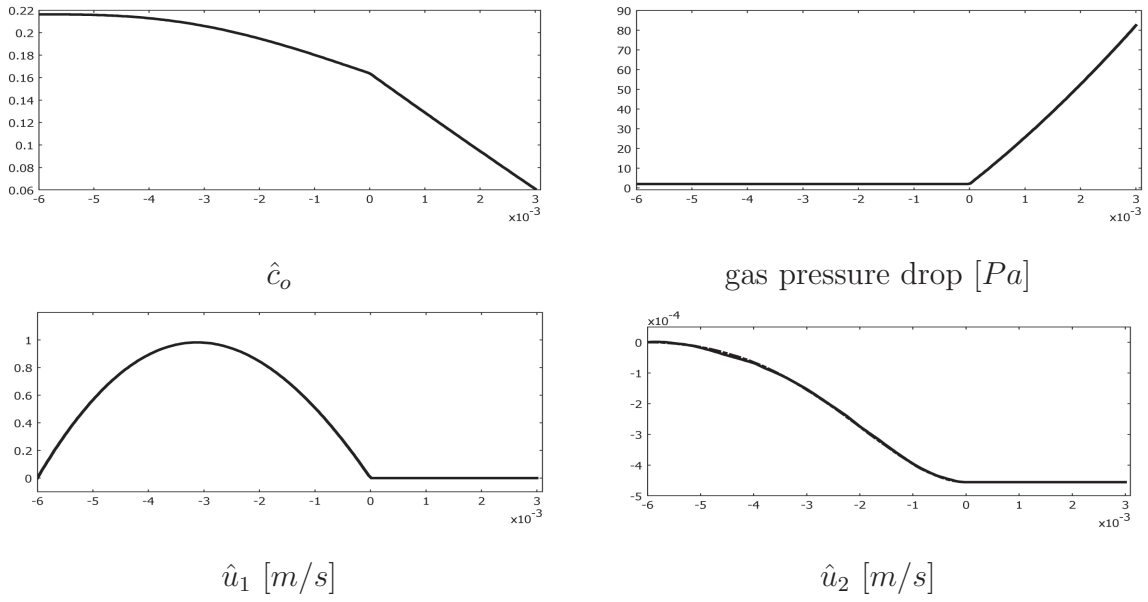

Figure 5.3: Comparison of the numerical solutions, obtained along a vertical cross-section at $x = 0.2m$, obtained using Mesh 1 (solid line) and Mesh 2 (dashed line). The curves are superposed. The abscissa of the graphs is the y-coordinate $[m]$ along the cross section.

length $l = 0.4m$ and then for the short air channel ($l = 0.02m$) introduced in [15]. For both geometries, several cases are considered by choosing different values of the parameters a, b, and e.

Recall that the optimal shape is computed with the gradient method and that steps refer to the iterations of this method. For every iteration of the Gradient method, it is required to find the numerical solutions of the state and adjoint problems as well as computing the shape gradient of the cost functional E. Solving the state and adjoint problems, for every given η, takes about one minute for the simplified model and two minutes for the general model. However, solving for η using the Bisection method requires 14 iterations to meet the tolerance. Therefore, every iteration of the gradient method requires about 14 minutes for the simplified model and 28 minutes for the general model. Hence, finding an optimal shape Γ in 25 Gradient method

iterations requires about 6 hours.

5.5.1 Long air channel: $l = 0.4m$

Case 1: $a = 1$, $b = e = 0$

In this case, it is required to find the optimal shape of the air channel so that the oxygen mass flux or the current density is as uniform as possible on the membrane. With the initial geometry, the oxygen mass flux on M is not uniform and decreases along the air channel as shown in Figure 5.8. Unlike the initial geometry, the optimized geometry leads to a more uniform oxygen mass flux on M (see Figure 5.8) and therefore a more uniform current density on M. In turn, the cathode catalyst layer is used efficiently. Also, having a uniform oxygen mass flux on M makes the water mass flux uniform, which is very useful to avoid accumulation of water in the cell and also to avoid the dry out of the membrane.

In comparison with the initial geometry, note that the optimized geometry of the air channel is wider near the inlet and narrower near the outlet in order to have the oxygen mass flux uniform.

Table 5.4 shows that the optimized geometry not only decreases the total variance of the oxygen mass flux, but also increases the total oxygen mass flux on the membrane. One drawback, however, is that the optimized geometry leads to an increase in the pressure drop, which is due to the narrow channel shape near the outlet.

The last two figures in Figure 5.8 present the convergence of the air channel wall, Γ, while approaching the optimal shape design of the air channel and the associated oxygen mass flux on the membrane $N_{\hat{c}_o}$. These figures show that the convergence is fast enough as the geometry obtained at step 10 is very close the final one.

Case 2: $b = 1$, $a = e = 0$

In this case, it is required to find the optimal shape of the air channel so that the total oxygen mass flux is maximized on the membrane, which is equivalent to maximizing the total current generated. Figure 5.9 shows that the optimal channel shape turns to be the one with smallest width. Yet having the air channel as such would increase the pressure drop as noted in Table 5.4. Note also that with the optimized geometry, the oxygen mass flux or the current density is maximized but not uniform on the membrane, resulting in a non-optimal use of the membrane catalyst.

Case 3: $e = 1$, $a = b = 0$

In this case, it is required to find the optimal shape of the air channel minimizing the pressure drop between the inlet and the outlet. Figure 5.10 shows that the optimal channel shape turns to be the one with largest width. As shown in Figure 5.10 and Table 5.4, the optimal geometry leads to minimal pressure drop, but smaller, nonuniform oxygen mass flux on the membrane.

Case 4: $a = 1, b = 3.3e - 6$, $e = 0$

In this case, the problem is to find the optimal shape of the air channel so that oxygen mass flux is made uniform but also maximum on the membrane. As shown in Figure 5.11 and Table 5.4, the optimal shape design maximizes the oxygen mass flux (or the current density) while keeping the flux relatively uniform on the membrane. Note also that the pressure drop has increased due the narrow channel shape near the outlet.

Case 5: $a = 1, e = 3.5e - 10$, $b = 0$

In this case, it is required to find the optimal shape of the air channel minimizing the total variance of the oxygen mass flux on the membrane and minimizing the

pressure drop between the inlet and the outlet. Figure 5.12 and Table 5.4 show an improvement in the design meeting these two objectives.

In this case it is hard to satisfy the two objectives as the pressure drop increases when the variance of the oxygen mass flux decreases, see case 1 for example.

To compare these cases at different E_{cell} voltages, it is essential to find the polarization curve corresponding to each optimized geometry. This helps us compare the the averaged current densities of the above cases at different cell voltages. Figure 5.13 presents the polarization curves corresponding to the optimal shape designs obtained in the above cases.

The polarization curve for the initial geometry is denoted by case 0 with black color. All cases have almost same current density at low voltages. The polarization curve for case 1 shows that the current density is increased while it is uniform on the membrane. The polarization curve for case 2 shows the maximum current density as required, yet the pressure drop is very high. An intermediate case between case 1 and case 2 is case 4, where it is required to have maximal, and uniform current density. The polarization curve corresponding to this case shows a remarkable improvement in the current density in comparison with that in case 0. In addition, the pressure drop is reasonable in comparison with the one obtained from case 2. The least pressure drop is achieved by case 3, where in this case the polarization curve shows the least current density in comparison with the other cases. An intermediate case between case 1 and case 3 is case 5, where the polarization curve shows a little increase in the current density.

5.5.2 Short air channel with $l = 0.02m$ and $\varepsilon = 0.4$

Small fuel cells are important since they are needed for small devices. In this subsection, the fuel cell considered has the same dimensions as in [15], and the system is binary involving oxygen and water vapor. The objective of this subsection is to solve

the optimization problem for the short air channel ($l = 0.02m$).

First, let us comment on the steady state solution with the initial geometry. Note that in Figure 5.14, the depletion of the oxygen along the channel and across the GDL is very small due to the small size of the fuel cell. Also, the variance of the oxygen mass flux on the membrane is already small enough. However, some design improvements can still be made by having a uniform current density on the membrane, and a lower pressure drop between the inlet and the outlet.

Case 1: $a = 1$**,** $b = e = 0$

In this case, it is required to minimize the variance of the oxygen mass flux on the membrane, which is equivalent to have a uniform current density on the membrane. Figure 5.14 and Table 5.5 show that the optimized geometry of the air channel leads to a smaller variance of the oxygen mass flux on the membrane. However, the total oxygen mass flux on the membrane negligibly decreased, unlike the increase observed for the same case with the long air channel (compare with Figure 5.8 and Table 5.4). As for the long channel geometry, this case results in an increase in the pressure drop.

Case 2: $b = 1$**,** $a = e = 0$

In this case, it is required to find the optimal air channel shape maximizing the oxygen mass flux on the membrane. Figure 5.15 shows that the optimal channel shape found is the one with the smallest width possible. This causes the pressure drop to increase dramatically while the increase in the total oxygen mass flux is negligible, as noted in Table 5.5.

Case 3: $e = 1$**,** $a = b = 0$

In this case, it is required to find the optimal air channel shape minimizing the pressure drop. Figure 5.16 shows that the optimal shape is the one with maximum

width. More interestingly, as shown in Table 5.5, the total oxygen mass flux negligibly decreased though the width of the air channel is set to the maximum allowed, while the pressure drop is a lot smaller. Hence, the optimized geometry leads to a minimal pressure drop while still having the total oxygen mass flux very close to the one in the initial case, or even the geometry with maximal total oxygen flux on M.

Case 4: $a = 1$**,** $e = 6.3e - 14$**,** $b = 0$

From the above cases, it follows that it is better to consider wider air channels which contribute to decrease the pressure drop with almost the same total oxygen mass flux on the membrane. Since the variance of the oxygen mass flux is important as well, it is interesting to consider the present case.

This case requires to find the optimal channel shape that minimizes the total variance of the oxygen mass flux and minimizes the pressure drop. Figure 5.17 and Table 5.5 show that the optimized geometry leads to the required objectives.

5.6 Long versus short channel design

Let us make some remarks on the differences of impact when designing long and short air channels. For long air channels, the impact of the optimal design on values of the cost functional is evident in all cases: the total oxygen mass flux on the membrane notably increased while its variance decreased, and the pressure drop between the inlet and outlet decreased.

However, for short air channels the depletion of the oxygen mass fraction is very small in both the air channel and GDL. This is due to the small size of the fuel cell. Consequently, the variance of the oxygen mass flux is small on the membrane. Hence, redesigning the air channel cannot improve a lot the oxygen mass flux or its variance on the membrane. Yet, optimal design can decrease the pressure drop between the inlet and outlet, while maintaining almost the same oxygen mass flux on

Table 5.4: Values of the cost functional corresponding to different cases, for the long channel geometry

Case Number	Step	Total Variance of N_O	Total N_O $[kg/s]$	$p_{in} - p_{out}$[Pa]	E
0	0	7.7e-010	2.3e-004	2.1	–
1	66	4.9e-011	2.4e-004	68.8	4.9e-011
2	1	6.4e-010	2.4e-004	255.4	-2.4e-004
3	1	1.7e-009	2.1e-004	0.080	0.080
4	61	5.6e-011	2.4e-004	88.4	-7.3e-010
5	51	4.5e-010	2.337e-004	2.8	1.49e-009

Table 5.5: Values of the cost functional corresponding to different cases, for the short channel geometry

Case Number	Step	Total Variance of N_O	Total N_O $[kg/s]$	$p_{in} - p_{out}$ $[Pa]$	E
0	0	2.8e-013	1.34608e-005	4.4	–
1	96	5.2e-014	1.34607e-005	99.2	5.2e-014
2	23	2.849e-013	1.34609e-005	545.6	-1.34609e-005
3	1	5.3e-013	1.344e-005	0.17	0.17
4	27	1.6e-013	1.345e-005	1.2	2.4e-013

the membrane.

In conclusion, redesigning the cathode air channel is effective for both long and short channels.

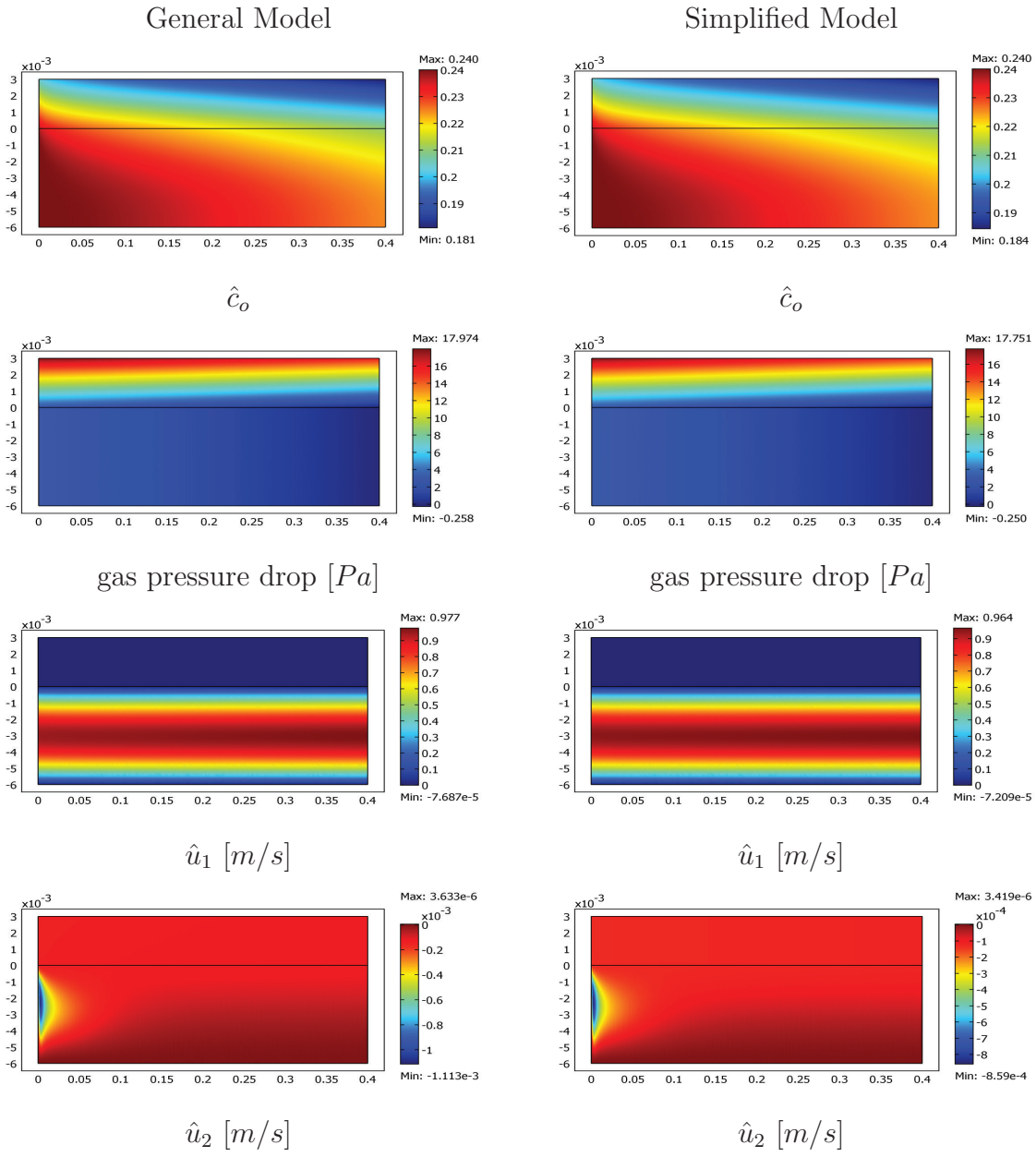

Figure 5.4: Surface plot of the numerical solutions for the simplified (at right) and general (at left) models for the long geometry. The coordinates of the geometry are in meters.

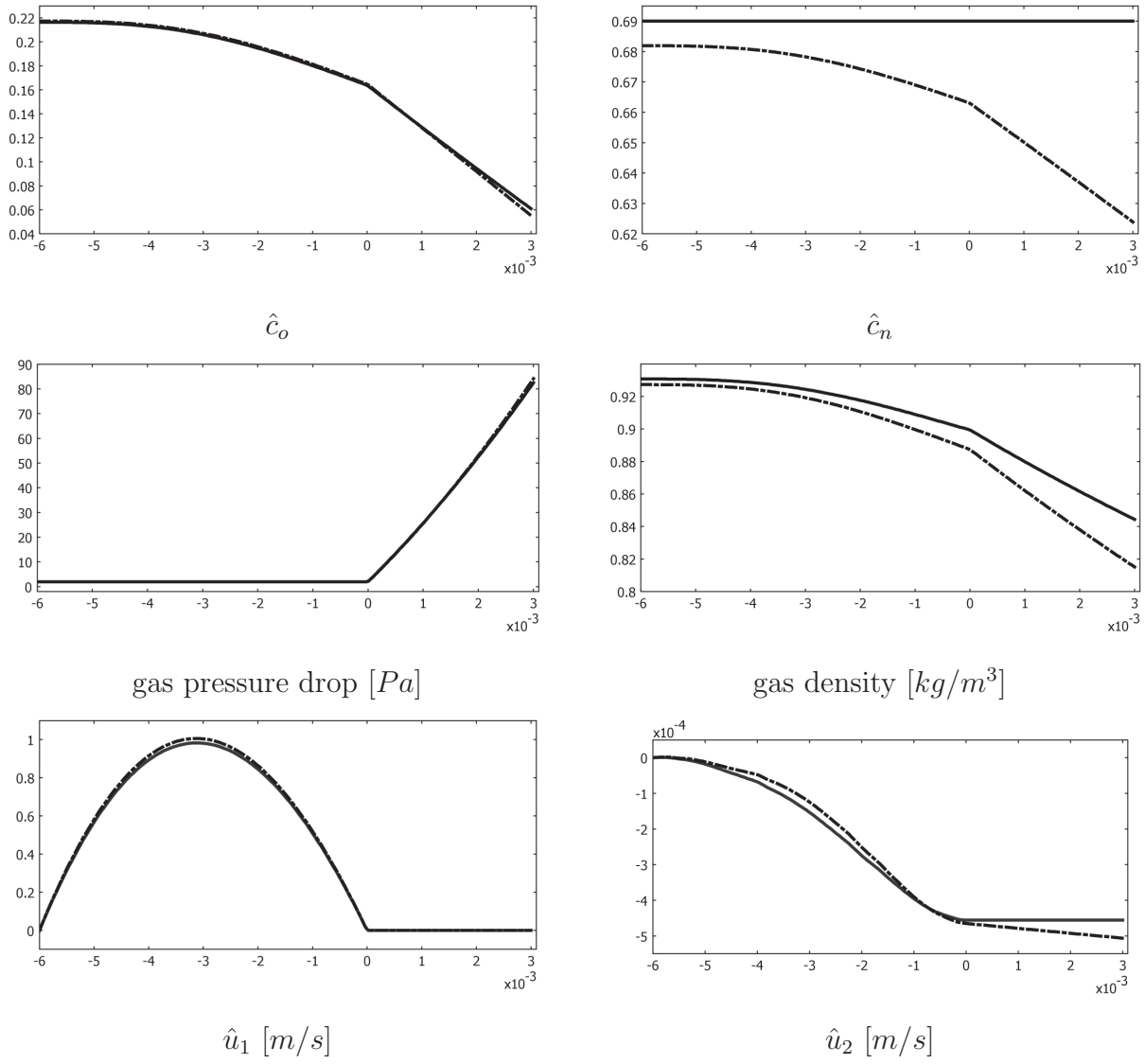

Figure 5.5: Solution of the simplified model (solid line) and general (dashed line) models on a vertical cross-section at $x = 0.2m$. The abscissa of the graphs is the y-coordinate $[m]$ along the cross section.

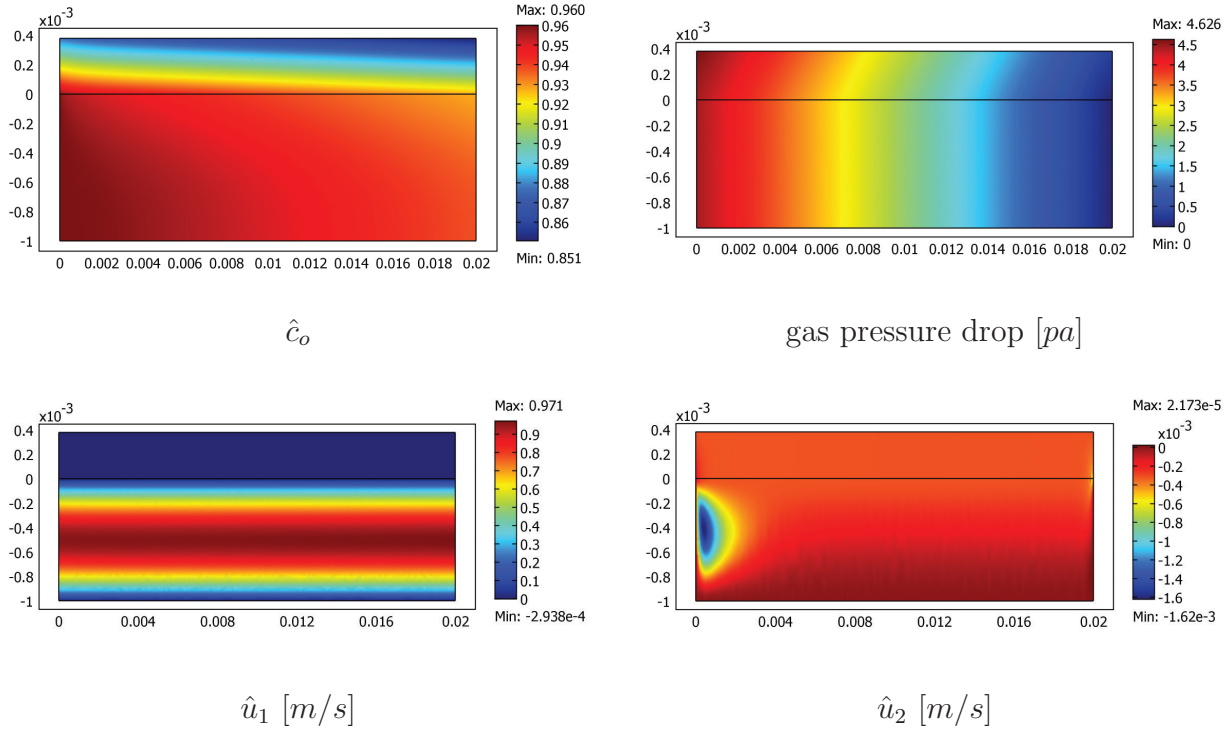

Figure 5.6: The numerical solution of the simplified model for the short air channel geometry. The coordinates of the geometry are in meters.

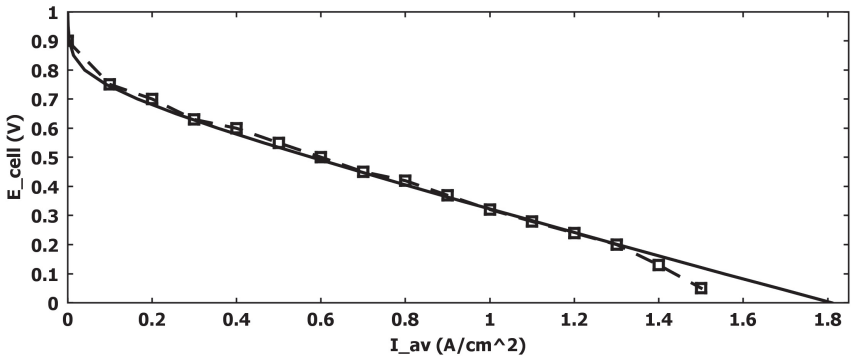

Figure 5.7: Comparison of the polarization curve obtained from the simplified model (solid line) with the one found experimentally in [15] (dashed line).

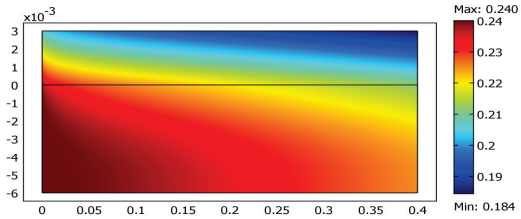

$\hat{c}_o$

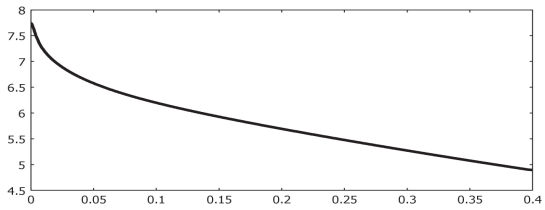

$N_{\hat{c}_o,y}$ $[10^{-4}kg/(m^2 \cdot s)]$ on M (initial geometry)

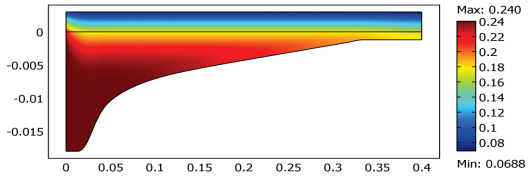

$\hat{c}_o$

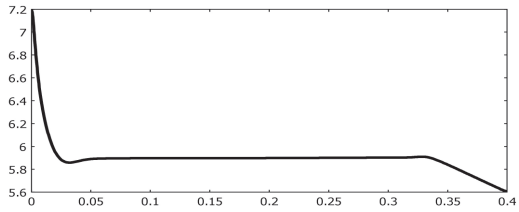

$N_{\hat{c}_o,y}$ $[10^{-4}kg/(m^2 \cdot s)]$ on M (optimized geometry)

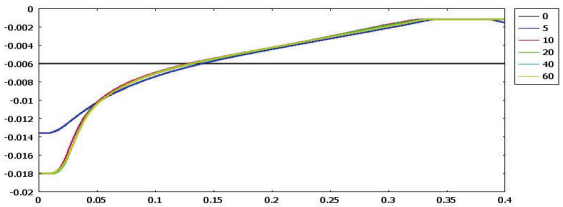

shape of the boundary Γ after n steps

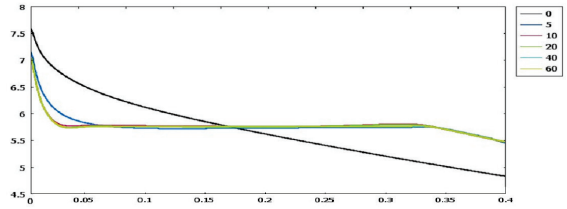

convergence of $N_{\hat{c}_o,y}$ $[10^{-4}kg/(m^2 \cdot s)]$ on M

Figure 5.8: The numerical solution while minimizing only the total variance of the oxygen mass flux on M, for the long channel geometry ($a = 1,\ b = e = 0$)

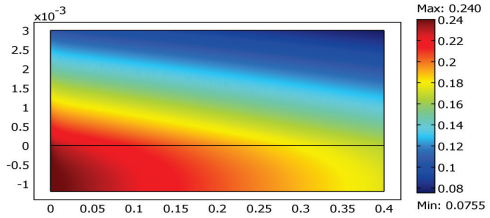

$\hat{c}_o$

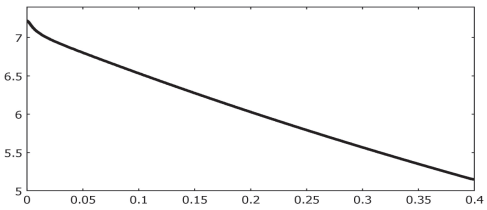

$N_{\hat{c}_o,y}$ $[10^{-4}kg/(m^2 \cdot s)]$ on M (optimized geometry)

Figure 5.9: The numerical solution while maximizing only the oxygen mass flux on M, for the long channel geometry ($b = 1,\ a = e = 0$)

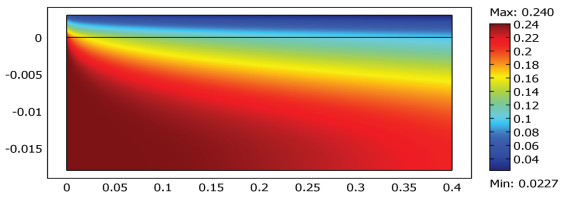

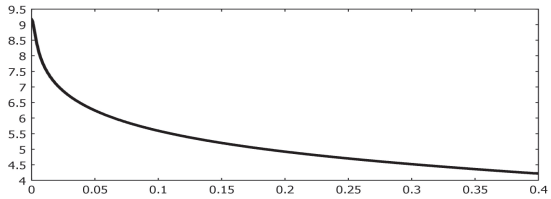

$\hat{c}_o$ $N_{\hat{c}_o,y}$ $[10^{-4}kg/(m^2 \cdot s)]$ on M (optimized geometry)

Figure 5.10: The numerical solution while minimizing only the pressure drop between the inlet and the outlet, for the long channel geometry ($e = 1$, $a = b = 0$)

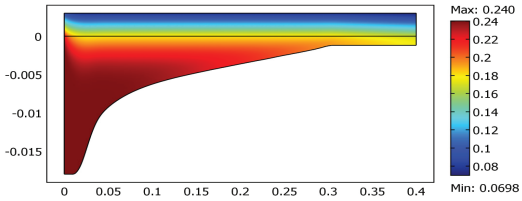

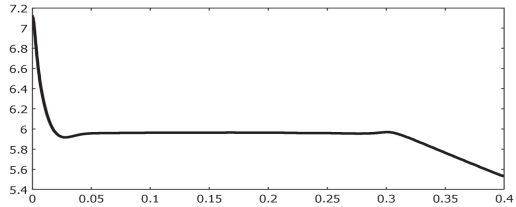

$\hat{c}_o$ $N_{\hat{c}_o,y}$ $[10^{-4}kg/(m^2 \cdot s)]$ on M (optimized geometry)

Figure 5.11: The numerical solution while minimizing the variance of the oxygen mass flux and maximizing the flux on the membrane, for the long channel geometry ($a = 1, b = 3.3e-6$, $e = 0$)

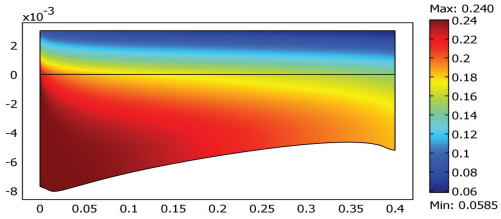

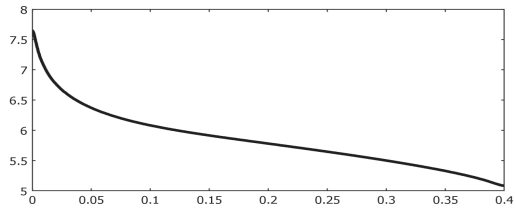

$\hat{c}_o$ $N_{\hat{c}_o,y}$ $[10^{-4}kg/(m^2 \cdot s)]$ on M (optimized geometry)

Figure 5.12: The numerical solution while minimizing both the variance of the oxygen mass flux on the membrane and the pressure drop between the inlet and the outlet, for the long channel geometry ($a = 1, e = 3.5e-10$, $b = 0$)

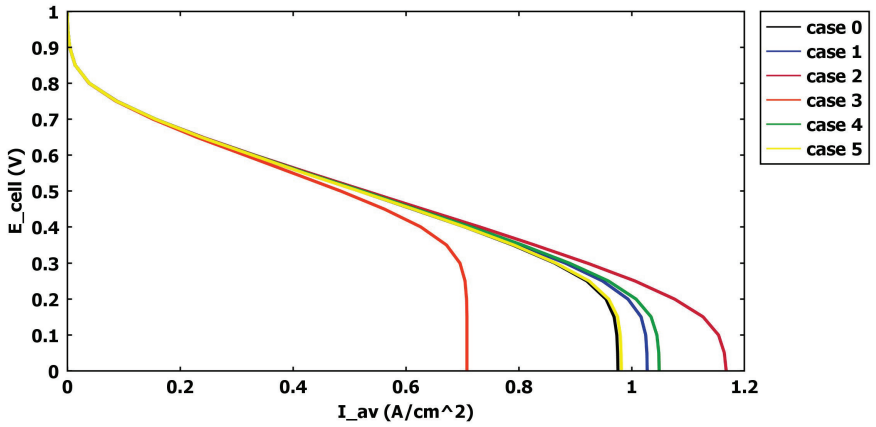

Figure 5.13: The polarization curves corresponding to the optimization cases considered.

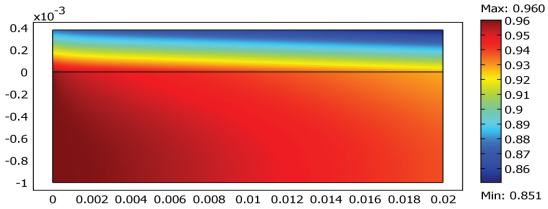

$\hat{c}_o$

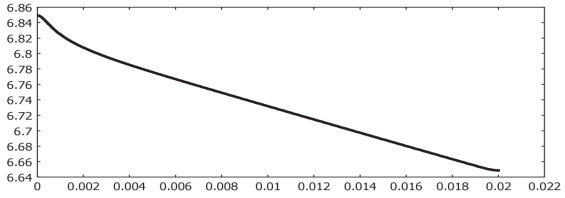

$N_{\hat{c}_o,y}$ $[10^{-5}kg/(m^2 \cdot s)]$ on M (initial geometry)

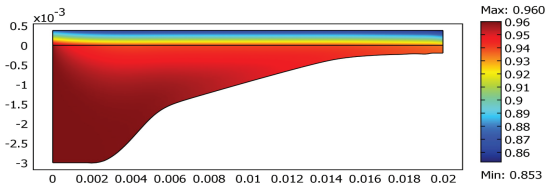

$\hat{c}_o$

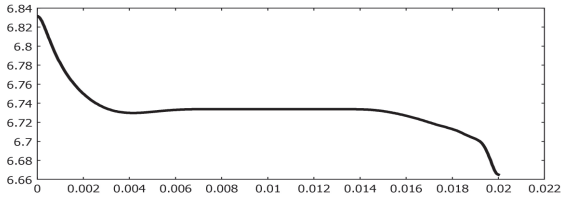

$N_{\hat{c}_o,y}$ $[10^{-5}kg/(m^2 \cdot s)]$ on M (optimized geometry)

Figure 5.14: The numerical solution while minimizing only the total variance of the oxygen mass flux on the membrane, for the short channel geometry ($a = 1$, $b = e = 0$)

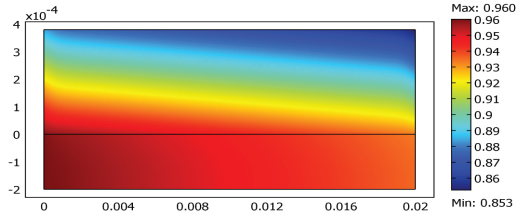

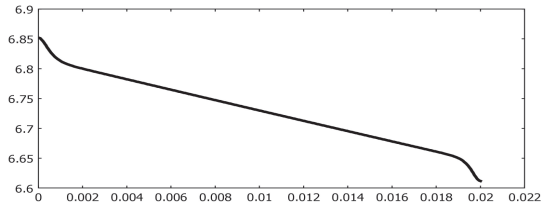

$\hat{c}_o$ $N_{\hat{c}_o,y}$ $[10^{-5}kg/(m^2 \cdot s)]$ on M (optimized geometry)

Figure 5.15: The numerical solution while maximizing only the total oxygen mass flux on the membrane, for the short channel geometry ($b = 1$, $a = e = 0$)

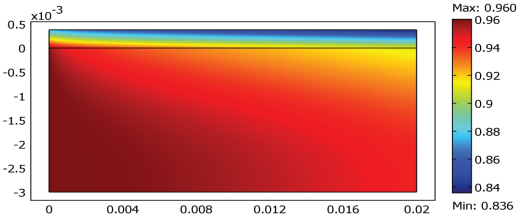

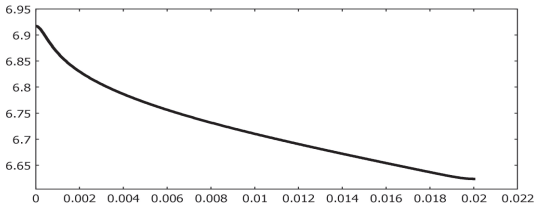

$\hat{c}_o$ $N_{\hat{c}_o,y}$ $[10^{-5}kg/(m^2 \cdot s)]$ on M (optimized geometry)

Figure 5.16: The numerical solution while minimizing only the pressure drop between the inlet and the outlet, for the short channel geometry ($e = 1$, $a = b = 0$)

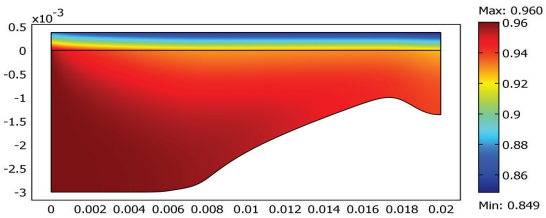

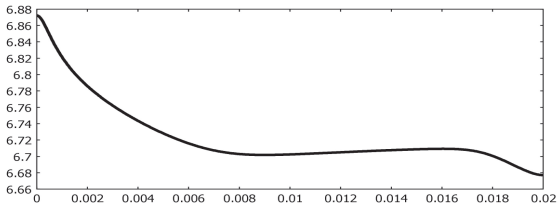

$\hat{c}_o$ $N_{\hat{c}_o,y}$ $[10^{-5}kg/(m^2 \cdot s)]$ on M (optimized geometry)

Figure 5.17: The numerical solution of minimizing both the total variance of the oxygen mass flux the membrane and the pressure drop between the inlet and the outlet, for the short channel geometry ($a = 1$, $e = 6.3e - 14$, $b = 0$)

Chapter 6

Conclusion

This chapter summarizes the contributions of the thesis. It also lists interesting future work that could result from our investigations.

6.1 The contribution of the thesis

In chapter 2, the thesis pays a particular attention in modeling the cathode part of the fuel cells by considering the following model parameters as variables: the gas mixture density, the mixture viscosity, and the reaction taking place at the cathode/anode interface. These parameters are taken constants by many authors to simplify the model, yet without investigation. Investigating the sensitivity of these parameters is done by considering two models: a general model and a simplified model assuming constant gas mixture density and constant nitrogen mass fraction. This led to simplify the general model to reduce the cost of numerical computations after careful comparison with the general model to evaluate the sensitivity of these parameters. Chapter 2 also contributes in that it couples the model used by [22] with a model for the reaction kinetics to obtain polarization curves. A new optimization problem was stated that includes a cost functional E representing the fuel cell performance and

the shape of the gas channel as design variable.

Chapter 3 consists of three mathematical analysis parts. In the first part, the shape gradient of the cost functional E is calculated by using the theory of shape calculus and an adjoint system. This is a primary step for solving the shape optimization problem in chapter 2 with the least computational expenses. The second part of this chapter proves the existence of the shape derivatives of the state variables $\hat{c}$, $\hat{\mathbf{u}}$, $\hat{p}$ and p_{in}, using the implicit mapping theorem, Sobolev embeddings, and fixed point formulation. The shape differentiability of the cost functional E is also proved. Existence of the shape derivative of such complex problems coupling several PDEs over several domains is rarely discussed in the literature. The third part proves the existence and uniqueness of the solution of the adjoint system, which is needed to compute the shape gradient. In the second and the third part, both the volumetric flow rate ϕ at the channel inlet and the oxygen mass fraction c_{in} at the channel inlet are assumed to be small enough. To our knowledge, the shape optimization and the analysis of the related problems have never been done for fuel cell applications.

Chapter 4 presents the numerical methods used to solve the shape optimization problem. This involves the finite element formulation for the steady state and adjoint problems. We proposed a method to compute the reaction rate H_m for arbitrary cell voltage E_{cell}. This problem is resolved by using the Bisection method. Resolving this problem makes it possible to compute the entire polarization curve, which is a tool to evaluate the efficiency of the fuel cell and validate the model. A fixed point method was attempted, as is often done to solve nonlinearities in fuel cell problems, but could not provide the whole polarization curve. We think that the Bisection method as implemented here is a simple and powerful alternative.

In chapter 5, the numerical solution of the simplified and general models are computed and compared. The conclusion of the comparison is that the assumptions made in the simplified model are reasonable. Also, the simplified model is shown to be able to produce a valid polarization when compared to the experimental one

in [15]. Both short and long air channels are considered to solve different shape optimization cases while treating single and mixed objectives. A main contribution in this chapter is that these cases are compared by considering their polarization curves along with the cost functional E. To our knowledge, this consideration is not found in the literature, where only polarization curves are used.

We found that designing long and short air channels has a different impact on increasing the current density of the fuel cell. Designing long air channels leads to a relatively large increase in the current density. However, for short air channels this objective is already met before redesigning the air channel, which refers to the high oxygen mass fraction on the membrane. On the other hand, designing both short and long air channels has a notable improvement on making the reaction rate uniform on the membrane and decreasing the pressure drop between the inlet and outlet of the air channel.

6.2 Future work

There is still some interesting future work:

1. Considering the three dimensional shape optimization problem since it reflects the real situation. One challenge will be treating the computational expense.

2. Finding the optimal design of the cathode/anode interface M instead of Γ. This could lead to a greater impact on the performance of the fuel cell. Another controlling parameter to consider is the porosity ε.

3. Investigating if the existence and uniqueness of the steady state and adjoint problems can be proved with ϕ or c_{in} not necessarily small.

Bibliography

[1] K. Atkinson and W. Han. *Theoretical Numerical Analysis: a Functional Analysis Framework, Texts in Applied Mathematics 39*. Springer, 2001.

[2] R. Byron Bird, W. E. Stewart, and E. N. Lightfoot. *Transport Phenomena*. John Wiley and Sons, Inc., 2002.

[3] R. Bradean, K. Promislow, and B. Wetton. Transport phenomena in the porous cathode of a proton exchange membrane fuel cell. *Numerical Heat Transfer, Part A: Applications*, 42(1-2):121–138, 2002.

[4] C. H. Cheng, H. H. Lin, and G. J. Lai. Design for geometric parameters of PEM fuel cell by integrating computational fluid dynamics code with optimization method. *Journal of Power Sources*, 165(2):803–813, 2007.

[5] M. C. Delfour and J. P. Zolésio. *Shapes and Geometries: Analysis, Differential Calculus, and Optimization*. Siam, 2001.

[6] T. Gallouët and A. Monier. On the regularity of solutions to elliptic equations. *Rendiconti di Mathematica*, 19(VII):471–488, 1999.

[7] D. Gilbarg and N. S. Trudinger. *Elliptic Partial Differential Equations of Second Order*. Springer-Verlag, Berlin, second edition, 1983.

[8] J. Gopalakrishnan and W. Qiu. Partial expansion of a Lipschitz domain and some applications. *Frontiers of Mathematics in China*, 2012.

[9] P. Grisvard. *Singularities in Boundary Value Problems*. Springer-Verlag,Masson, 1992.

[10] M. Grujicic and K. Chittajallu. Design and optimization of polymer electrolyte membrane (PEM) fuel cells. *Applied Surface Science*, 227:56–72, 2004.

[11] M. Grujicic and K. Chittajallu. Optimization of the cathode geometry in the polymer electrolyte membrane (PEM) fuel cells. *Chemical Engineering Science*, 59:5883–5895, 2004.

[12] J. Haslinger and R. A. E. Makiner. *Introduction to Shape Optimization: Theory, Approximation and Computation*. SIAM, 2003.

[13] A. Jamekhorshid, G. Karimi, and I. Noshadi. Current distribution and cathode flooding prediction in a PEM fuel cell. *Journal of the Taiwan Institute of Chemical Engineers*, 42:622–631, 2011.

[14] M. J. Kermani and J. M. Stockie. Heat and mass transfer modeling of dry gases in the cathode of PEM fuel cells. *International Journal of Computational Fluid Dynamics*, 18(2):153–164, February 2004.

[15] N. Khajeh-Hosseini-Dalasm, K. Fushinobu, and K. Okazaki. Three-dimensional transient two-phase study of the cathode side of a PEM fuel cell. *International Journal of Hydrogen Energy*, 35:4234–4246, 2010.

[16] A. Kumar and R. G. Reddy. Effect of channel dimensions and shape in the flow-field distributor on the performance of polymer electrolyte membrane fuel cells. *Journal of Power Sources*, 113:11–18, 2003.

[17] J. L. Lions and E. Magenes. *Non-Homogeneous Boundary Value Problems and Applications*, volume I. Springer-Verlag, 1972.

[18] J. L. Lions and E. Magenes. *Non-Homogeneous Boundary Value Problems and Applications*, volume II. Springer-Verlag, 1972.

[19] A. Mawardi, F. Yang, and R. Pitchumani. Optimization of the operating parameters of a proton exchange membrane fuel cell for maximum power density. *The Journal of Fuel Cell Science and Technology*, 2(2):121–135, 2005.

[20] D. Mitrović and D. Žubrinić. *Fundamentals of Applied Functional Analysis.* Addison Wesley Longman Limited, 1998.

[21] A. Novruzi. Existence of optimal shape for a system of conservation laws in a free air-porous domain. *Quarterly of Applied Mathematics*, LXIV(4):641–661, 2006.

[22] A. Novruzi, K. Promislow, and B. Wetton. 3D hydrogen fuel cell fluid dynamics computation. *ECCOMAS*, 24-28 July 2004.

[23] C. Pozrikidis. *Fluid Dynamics: Theory, Computation, and Numerical Simulation.* Springer, second edition, 2009.

[24] A. Quarteroni and A. Valli. *Numerical Approximation of Partial Differential Equations.* Springer-Verlag, 1994.

[25] M. Renardy and R. C. Rogers. *An Introduction to Partial Differential Equations.* Springer-Verlag, second edition, 2004.

[26] M. Santis, S. A. Freunberger, A. Reiner, and F. N. Buchi. Homogenization of the current density in polymer electrolyte fuel cells by in-plane cathode catalyst gradients. *Electrochimica Acta*, 51:5383–5393, 2006.

[27] M. Secanel, B. Carnes, A. Suleman, and N. Djilali. Numerical optimization of proton exchange membrane fuel cell cathodes. *Electrochimica Acta*, 52(7):2668–2682, 2007.

[28] M. Secanel, K. Karan, A. Suleman, and N. Djilali. Optimal design of ultra-low platinum PEMFC anode electrodes. *Journal of The Electrochemical Society*, 155(2):B125–B134, 2008.

[29] M. Secanel, K. Koran, A. Suleman, and N. Djilali. Multivariable optimization of PEMFC cathodes using agglomerate model. *Electrochimica Acta*, 52(22):6318–6337, 2007.

[30] M. Secanel, R. Songprakorp, N. Djilali, and A. Suleman. Optimization of a proton exchange membrane fuel cell membrane electrode assembly. *Structural and Multidisciplinary Optimization*, 40:563–583, 2010.

[31] J. Simon. Differentiation with respect to the domain in boundary value problems. *Numerical Functional Analysis and Optimization*, 2(7, 8):649–687, 1980.

[32] D. Song, Q. Wang, Z. Liu, T. Navessin, M. Eikerling, and S. Holdcroft. Numerical optimization study of the catalyst layer of PEM fuel cell cathode. *Journal of Power Sources*, 126(1-2):104–111, 2004.

[33] E. L. Sudnikov. The viscosity of moist air. *Journal of Engineering Physics and Thermophysics*, 19:1036–1037, 1970.

[34] R. Temam. *Navier-Stokes Equations. Theory and Numerical Analysis*. North-Holand Publishing Company, 1977.

[35] P. T. Tsilingiris. Thermophysical and transport properties of humid air at temperature range between 0 and 100 C. *Energy Conversion and Management*, 49:1098–1110, 2008.